Groundwater Upwelling Velocities in Remediation Areas, Onondaga Lake Bottom Subsite

S.S. PAPADOPULOS & ASSOCIATES, INC.
Environmental & Water-Resource Consultants

December 29, 2010

7944 Wisconsin Avenue, Bethesda, Maryland 20814-3620 • (301) 718-8900

Table of Contents

Page

Table of Contents (Continued)

List of Figures

Table of Contents (Continued)

List of Tables

List of Attachments

Executive Summary

This report describes the results of extensive field and analytical studies that have quantified the discharge of groundwater to the areas in Onondaga Lake where a sediment cap will be placed as part of the remedial activities undertaken to meet the requirements of the Record of Decision (ROD) for the Onondaga Lake Bottom Subsite. The data and evaluations described in this report provide an excellent foundation for the design of the remedy for Onondaga Lake. The upwelling velocities that are described in this report will be used in the chemical isolation model for purposes of cap design.

The current rates of groundwater discharge in much of Remediation Areas A and E and in the center section of Remediation Area C, which are similar to discharge rates expected after placement of the isolation cap, have been delineated based on the analysis of chloride depth profiles at over 200 locations within and in the vicinity of these remediation areas. In Remediation Area B, Remediation Area D, and the northern and southern sections of Remediation Area C, the rates of groundwater discharge after placement of the isolation cap will be significantly lower than current rates as the result of the construction and operation of hydraulic containment systems along the shoreline. Groundwater discharge rates after placement of the isolation cap in these remediation areas were calculated based on groundwater flow rates upward through the underlying regional confining unit (the silt and clay unit), as the containment systems will capture all groundwater flow to the lake above this unit.

This report describes methods that were implemented in the field to measure groundwater discharge rates, which are commonly referred to as upwelling velocities, within the remediation areas. The evaluation of upward groundwater velocity through the sediment, based on the change in chloride concentrations with depth in sediment pore water, was determined to be the best method for quantifying current upwelling velocities in the remediation areas. This report describes the theoretical basis for the use of this method to measure upwelling velocities and describes the extensive data collected on chloride concentrations in sediment pore water to accurately delineate the current distribution of upwelling velocities within the remediation areas. The mean upwelling velocities determined from this method in Model Areas A1, A2, and C2 and Remediation Area E are 1.3 cm/yr, 4.1 cm/yr, 2.7 cm/yr and 1.49 cm/yr, respectively; upwelling velocities in all of these areas will be minimally affected by the hydraulic containment systems.

In the remediation areas located offshore of proposed hydraulic containment systems, the long-term upwelling velocity after remedy implementation will be equal to the rate of groundwater movement through the regional confining unit. These containment systems are assumed to operate for the life of the remedy. The vertical hydraulic conductivity of the regional confining unit was estimated by the testing of 40 core samples collected from the silt and clay within the remediation areas; these data were combined with estimates of the hydraulic gradient across the regional confining unit and the thickness of the silt and clay unit to calculate the upward groundwater flow through the unit. The uncertainty in this calculation was evaluated based on estimates of the uncertainty in vertical hydraulic conductivity, hydraulic gradients and thickness. The mean estimated long-term upwelling velocities through the regional confining unit were estimated to be less than 2 cm/yr in all areas proposed for capping that are located offshore of proposed hydraulic containment systems.

Section 1
Introduction

This technical report describes groundwater discharge to the areas in Onondaga Lake where a sediment cap will be placed as part of the remedial activities undertaken to meet the requirements of the ROD for the Onondaga Lake Bottom Subsite. The areas where a sediment cap will be constructed have been geographically grouped into five subareas termed Remediation Areas A through E. The locations of the remediation areas, which have a total area of about 400 acres, are shown on Figure 1. For purposes of cap design, Remediation Area D has been subdivided into four subareas: SMU2-ILWD, western, center, and eastern; Remediation Area A has been subdivided into Model Area A1 and Model Area A2; and Remediation Areas B and C have been subdivided into Model Area B2, Model Area B1/C1, Model Area C2, and Model Area C3.[1] The locations of the remediation areas and model areas are shown on Figure 1.

Groundwater discharge to Onondaga Lake has been evaluated in detail because groundwater flux through lake sediments can transport contaminants in the sediments into the upper layers of the cap. As a result, understanding the groundwater discharge that will occur through the sediment cap after placement is essential for predicting the long-term performance of the sediment cap. In the analytical and numerical models developed to simulate the performance of the sediment cap (see Appendix B), the parameter describing the rate of groundwater discharge is referred to as the "Darcy velocity." The Darcy velocity is the rate at which groundwater moves upward through the sediment cap. The Darcy velocity is frequently called the "upwelling velocity." The upwelling velocities that are described in this report have been used as inputs to the chemical isolation model used for cap design (see Appendix B).

In much of Remediation Areas A and E, and in Model Area C2, it is anticipated that groundwater discharge through the cap will be similar to that which is occurring today. As a result, evaluations of groundwater discharge following construction of the cap have focused on understanding and quantifying existing rates of groundwater discharge in these areas.

Hydraulic containment systems constructed or proposed for construction along the shoreline reduce the groundwater discharge to the lake in Remediation Areas B and D, and portions of Remediation Areas A and C, to negligible levels by capturing all groundwater flow towards the lake above the regional confining unit (Figure 1). In these areas, evaluations of groundwater discharge following construction of the cap have focused on understanding the component of groundwater discharge that will not be captured by the hydraulic containment

[1] For purposes of chemical isolation layer design, each remediation area was subdivided into distinct model areas as shown on Figure 1. In this report, estimates of upwelling velocities in each of the model areas are developed. The methods used to delineate the model areas are presented in Appendix B. Additional detail on how the influence of groundwater conditions factored into model area delineation are provided in Sections 2, 5 and 8 of this appendix. For purposes of evaluation alternatives in the Feasibility Study, Onondaga Lake was separated into eight areas or sediment management units (SMU) for ease of evaluating alternatives in different portions of the lake. The SMU delineations are shown on Figure 1. For the purpose of this document, portions of the lake remedy are referred to in terms of the remediation areas /model areas rather than the SMU delineations.

systems and continue to flow through the cap following completion of the remedy. The existing rates of groundwater discharge in these remediation areas provide only an upper bound estimate of the amount of groundwater discharge that will occur following construction of the hydraulic containment system. The dominant component of groundwater discharge following construction of the cap will be upward groundwater flow through the underlying regional confining unit. Thus, the evaluations described in this report focused on quantifying groundwater flow through the regional confining (silt and clay) unit.

A detailed description of groundwater flow to Onondaga Lake is contained in Appendix D: Part A to the Onondaga Lake Feasibility Study (FS) titled “Groundwater Flow to Onondaga Lake” (Parsons 2004). In addition, following publication of the FS, the United States Geological Survey (USGS) published an analysis of groundwater flow in the unconsolidated sediments underlying Onondaga Lake and the contiguous glacial valleys (Yager and others 2007a, 2007b; and Kappel and Yager, 2008). The major findings of these studies are summarized in this report.

The analyses of groundwater discharge described in Appendix D of the FS indicated that in areas offshore of where a hydraulic containment system would be constructed upwelling velocities would be less than 2 cm/yr with the containment system in operation. Upwelling velocities in Remediation Areas A and E, without a hydraulic containment system, were estimated during the FS to be higher in near shore areas. Upwelling velocities in Remediation Area A ranged from 300 cm/yr within 20 ft. of the shoreline to less than 2 cm/yr beyond 700 ft. from the shoreline, and upwelling velocities in Remediation Area E ranged from 70 cm/yr near the shoreline to less than 2 cm/yr beyond 300 ft. from the shoreline.

This report focuses on the studies and investigations that have been conducted since the FS was completed to better quantify groundwater discharge to the five remediation areas. Seepage meters and chloride-depth profiles of the sediments were the field methods employed in the pre-design investigations (PDI) to quantify groundwater discharge rates. These methods and the results of these methods are described in this report as well as other methods that were considered to quantify groundwater discharge rates. In addition, as part of the pre-design investigations, many borings have been advanced into the sediments beneath the remediation areas. The data from these borings have provided a good understanding of the characteristics of the sediments and the thickness and continuity of the major stratigraphic units including the regional confining unit. This information has allowed the development of a better understanding of groundwater flow within the sediments than existed at the time the FS was prepared.

The chloride-depth profile method was judged to be the most reliable and accurate method for quantifying the relatively low groundwater discharge rates through the sediments in the remediation areas. This method relies on the observation that the pore waters in the sediments beneath Onondaga Lake have significantly higher chloride concentrations than the lake water as the result of natural brines beneath the lake and migration of leachate from the wastebeds along the shoreline of Onondaga Lake. As a result, there is a significant chloride concentration gradient from the sediments to the lake. The change in chloride concentration with depth below the lake/sediment interface provides information on the rate of upward groundwater flow through the sediment.

The shape of the chloride-depth profile is a function of chloride migration by advection with groundwater and chemical diffusion. If there is no advective transport with groundwater, the chloride-depth profile will be linear as a result of diffusion. If there is upward groundwater flow, the chloride depth profile will be convex, with the convexity a function of the magnitude of the groundwater flow, as shown on the figure below. Analysis of the convexity of the profile is the method that was used to quantify groundwater upwelling velocities. This method is useful for analyzing upwelling velocities that are less than about 50 cm/yr. At greater upwelling velocities, the chloride concentrations do not change significantly with depth.

The figure to the right shows a plot of chloride concentrations in pore water versus depth at a boring located in Remediation Area E (OL-VC-60154). This figure illustrates the large changes in chloride concentrations that occur with depth below the sediment-water interface. The measured chloride data are plotted as dots and chloride concentrations increase from about 359 mg/L at the sediment-water interface to over 15,000 mg/L at a depth of about 9 ft. below the sediment-water interface. The measured chloride data follow a convex profile indicating a relatively small upwelling velocity. Also shown on the figure are the expected chloride depth profiles for upwelling velocities of 0.1 cm/yr, 1 cm/yr, 10 cm/yr and 100 cm/yr. These expected chloride depth profiles illustrate the significant effect that changes in upwelling velocities have on the shape of the chloride depth profile. For example, the chloride depth profile with an upwelling velocity of 1 cm/yr is significantly different than that with an upwelling velocity of 10 cm/yr. The measured chloride data shown on the figure follow a trend similar to that expected with an upwelling velocity of about 1 cm/yr.

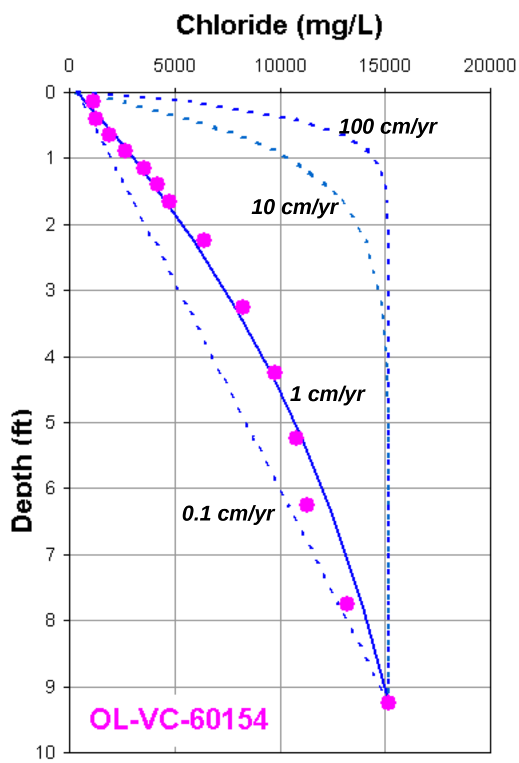

The remainder of this report is organized into eight sections; Section 2 through Section 9. Section 2 of this report describes groundwater conditions in the remediation areas. Section 3 describes the methods used to determine upwelling velocities and compares the methods. Section 4 describes the method used to analyze chloride-depth profiles to calculate upwelling velocities. Section 5 describes upwelling velocities for cap design in remediation areas located in areas without onshore hydraulic containment systems. Section 6 describes an evaluation of uncertainty in calculated upwelling velocities. Section 7 describes analyses of upward groundwater flow through the silt and clay unit, and Section 8 describes upwelling velocities for cap design in areas with onshore hydraulic containment systems. Conclusions are presented in Section 9, and the references cited in the report are listed in Section 10.

Section 2
Groundwater Conditions in Remediation Areas

Geologic Setting

Onondaga Lake overlies a deep, northwest-trending glacial trough in the Vernon Shale, the bedrock formation beneath and in the vicinity of the lake. A schematic block diagram of the southeastern end of the lake, which illustrates the trough, is shown on Figure 2. The trough averages about 300 ft. deep along the axis of the lake and is filled primarily with unconsolidated, fine-grained sediments, although a coarse-grained unit typically occurs overlying till near the base of the unconsolidated sediments. The thickness of the unconsolidated sediments decreases rapidly away from Onondaga Lake, except in the valleys of the main tributaries, which are also underlain by unconsolidated sediments. The stratigraphic sequence observed in most borings advanced beneath the lake and adjacent upland areas are similar:

- Surficial sediments typically described as silt with fine sand and fill material
- Gray clayey marl, gray-brown clayey silty marl (marl unit)
- Brown-gray clay, gray-brown silt and clay (silt and clay unit also termed regional confining unit)
- Gray-brown silt with sand layers (fine sand and silt unit)
- Sand, sometimes with gravel (sand and gravel unit)
- Till, dense clay and silt with sand and gravel (till unit)
- Green, red and gray shale (bedrock)

The silt and clay unit is an important regional confining unit or aquitard that impedes upward groundwater flow to the lake. This unit has been interpreted to be continuous beneath the entire lake, consistent with the interpretation in the USGS report by Yager and others (2007b). A thickness map of this unit based on interpretation of boring logs is shown on Figure 3.

Hydrogeologic cross sections through Remediation Areas A, D and E are shown on Figures 4 to 6 and locations of these sections are shown on Figure 1. These cross sections, at a minimum, depict the silt and clay unit and overlying sediments. Where information is available on the geologic units below the silt and clay unit, this information is also shown. The sections are annotated with notes from the boring logs regarding lithologic observations within each of the geologic units. In general, the marl is described as silt and/or silt and clay though in some logs the marl was noted as consisting of gravel and/or sand sized sediments. In Remediation Area D, relatively thick deposits of Solvay waste generated from the production of sodium carbonate (soda ash) by the Solvay process and other materials contained within the in-lake waste deposits overlie the marl unit (Figure 5). Additional hydrogeologic cross sections are contained in Attachment I.

Onondaga Lake and Groundwater Flow

Onondaga Lake, oriented along a northwest-southeast axis, is approximately 4.5 miles long and one mile wide. The lake has a mean depth of 36 ft. and a maximum depth of 65 ft. which occurs in the southern part of the lake. The average lake level during the past 20 years was

362.9 ft. above mean sea level (AMSL),[2] based on records from the USGS gage on Onondaga Lake (Site 04240495, Onondaga Lake at Liverpool, New York). The surface area of the lake at this elevation is approximately 4.5 square miles, and the volume is approximately 34,600 million gallons. Surface water inflows and outflows from the lake average about 470 cubic ft. per second based on average flows between 1998 and 2002 (Onondaga County, 2003). The groundwater component of the lake water budget is small, estimated to be less than 0.5 percent of surface water inflows (Parsons, 2004). Precipitation on the lake and evaporation from the lake are approximately equal; therefore, the net water budget associated with precipitation and evaporation is small. The average residence time of water in the lake is approximately 100 days.

Regional groundwater flow in both the bedrock and the unconsolidated sediments is towards the valleys of the major tributaries of the lake. Groundwater discharge areas include seven major tributaries: Ninemile Creek, Geddes Brook, Harbor Brook, Bloody Brook, Onondaga Creek, Saw Mill Creek, and Ley Creek. Groundwater flow towards and into the lake originates primarily as precipitation that infiltrates into the unconsolidated sediments bordering the lake. Because the saturated unconsolidated sediments are restricted to a relatively narrow band on either side of the lake, the total recharge area is relatively small, and as a result, recharge to and discharge from the unconsolidated sediments is relatively small. Most of the groundwater in the unconsolidated sediments that flows toward the lake discharges to the tributaries and to ditches and drains along the shoreline with the remainder discharging in near-shore areas of the lake. This occurs, in part, because of the thickening wedge of fine-grained, low-permeability materials beneath the lake and because of dense sodium-chloride brines in the unconsolidated sediments beneath the lake.

Most of the groundwater discharge that occurs to the lake is the result of groundwater flow through the marl and overlying units from the upland areas. These units are typically fine grained, though there are some sand stringers or lenses, as shown on the hydrogeologic cross sections. As a result, groundwater flow rates through these units are not large and most of the groundwater discharge occurs near shore in the littoral zone.

Some groundwater discharge to the lake occurs as the result of upward groundwater flow through the silt and clay unit from the deeper permeable units. The sand and gravel unit and the overlying fine sand and silt unit are the primary deeper permeable units (see Figure 2). These units are primarily recharged where they subcrop around the perimeter of the lake. Groundwater levels in the sand and gravel along the lakeshore are typically well above the lake level indicating the potential for upward groundwater flow. The vertical hydraulic conductivity of the silt and clay unit is estimated to be on the order of 10^{-7} cm/sec and, thus, the total upward groundwater flow through this unit is very small. The potential upward groundwater flow through the silt and clay unit is described in detail in Section 7.

The presence of natural sodium-chloride brines in the unconsolidated sediments beneath the lake complicates the understanding of local groundwater flow conditions. In the past, discharge of brines at salt springs was reported to have occurred around much of the shoreline of

[2] Vertical datum in this report is referenced to the North American Vertical Datum of 1988 (NAVD 88).

the southern basin of the lake (Kappel, 2000). These discharges likely occurred in areas where the silt and clay unit thinned or disappeared along the shoreline. The natural discharge of brines has ceased due to extraction of brines from wells along the shoreline. From 1797 to 1917, over 11.5 million tons of finished salt were produced from the springs and wells along the southern shoreline of the lake (USGS, 2000). This represents the salt content from the constant production of 500 gallons per minute (gpm) of brine with a chloride concentration of 60,000 mg/L over this period.

In addition to the natural sodium-chloride brines, there are natural mixed cation brines in the bedrock. These brines formed by the dissolution of evaporate beds within the Vernon Shale and overlying bedrock units. These brines are enriched in calcium, magnesium, and bromide relative to the sodium-chloride brines. In addition to the natural brines, some brines in the subsurface result from seepage of leachate[3] from the wastebeds. These brines are comprised primarily of sodium, calcium, and chloride. The wastebed leachates typically have sodium to calcium ratios that are less than 1, whereas the natural sodium-chloride brines have sodium to calcium ratios that are greater than 10. The mixed cation brines typically have sodium to calcium ratios in the range of 1.4 to 4. The mixing of relatively fresh groundwater, natural sodium-chloride brines, natural mixed cation brines, and leachate from the wastebeds have created a wide variety of groundwater quality types in the vicinity of Onondaga Lake. The distribution of groundwater quality provides information on groundwater migration and origin.

Hydraulic Containment Systems

Hydraulic containment systems along the shoreline are an integral part of the lake remedy and remedies for the adjacent upland areas. Two types of hydraulic containment systems have been proposed; containment systems with a barrier wall and containment systems without a barrier wall.

The hydraulic containment systems incorporating a barrier wall will extend along the shoreline from the Willis-Semet area to south of the mouth of Harbor Brook, a total distance of about 6,800 ft. These hydraulic containment system consists of five primary elements: 1) an impermeable barrier or wall seated in the upper portion of the silt and clay unit; 2) a gravel filled drain, completed to an elevation that is several feet below the elevation of the lowest recorded lake level, with a collection pipe embedded within, 3) wick drains within the lower portion of the fill and within the marl unit, 4) pumps to maintain the water level in the drain below lake level, and 5) a water treatment facility. These hydraulic containment systems are designed to capture the groundwater flowing towards the lake in the materials above the silt and clay unit. In addition, the drains will capture some flow from the underlying units by increasing hydraulic gradients across the confining unit. A schematic of the hydraulic containment system with a barrier wall is shown on Figure 7. A 2,850 ft. section of the hydraulic containment system has already been completed adjacent to the southern section of Remediation Area C and part of

[3] Leachate refers to the liquid with a high total dissolved solids concentration that was discharged to the wastebeds during the period when the wastebeds were active. The leachate had a total dissolved solids concentration of about 100,000 mg/L and was a calcium-sodium-chloride type water (Effler, 1996).

Remediation Area D (Willis/Semet IRM Barrier Wall). The impermeable barrier in this area consists of a sealed joint sheet pile wall.

Two segments of a hydraulic containment system without a barrier wall are proposed along the shoreline of Wastebeds 1-8; an approximately 1,400 ft. segment east of the mouth of Ninemile Creek and an approximately 6,000 ft. segment along the east side of the wastebeds extending northward from Ditch A (Figure 1). These segments of the hydraulic containment system will consist of four components: 1) a gravel filled drain, completed to an elevation that is several feet below the elevation of the lowest recorded lake level, with a collection pipe embedded within, 2) wells or wick drains within the lower portion of the fill and within the marl unit, 3) pumps to maintain the water level in the drain below lake level, and 4) a water treatment facility. These hydraulic containment systems will be designed to capture all groundwater flowing towards the lake from Wastebeds 1-8 in the marl and overlying fill units. A schematic of the hydraulic containment system without a barrier wall is also shown on Figure 7.

Groundwater Flow Model

A groundwater flow model has been developed to aid in the evaluation and design of the remedy for Onondaga Lake. The flow model has assisted in the development of the current understanding of groundwater flow conditions in the vicinity of the lake, which guided the detailed studies undertaken to quantify upwelling velocities. The model has been used to quantify the rates and direction of groundwater flow in the unconsolidated materials and in the upper bedrock in the vicinity of Onondaga Lake and to quantify groundwater discharge in the vicinity of Onondaga Lake. The model domain encompasses an area of approximately 30 square miles including all of Onondaga Lake and areas to the west and southwest of the lake. Revisions have been made to the model since the FS; the revised model, referred to as model Version 3.0 (S.S. Papadopulos & Associates, Inc. and O'Brien and Gere, 2009), received conditional approval by the NYSDEC on June 15, 2010. Version 1.0 of the groundwater model is described in Appendix D to the FS (Andrews and Swenson, 2004; and Swenson and Andrews, 2004).

Groundwater Conditions and Model Area Development

Groundwater discharge was an important consideration in developing the cap modeling areas for chemical isolation layer design as shown on Figure 1 and described in Appendix B. Model areas were developed to address variability in conditions across individual remediation areas to allow for robust cap designs, specific to the conditions in a particular portion of the overall remediation area. For example, the groundwater discharge at the mouth of Ninemile Creek is higher than that at other locations within Remediation Area A; therefore, to account for this spatial difference in groundwater upwelling velocities in the chemical isolation layer design, the region of higher upwelling was modeled separately from the remainder of the remediation area (and model inputs were specified separately for the two distinct areas).

In Remediation Area A, following collection of the Phase V and VI chloride-depth profiles it was determined that velocities near the mouth of Ninemile Creek were elevated compared to those in other parts of Remediation Area A. This finding was consistent with the understanding of the underlying sediment/soil structure near the mouth of Ninemile Creek. To explicitly consider the higher upwelling velocity in this area in the cap design, Model Area A2 was differentiated from the remainder of Remediation Area A, which was defined as Model Area A1.

In Remediation Area B, the primary factor in delineating model areas was contaminant concentration. However, the calculated upwelling velocities following onshore hydraulic control suggest higher upwelling velocities in the southeastern half of Remediation Area B. Therefore, separate groundwater upwelling distributions were developed for Model Area B1/C1 and B2 such that the higher upwelling velocities in B2 were specifically considered in the cap design for that area.

The influence of the onshore hydraulic containment system was an important consideration in the delineation of model areas within Remediation Area C. The first priority in this area was the concentration and distribution of contaminants; however, the approximate influence of the hydraulic containment system was generally consistent with the delineation based on contaminant distribution. The onshore hydraulic containment system will control upwelling velocities in Model Areas C1 and C3, as shown on Figure 1. In Model Area C2 upwelling velocities will be only minimally affected by the hydraulic containment systems and thus upwelling velocities were based on chloride depth profiles measured in the vicinity of Model Area C2.

Similar to Remediation Area B, Remediation Area D was modeled as four separate areas primarily due to contaminant concentration and distribution. However, groundwater velocities across Remediation Area D generally decrease moving east from the SMU 2 ILWD Area to the Eastern Area. As a result, groundwater distributions were developed for the cap model in each of the four areas of Remediation Area D.

For purposes of cap modeling Remediation Area E was subdivided into three model areas based on contaminant concentrations and distribution. However, a close review of the groundwater data and underlying geology in Remediation Area E shows a consistent silt/clay unit thickness and does not give any reason to expect spatial variability in upwelling velocities in the offshore areas. This is supported by the scatter in the upwelling data, lack of a clear spatial pattern throughout Remediation Area E, and similarity in upwelling statistics among the data from within each of the three modeling areas. Therefore, the chemical isolation layer design modeling does not use different groundwater upwelling rates in the three model areas, and rather bases each on the full upwelling data set from Remediation Area E.

Section 3
Measurements of Upwelling Velocities

Three types of field methods were implemented in an attempt to quantify groundwater discharge rates to the remediation areas in Onondaga Lake; 1) a piezometer-based method to measure hydraulic heads in the sediment pore waters, 2) seepage meters to directly measure groundwater discharge, and 3) measurement of chloride concentration profiles below the sediment-water interface to estimate groundwater flow rates through the sediments. The piezometer-based method consisted of a network of piezometers with recording devices that were installed within the lake sediments in late 2002 and monitored through July 2003 as part of a study known as the Groundwater Upwelling Investigation (Parsons, 2003). The intent of this method was to measure upward hydraulic gradients within the lake sediments and to covert the hydraulic gradients to upwelling velocities using estimates of the vertical hydraulic conductivity of the sediments. Two studies were conducted to evaluate the use of seepage meters, which directly measure groundwater discharge. An initial study was conducted with six meters in 2005 and a second study was conducted with thirteen seepage meters in 2007. Several field methods were also evaluated to measure and/or estimate sediment chloride concentrations; measurement of sediment conductivity using a direct push conductivity probe, Vibracore sampling with centrifugation of sediment samples to obtain sufficient pore water for analysis of chloride, and in-situ peepers. Each of the field methods implemented in an attempt to quantify groundwater discharge rates is described below. The work plan for the data collection activities and quality assurance plans are described in numerous documents prepared by Parsons (2003, 2005a, 2005b, 2006, 2007a, 2007b, 2007c, 2007e, 2007f, 2007g, 2007h, 2007i, 2008a, 2008b, 2008c, 2008d, 2008e, 2008f, 2008g, 2009a, 2009b, 2009c, 2009d, 2009e, and 2009f).

In addition to the quantitative methods implemented in the field, an additional method was used to qualitatively screen the lake bottom for locations with potentially anomalous groundwater discharge rates such as subaqueous springs and seeps. This method consisted of towing a conductivity and temperature sensor near the lake bottom and analyzing the data for anomalous temperature and conductivity readings that might potentially indicate areas of elevated groundwater discharge. Two surveys were conducted: one in 2005 and a second in 2007. This qualitative investigation of groundwater discharge is described below followed by a discussion of the quantitative methods.

Other techniques for estimating groundwater fluxes were considered but rejected as not feasible for use in Onondaga Lake. An excellent review of field techniques for estimating water fluxes between groundwater and surface water has been published by the USGS (Rosenberry and LaBaugh, 2008). A technique frequently used for quantitatively estimating groundwater fluxes is temperature. The seminal paper regarding this issue is Bredehoeft and Papadopulos (1965) “Rates of vertical groundwater movement estimated from earth’s thermal profile.” Temperature techniques for estimating groundwater velocities, as noted by Sayles and Jenkins (1982), work best for upwelling velocities of greater than 50 cm/yr. A recently developed technique for using temperature to quantify groundwater discharge is based on collecting time-series data at various depths below the sediment-water interface and evaluating how the temperature signal is attenuated with depth. A description of this method is contained in Keery and others (2006). An evaluation of this method indicated that the resolution of this method was on the order of 200 cm/yr. Recent advances in fiber-optic temperature sensing have indicated the potential of this technique to accurately define temperatures at the sediment water interface but the technique does not yet lend itself to the quantitative estimation of upwelling velocities (Day-Lewis and others, 2006).

Temperature and Conductivity Survey

Two temperature and conductivity surveys were conducted in the lake to identify areas of groundwater discharge. These surveys were designed to qualitatively identify areas of groundwater discharge, but not to quantify the rate of groundwater discharge. The areas of potential groundwater discharge identified by these methods were then investigated by other methods in an attempt to quantify the discharge rates.

The first survey was conducted on September 7 and 8, 2005 using a Hanna S6T2 temperature and conductivity meter that was towed near the lake bottom from a slowly moving boat. Measurements were conducted in transects along the shoreline east of Ninemile Creek and conducted along the northern portion of the shoreline in Remediation Area E. The measurements along the shoreline east of Ninemile Creek did not identify potential groundwater discharge areas, as neither temperature nor conductivity changed significantly across the survey transects. In Remediation Area E, one potential upwelling location, which was identified by an approximately 1.5°F decrease in temperature and an increase in conductivity, was observed. A seepage meter was located at the observed temperature and conductivity anomaly (meter 60052 as described below).

A second and much more comprehensive temperature and conductivity survey was conducted from April 24 to 26, 2007 in Remediation Areas A and E. For these surveys, a YSI 6600 series multi-parameter sonde was used to measure water temperature, specific conductance, salinity, dissolved oxygen, turbidity, and sensor depth. The sensor was mounted in a custom built steel cage and towed with a 15-ft. jon boat as close to the bottom as possible. As an initial calibration step, the unit was tested on a known brine spring in Onondaga Creek to ensure it would identify a large anomaly in the groundwater discharging through the sediments. This screening step was successful in identifying the location of a large spring in lower Onondaga Creek. The survey was conducted by running transects approximately 25 ft. apart along the shoreline from water depths of about two ft. to six ft. Figures displaying the temperature and conductivity data collected during this survey are contained in Attachment II. For the most part, the temperature and conductivity patterns are consistent and uniform with very few anomalies suggesting potential groundwater seeps. One distinct anomaly of higher conductivity was observed along the shoreline east of the mouth of Ninemile Creek and a seepage meter cluster was located in this area (Seepage Meter Cluster 4-2 as described below). Another conductivity anomaly was observed adjacent to the shoreline east of Harbor Brook and a seepage meter cluster was located in this area (Cluster 7-1 as described below).

Groundwater Upwelling Investigation – 2003

A groundwater upwelling study was conducted in Remediation Area A near the mouth of Ninemile Creek and in Remediation Areas C and D in 2002 and 2003 (Parsons, 2003). The study consisted of vibrating wire piezometers emplaced in pairs at depths of 4.5 and 14.5 ft. below the sediment-water interface at three or four locations along each of six transects oriented approximately perpendicular to the shoreline. The locations of the piezometers are shown on Figure 8. Hydraulic pressures were recorded every twelve hours at these locations from December 27, 2002 through August 1, 2003.

The data from the one transect with three sets of piezometers in Remediation Area A provided relatively consistent estimates of hydraulic heads in the sediments. The piezometer pairs in the transect in Remediation Area A were located 25 ft., 538 ft. and 1,011 ft. from the shoreline. The sediments along this transect are primarily silts with some sands and clays (refer to hydrogeologic cross-section shown on Figure 4; the cross-section trace is shown in Figure 1).

The average upward hydraulic gradient, during the period investigated, calculated as the pressure head difference between the piezometers at a depth of 14.5 ft. and the one at a depth of 4.5 ft., ranged between 0.01 and 0.027 ft. per foot at the three piezometer pairs (Attachment III). The estimated vertical hydraulic conductivity of the sediments based on the lithologic characteristics of the sediments between a depth of 4.5 ft. and 14.5 ft. is approximately 10^{5} cm/sec. Based on this estimate of the hydraulic conductivity, the upwelling velocity along the transect ranges from about 3 to 8 cm/yr, with the range merely reflecting the variability in the estimate of the hydraulic gradient. There is also uncertainty associated with the hydraulic conductivity estimate.

The piezometer-based method was determined not to be a suitable method for estimating groundwater discharge rates to the lake for purposes of cap design. There were two main reasons why it was judged to not be suitable: 1) it is logistically difficult to collect data from a large number of locations, and 2) it is difficult to obtain reliable estimates of pore water pressures from the vibrating wire piezometers for reasons that could not be fully explained. It is hypothesized that the accumulation of biogenically generated gas in the sand packed interval in which the piezometers were placed led to anomalous pressure measurements.

Seepage Meter Investigations

Two seepage meter investigations were conducted during pre-design investigations for the lake. One was conducted with six seepage meters as part of the Phase I Pre-Design Investigations in 2005 and the second was conducted with 13 seepage meters as part of the Phase III Pre-Design Investigations in 2007. The seepage meters used in this study were an adaptation of the type of seepage meter described by Lee (1977).[4] These two seepage meter investigations are described below.

[4] A useful review of seepage meters is contained in Rosenberry (2005) and Roseberry and LaBaugh (2008). The use of seepage meters to investigate groundwater discharge to lakes in central New York is discussed in Schneider and others (2004) and Sebestyen and others (2001).

Seepage Meters – Phase I Investigation

The seepage meters used in the Phase I Investigation were constructed with two-foot diameter PVC housing and an interior acrylic dome. Each meter consisted of two sections: a lower section that was installed into the sediment, and an upper section that housed the dome and a thin-walled Teflon sample bag. The two sections joined at a sealed male-to-female fitting to ensure that there was no leakage. The seepage meters were installed as a two-step process. First, the lower section of the seepage meter was slowly pushed 12 to 18 in. into the lakebed. After a stabilization period of at least 24 hours, the top and bottom sections of the meter were attached with a gasket to create a water-tight seal and bolted together using threaded steel rods. Finally, the four-liter measurement bags were prefilled with 60 ml of water and attached to the seepage meters.

Three seepage meters were installed in Remediation Area A and three were installed in Remediation Area E at the locations shown on Figures 9 and 12. One of the meters installed in Remediation Area A was located adjacent to a piezometer pair installed as part of the upwelling investigation described above. The meters in Remediation Area A were installed between 325 ft. and 820 ft. from shore, and the meters in Remediation Area E were installed between 200 ft. and 430 ft. from shore based on access and water depth constraints. The meters were monitored approximately weekly from September 16 through November 15, 2005.

There was significant variability in the weekly measurements of upwelling velocities at each of the meters, even though the piezometer data indicated that hydraulic gradients were relatively constant during the period of the study. An analysis of the data that were collected indicates that the volume of water collected in the seepage meter bags was influenced by multiple factors in addition to the ambient flux of groundwater through the sediments. Initially following seepage meter installation, gas production from decaying vegetation appears to have significantly influenced the rate of water accumulation, and as a result, data from the early period are not useful for estimating groundwater fluxes through the sediments. Settlement of the seepage meters was also a major factor influencing the rate of water accumulation resulting from high winds and resulting waves impart forces on the meters. A very small amount of settlement results in a relatively large volume of water accumulation in the collection bags relative to the amount of water accumulation from the ambient seepage flux. As a result, the groundwater flux through the sediments could not accurately be estimated directly from the water that accumulated in the seepage meter collection bags. The measured weekly upwelling velocities at the six seepage meters are shown on figures in Attachment IV.

Lake levels were relatively stable and gas production, at five of the six meters, was relatively constant during the period October 27 to November 15, 2005. Therefore, the amount of water that accumulated in the collection bags during this period can be attributed both to settlement (in part caused by wind and wave action) and ambient groundwater flux. Based on data from this period, the median combined settlement-induced flux and groundwater flux at each of the meters, with the exception of 60053 (SM-6) where gas production varied significantly during this period, are the following:

40013 (SM-1) – 19 cm/yr
40014 (SM-2) – 4 cm/yr
40015 (SM-3) – 44 cm/yr
60051 (SM-4) – 9 cm/yr
60052 (SM-5) – 10 cm/yr

These fluxes represent an upper bound estimate of the groundwater flux as it is likely that the settlement induced flux was significant but insufficient reference data were available to determine the exact amount of settlement.

Seepage Meters – Phase III Investigation

The seepage meters used in the Phase I Investigation were redesigned for the Phase III Investigation based on issues identified with the original meters. The meters were redesigned to reduce impacts of waves (e.g., wave breaks, stabilization poles, etc.) and to reduce settlement. In addition, larger volume bags were used for sample collection and control bags were used at each meter to assess outside factors influencing water accumulation in the bags. The control bags were based on the design described in Cable and others (2004). In addition, wave height was monitored to account for any influences caused by wave action, centimeter scale measurements of meter elevations were made to assess settlement, and water levels were monitored in the lake and in on-shore monitoring wells to assess changes in horizontal gradients towards the lake during the investigation. A photograph of a redesigned seepage meter is shown in Attachment IV.

Seepage meters were installed at five locations during the Phase III Investigation: three in Remediation Area A, and two in Remediation Area E. Multiple meters were used at each location to assess the reproducibility of results. At three of the locations, three seepage meters were installed in close proximity to each other. At the other two locations, two meters were installed in close proximity to one another. The seepage meters were located as follows:

- Cluster 4-1 was located near the shoreline approximately 900 ft. east of Ninemile Creek to evaluate a temperature and conductivity anomaly at this location. These meters are labeled 40097, 40098, and 40122 on Figure 9.
- Cluster 4-2 was located about 1,300 ft. east of Ninemile Creek to evaluate a temperature and conductivity anomaly at this location. These meters are labeled 40095 and 40096 on Figure 9.
- Cluster 4-3 was located approximately 1,600 ft. east of Ninemile Creek to evaluate potential groundwater discharge from the distal end of a buried former channel of Ninemile Creek. These meters are labeled 40099, 40100, and 40101 on Figure 9.
- Cluster 7-1 was located approximately 350 ft. east of Harbor Brook to evaluate a conductivity anomaly at this location. These meters are labeled 70067, 70068 and 70069 on Figure 12.
- Cluster 7-2 was located approximately 1,000 ft. east of Harbor Brook. These meters are labeled 70065 and 70066 in Figure 12.

The seepage meters were monitored approximately weekly from June through August, 2007. The measured upwelling velocities at each of the seepage meter clusters are shown on figures in Attachment IV.

The results of the Phase III seepage meter study indicated that seepage meters are not a reliable method for measuring small upwelling velocities in Onondaga Lake. The results indicated that seepage meters do not consistently provide a reliable estimate of the "true" upwelling velocity. This conclusion is based on the following observations:

- The seepage meter data from the near-shore portion of Remediation Area A indicate negligible groundwater discharge whereas other lines of evidence (pore water chloride profiles and groundwater modeling) indicate that quantifiable groundwater discharge is occurring.
- The upwelling velocities at seepage meter pairs and triplicates showed little correlation between/among meters.
- The upwelling velocities calculated from the control bags were of the same order of magnitude as the rates calculated from the meters. In addition, upwelling velocities calculated from the control bags do not correlate temporally among locations.

Overall, the lack of reproducibility between/among meters at the five cluster locations indicated that the seepage meters were not a reliable method for estimating upwelling velocities of the magnitude that occur in Onondaga Lake. Therefore the data collected in the seepage meter investigations were not used for the development of the upwelling estimates for the cap design.

Chloride-Depth Profiles

Effler and others (1990) noted that chloride concentrations in the shallow sediments beneath Onondaga Lake increased nearly linearly with depth. They noted that this indicated a diffusive flux of chloride to the lake from a deep source of chloride. The source of chloride is now understood to be primarily halite brines within the glacial deposits that fill the Onondaga Trough and leachate from seepage from the wastebeds. TAMS (2002) noted that the chloride gradients beneath Onondaga Lake were not truly linear and that the deviation from linearity could be used to estimate the upwelling velocity.

The use of chemical concentration gradients in sediments to investigate upwelling velocities was first reported in the literature in 1982 when two studies were published that quantified upwelling velocities in the Pacific Ocean. One study used calcium and magnesium ion gradients to quantify upwelling velocities in the range of 1 cm/yr to 20 cm/yr near the Galapagos Islands, and the other study in the equatorial East Pacific Ocean quantified upwelling velocities of about 20 cm/yr using calcium ion gradients and the ratio of helium-4 to helium-2 (Maris and Bender, 1982; Sayles and Jenkins, 1982). Additional studies that have described the use of chemical concentration gradients in sediments to estimate upwelling velocities include Berg and Risgaard-Petersen (1998), Maris and others (1984), and Anati (1994). All of these studies have indicated that the use of chemical concentration gradients is a useful method for quantifying upwelling velocities that are less than approximately 50 cm/yr. Groundwater flow rates through lake sediments were also evaluated using tritium and chloride concentration depth profiles in sediments by Cornett and others (1989).

The section below describes the theoretical basis for the use of chemical concentration gradients in sediments to estimate upwelling velocities, the field methods that were investigated for measuring and/or estimating chloride concentrations in pore water, and the method of data evaluation.

Description of Method

At steady state conditions, the governing equation for vertical migration of chloride by advection with groundwater and diffusion is:

$$0 = -v\frac{\partial c}{\partial z} + D\frac{\partial^2 c}{\partial z^2} \qquad \text{for} \quad 0 \le z \le L \tag{1}$$

with the following boundary conditions:

$$c(z,0) = c_o; \quad c(0,t) = c_o; \quad \text{and } c(L,t) = c_L$$

where:
- c = chloride concentration,
- c_o = chloride concentration at upper boundary;
- c_L = chloride concentration at lower boundary;
- L = length of domain;
- v = seepage velocity (Darcy velocity divided by porosity);
- D = sum of diffusion and dispersion coefficients.

An analytical solution to this equation developed by Al-Niami and Rushton (1977) was used to solve Equation 1 and was implemented in a Microsoft Excel spreadsheet to analyze the chloride depth profiles. The upwelling velocity was calculated by solving Equation 1 in an iterative manner until there was a good correspondence between the calculated and the measured chloride depth profile.

In evaluating chloride-depth profiles using Equation 1, it is important to note that the steepest concentration gradients occur near the sediment-water interface. As a result, calculated upwelling velocities are most sensitive to the chloride data collected near the interface. In applying Equation 1 to the evaluation of upwelling velocities for purposes of this report, a preference was given to using only data from the upper 5 ft. of sediment to estimate the upwelling velocity as deviations from linearity, if there were any, were most pronounced in this depth range. All profiles, though, were analyzed using data from the upper 5 ft. as well as data from the entire depth profile, which typically consisted of data to a nominal depth of about 9 ft. below the interface.

Model Parameters

The use of Equation 1 to analyze steady-state concentration profiles requires the definition of the parameter D, which is the sum of the diffusion and dispersive coefficients. The parameter D is defined as:

$$D = \omega D^* + \alpha_L v \tag{2}$$

where D^* is the diffusion coefficient, ω is coefficient related to tortuosity and α_L is dispersion length.

The coefficient related to tortuosity is defined based on Boudreau (1996) as:

$$\omega = n/(1-\ln(n^2)) \tag{3}$$

where n is the porosity.

These parameters are a function of two characteristics of the sediment media, porosity and dispersion length; and a function of the diffusion coefficient of chloride in pore water. For purposes of the analysis of the chloride depth profiles from sediments of Onondaga Lake, the following values for these characteristics were used:

- A porosity value of 0.65 was used for evaluation of chloride depth profiles from Remediation Area C, a value of 0.75 was used for Remediation Area A, and a value of 0.70 was used for Remediation Area E. Sediment porosity was measured at multiple depths at 64 Vibracore locations; the average porosity at these 64 locations is shown on Figure 13. The available porosity data are listed in Attachment V.
- The dispersion length was calculated using equation (26) in Neuman (1990), which was developed to calculate the scale dependence of the dispersion length. This equation is: $\alpha_L = 0.0169L^{1.53}$, where L is length of the flow field in meters (note that equation requires that L be in units of meters). For a flow field length of 5 ft. the calculated dispersion length is about 0.1 ft. The use of this method to estimate the dispersion length and alternative methods for estimating the dispersion length are discussed in detail in Attachment XI.
- The effective diffusion coefficient for chloride was specified as 1.235 cm^2/day based on Felmy and Weare (1991) for a brine at 11° C.

An assumption implicit in the use of Equation 1 to estimate upwelling velocities is that the chloride concentrations in the sediments are at steady state; that is concentrations are not changing with time. A series of evaluations was conducted to determine the time required to reach steady state in shallow sediments after the sediments were disturbed. The calculations indicate that steady state is typically reached within a few decades. These calculations are described in Attachment VIII. In addition, it is assumed that chloride is neither being produced by dissolution nor lost by precipitation or sorption within the sediments. This is a valid assumption in most of the remediation areas but in some locations, particularly in areas with in-lake waste deposits, it appears that this assumption may not be valid. As a result, this method was not used to evaluate upwelling velocities in areas known to contain in-lake waste deposits.

Measurement of Sediment Chloride Concentrations

The initial method used to measure sediment chloride concentrations in sediment pore water was to collect cores using the Vibracore method, section the cores into 1.0 ft. intervals, centrifuge the cores, and then analyze the pore water for chloride and specific conductance. After evaluation of the data from the Phase I Pre-Design Investigation, it was determined that data at closer intervals were required for accurate analysis of the chloride-depth profiles. As a result, in Phase II the cores were sectioned into 0.5-ft. intervals. In Phase III, the upper 2 ft. of core were sectioned into 0.2 ft. intervals, but the pore water centrifuged from these small sections was only sufficient for analysis of chloride and specific conductance. All other pore water samples from Phase III were analyzed for common anions and cations, including chloride, and specific conductance. The cation-anion balance and the correlation between specific conductance and chloride were used to evaluate data quality.

In Phase II, the use of diffusion samplers (peepers) also was investigated for obtaining estimates of chloride concentrations in pore water. Fourteen extended peepers were installed at the five seepage meter clusters to approximate depths of 8 to 9 ft. The stainless steel peepers consist of a series of cells spaced at 0.5 ft. intervals that are filled with deionized water and covered with a membrane. Ions in the sediment pore water diffuse across the membrane and the peeper is kept in place ideally until equilibrium is reached between the cell and the pore water. The peepers in the Phase II investigation were left in place for approximately one week prior to retrieval. Pore water samples were collected from locations adjacent to each of the peepers and the concentrations measured in the pore water by centrifugation were compared to those determined from the peepers. In almost all cases, the measured chloride concentrations in the pore water were higher than the chloride concentrations in the peepers. This is consistent with the results of the laboratory study conducted by Jackson and Anderson (2007) that indicated that chloride equilibrium requires much longer deployment time than one week. Diffusion samplers were also installed in each of the five seepage meters cluster in the Phase III investigations. These samplers were left in place for approximately three to five weeks and in general the chloride concentrations determined from these diffusion samplers were also lower than those measured in centrifuged pore water. The chloride depth profiles determined from the diffusion samplers in Phase III are shown along with the chloride depth profile from a nearby vibracore location in Attachment XII.

Because it is labor intensive to collect and centrifuge core samples for pore water analyses and to use extended peepers, alternative techniques were investigated for rapidly estimating sediment pore water chloride concentrations. The most promising technique identified was the measurement of sediment conductivity with a probe advanced into the sediment and subsequent conversion of conductivity to equivalent chloride concentrations. The main technical weakness of this technique is that sediment conductivity is not the same as pore water conductivity as a conductivity probe in contact with sediment measures a response that is both a function of the sediment matrix and the characteristics of the pore water. In these investigations it was determined that there was a relatively good correlation between sediment conductivity and pore water conductivity. The relationship between sediment conductivity and pore water conductivity, though, is a function of sediment characteristics and at locations where sediment characteristics were variable, conductivity depth profiles were also variable as the result of changing sediment characteristics.

A Geoprobe SC4000 soil conductivity probe was used for measuring sediment conductivity. The probe uses a four-pole Wenner-type array; current is passed through the outer contacts of this array and voltage is measured on the inner two contacts. Conductivity and temperature measurements were made at 0.05 ft. intervals as the probe was advanced. Most probes were advanced to a depth of approximately 10 ft.

The conductivity data were converted to equivalent chloride concentrations using a conversion factor. A conversion factor of 0.89 was used to convert from conductivity in uS/cm^2 to mg/L chloride in Remediation Areas A, B and C and a factor of 0.80 was used in Remediation Areas D and E. These factors were developed from comparisons of pore water chloride and sediment conductivity data collected in close proximity to each other. The calculated upwelling velocities are not sensitive to the conversion factor as the conversion factor merely scales the chloride depth profile and does not affect the convexity of the profile. Attachment VI contains plots of chloride concentrations and conductivity versus depth for 31 locations where both pore water and sediment conductivity data were collected. In general, the shapes of the depth profiles are similar for both the pore water data and the sediment conductivity data.

There are inherent strengths and weaknesses with both methods used to construct chloride depth profiles. The chloride-depth profiles constructed from chemical analyses of pore water provide a more accurate estimate of actual changes in chemical concentrations with depth because the parameter of interest, chloride, is measured directly. The main weakness with the chloride-depth profiles developed from pore water is related to the fact that the measured concentrations represent an average concentration over the section of core analyzed. As a result, it is not possible to accurately define the chloride-depth profile very near the sediment-water interface where the chloride concentrations change rapidly with depth. The sediment-conductivity data collected with the Geoprobe conductivity probe, on the other hand, are an approximate analog for chloride concentrations in pore water, but because the probe does not measure pore water properties alone; variations in conductivity measurements with depth are also related to changes in the physical/chemical properties of the sediment. This method, though, allows variations in conductivity near the sediment water interface to be determined very precisely. Recognizing the strengths and limitations of the two methods leads to the conclusion that both methods can be used to provide reliable estimates of upwelling velocity.

Field Investigations

Chloride-depth profiles were constructed and used to calculate upwelling velocities at 356 locations within and in the vicinity of the Remediation Areas[5]. At 156 locations chloride-depth profiles were developed from analyses of pore water collected from cores during the Phase II, Phase III, Phase V and Phase VI Investigations, and at 245 locations chloride-depth

[5] Upwelling velocities were estimated from the analysis of 474 chloride-depth profiles collected at 356 locations; 167 profiles developed from pore water data and 307 profiles developed from sediment conductivity data. Data from 25 chloride-depth profiles were not analyzable.

profiles were developed from sediment conductivity data collected in the Phase III and Phase IV Investigation in 2007 and 2008[6]. Pore water data from 72 locations sampled as part of the Lake RI and 10 locations as part of the Phase I Pre-Design Investigation were not used for estimating upwelling velocities because of a limited number of depth-discrete samples collected at each location. In addition, sediment conductivity data collected as part of the DNAPL Investigation (Parsons, 2006) near the Causeway and in Phase II were not used for estimating upwelling velocities because of a lack of standardization in collection of the data. The table on the following page lists all of the investigations in which pore water and sediment conductivity data were collected, the number of locations at which data were collected, and comments regarding data collection.

Sediment conductivity data and pore water data could not be collected in some areas because of the presence of a Solvay crust and/or obstructions in the water. In Remediation Area D, the crust in the in-lake waste deposits prevented the collection of sediment conductivity and pore water data.

Initial Data Evaluations

The following steps were completed initially to evaluate the data that were collected:

1. Anion-cation balances were calculated for the pore water analyses; the balances are listed in Attachment V. In a number of instances, the error in the anion-cation balance was greater than twenty percent. Based on an evaluation of chloride concentrations and specific conductance, it was determined that the error was generally attributable to an under-reporting of cation concentrations. Plots were completed of conductivity versus chloride for data from each Vibracore location with applicable data, to identify chloride data that were outliers. These plots are contained in Attachment V.

2. Plots of conductivity versus depth and chloride versus depth were developed for each location with co-located Geoprobe and Vibracore data, and a relationship was developed between the conductivity values from the Geoprobe and the chloride concentrations from pore water collected from the cores. These plots are contained in Attachment VI for 31 locations with Geoprobe and Vibracore data. A linear factor relating the chloride concentration to conductivity was calculated using the Solver routine in Excel in which the sum of the squared differences between calculated chloride concentrations and observed chloride concentrations were minimized. The calculated factors for each of the thirty-one locations are listed in Attachment VI.

[6] At 31 locations chloride-depth profiles were developed from both pore water data and sediment conductivity data.

Pore-Water and Sediment Conductivity Data

Type	Study Phase	Date	Locations	Comments
Pore Water	RI	1992	72	Borings were advanced throughout the lake to a nominal depth of 3 ft. and generally three to five subsamples from each boring analyzed for chloride. These data were not used to calculate upwelling velocities because of limited depth-discrete data.
	Phase 1 PDI	2005	10	Sediment samples collected at nominal depths of 1, 3, and 5 ft. and pore water collected by centrifuging the samples. These data were not used to calculate upwelling velocities because of limited depth-discrete data.
	Phase II PDI	2006	13	Sediment samples collected at 1 ft. depth intervals to 10 ft. and pore water collected by centrifuging the samples.
	Phase III PDI	2007	21	Sediment samples collected at 1 ft. depth intervals to 10 ft. and pore water collected by centrifuging the samples. Collocated with seepage meters and Geoprobes.
	Phase III PDI Addendum 5	Dec 2007	30	Pore water collected by centrifuging sediments from approximate intervals of 0.0-0.3 ft., 0.3-0.5 ft., 0.5-0.8 ft., 0.8-1.0 ft., 1.0-1.3 ft., 1.3-1.5 ft., 1.5-1.8 ft., 2-2.5 ft., 3-3.5 ft., 4-4.5 ft., 5-5.5 ft., 6-6.5 ft., 7-7.5 ft., 8-8.5 ft., and 9-9.5 ft.
	Phase V	2009	23	Pore water collected by centrifuging sediments from intervals of 0-0.25 ft., 0.25-0.5 ft., 0.5-0.75 ft., 0.75-1.0 ft., 1.0-1.25 ft., 1.25-1.50 ft., 1.50-1.75 ft., 2.0-2.5 ft., 3.0-3.5 ft., 4.0-4.5 ft., 5.0-5.5 ft., 6.0-6.5 ft., 7.5-8.0 ft. and 9.0-9.50 ft..
	Phase VI	2010	69	Pore water collected by centrifuging sediment from same intervals as in Phase V.
Sediment Conductivity	DNAPL Investigation	2006	20	Advanced along the causeway in SMU 2 to a nominal depth of 45 ft. using a Geoprobe fitted with a MIPs and conductivity detector. These data were not used to estimate upwelling velocities.
	Phase II PDI	2006	68	Advanced using Geoprobe method to nominal depth of 10 ft. These data were not used to estimate upwelling velocities.
	Phase III PDI	2007	39	Advanced using Geoprobe method to nominal depth of 10 ft. in proximity to five seepage meters in SMU 4 and SMU 7.
	Phase III PDI Addendum 5	2007	82	Advanced using Geoprobe method to nominal depth of 10 ft.
	Phase IV PDI	2008	124	Advanced using Geoprobe method to nominal depth of 10 ft.

3. Plots of porosity versus depth were prepared for each of the Vibracore locations. These plots are contained in Attachment V. The porosity was determined in the laboratory according to method ATSM D-2216 from samples collected with Vibracore. An average porosity was calculated for each location and the average porosity values at each of the Vibracore locations are shown on Figure 13.
4. Plots of sodium and sodium-calcium ratio versus depth were prepared for each of the Vibracore locations. These plots are contained in Attachment V.

Section 4
Upwelling Velocities Calculated from Chloride-Depth Profiles

The chloride-depth profiles developed from pore water data and sediment conductivity data collected in the littoral zone in, and in the vicinity of, the remediation areas were analyzed using the procedures described in the previous section. Plots of the chloride-depth profiles are contained in Attachment VII. In total, as a result of duplicate and triplicate data collected at some locations, 474 chloride-depth profiles were developed for 356 locations. The analysis consisted of iteratively solving Equation 1, described in Section 3, using various values of the upwelling velocity until a "best fit" between the calculated and the measured chloride depth profile was obtained. The "best fit" was, in the ideal case, defined as a solution in which the sum of the squared differences between the measured and calculated chloride values was minimized. An example of the iterative process is illustrated below for the analysis of the pore water chloride data from location OL-VC-60154. An initial estimate of the upwelling velocity is 0.0 cm/yr, which produces a sum of the squared differences between the calculated and measured values (squared error) of 5220. A second estimate of the upwelling velocity of 2.0 cm/yr[7] produces a squared error of 2871, a third estimate of the upwelling velocity of 1.0 cm/yr produces a squared error of 184 cm/yr, and finally after many more iterations a final solution of 1.1 cm/yr is calculated with a squared error of 172.

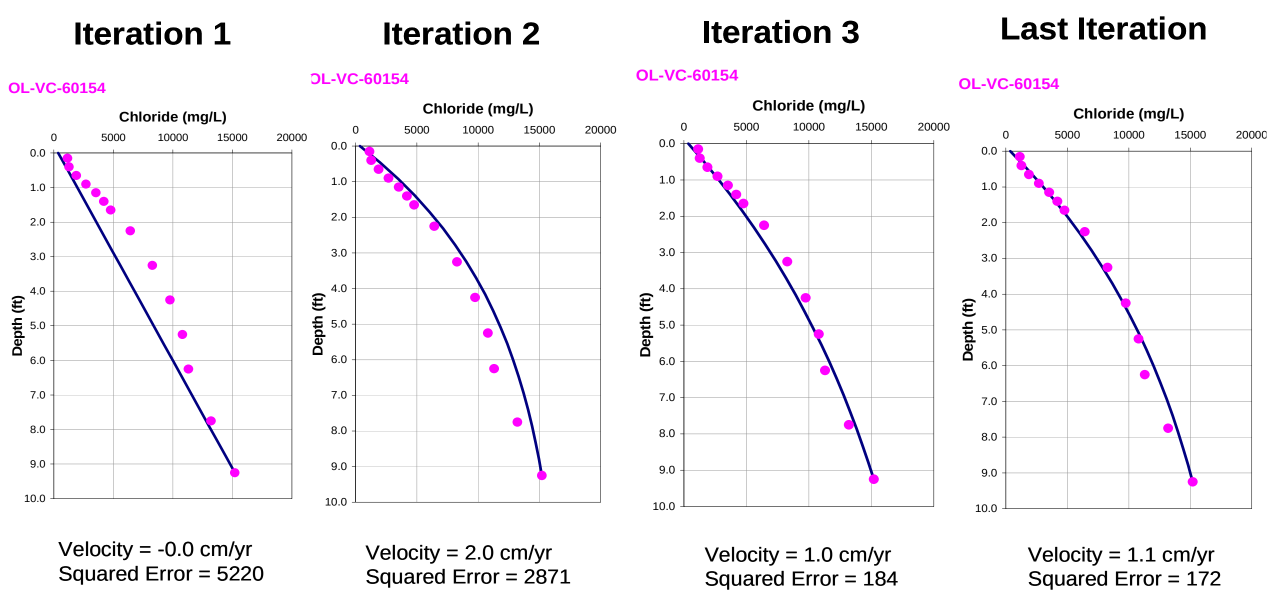

[7] In this text a positive upwelling velocity indicates groundwater flow towards the sediment-water interface. This direction is opposite the standard groundwater convention in which a "positive" velocity indicates downward flow. In Attachment VII, the standard groundwater convention was used; thus for location OL-VC-60154 the "best fit" velocity is listed as "-1.0" rather than "1.0" as described above.

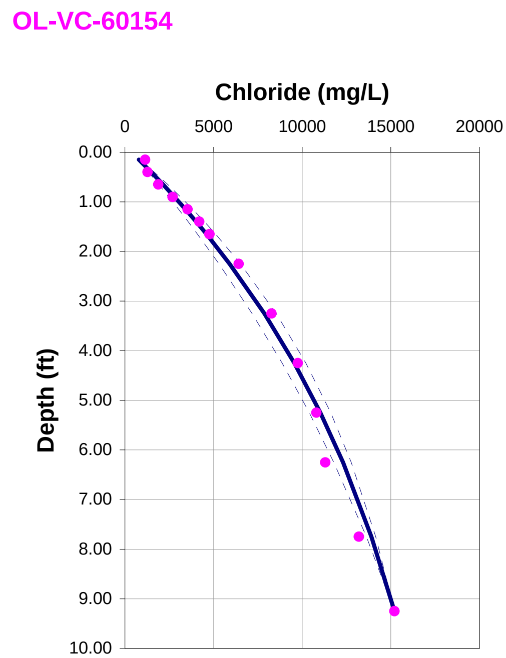

The iterative solutions were calculated with the assistance of the Solver routine in Excel,[8] which is designed to find the solution that minimizes the squared error. In this example, relatively small changes in the upwelling velocity produce large changes in the squared error; for example changing the velocity from 2 cm/yr to 1 cm/yr reduces the squared error from 2871 to 184. This sensitivity of the squared error to the velocity in this example indicates that the upwelling velocity can be accurately quantified from the measured data[9]. The upwelling velocities that were calculated for each of the chloride-depth profiles are shown on Figures 14 through 16 for Remediation Areas A, C, and E, respectively. On these figures, the values from the "best fit" solutions to Equation 1 for each of the chloride-depth profiles that were analyzed are shown on the plots in Attachment VII along with the parameter values used in solving Equation 1.

An example plot for pore water data from OL-VC-60154 is shown to the right. The solid line indicates the "best fit" solution with a velocity of 1.1 cm/yr, and the dashed lines indicate solutions for velocities of 1.1 ± 30% cm/yr. A rigorous quantitative evaluation of the uncertainty associated with the "best fit" solution is described in Section 6.

In analyzing the chloride-depth profiles, a "best fit" solution was calculated based on an analysis of data from the sediments within 5 ft. of the sediment-water interface and a "best fit" solution was calculated based on data from within the upper 10 ft. of the sediment-water interface. "Best fit" solutions were calculated using the two data sets to check the consistency of the calculated upwelling velocity and these results are shown on the plots in Attachment VII. In most cases, similar upwelling velocities were calculated using data from the upper 5 ft. and data from the upper 10 ft. In general for purposes of evaluating the spatial distribution of upwelling velocities, the higher of the two estimates was used and this value is posted on Figures 14 through 16[10].

---

[8] Microsoft Office Excel 2003 was used for these analyses.

[9] This example oversimplifies the analysis of the data from OL-VC-60154 since in determining the "best fit" solution both the velocity and the concentration at the lower boundary were adjusted in the iteration process.

[10] An exception was when the data from the upper five ft did not correspond to the "best-fit" depth profile as well as data from the upper 10 ft. (or vice versa); in these cases, the "best-fit" solution that better fits the data is the value listed on Table 1 and posted on Figures 14 through 16, and a comment is included in Table 1 and Table VII-1.

At some locations, the measured chloride-depth profile did not exhibit a smooth change in chloride concentrations with depth. As a result, the correspondence between the "best-fit" solution to Equation 1 and the measured data is poor. An example of a chloride-depth profile where the "best-fit" solution poorly matches the observed data is at location OL-GP-40182 where the chloride-depth profile was developed from sediment-conductivity data; the data from this location is shown on the figure to the right. A "best-fit" solution to the entire data set and a "best-fit" solution to the data near the sediment-water interface for this location are also shown on that figure. The upwelling velocity corresponding to the "best-fit" solution to the data near the interface is about 11 cm/yr and the velocity corresponding to the "best-fit" solution to the entire data set is about 2 cm/yr.

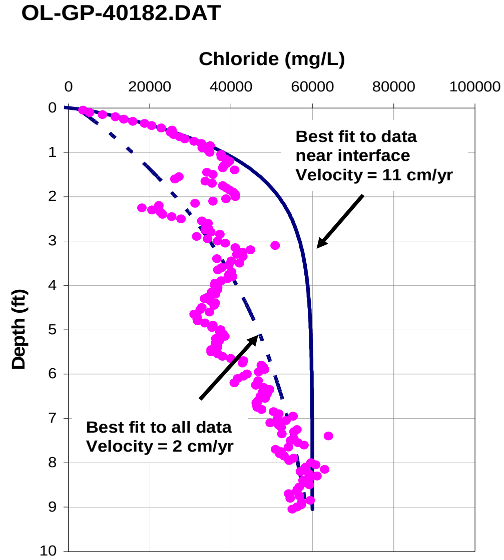

The calculated chloride-depth profiles of the "best-fit" solutions increase monotonically with depth whereas the data from OL-GP-40182 display significant scatter between a depth of about 1 ft. and 5 ft. below the sediment-water interface that is inconsistent with the calculated "best-fit" profiles. The deviation between the form of the measured data and the underlying model could be caused by a number of factors, but insufficient information is available to identify the main factors. It is suspected that a major factor is a poor correspondence between the sediment conductivity reading and the conductivity of the pore water due to variations in lithology with depth and variations in the contact between the probe and the sediment with depth. The sediment-conductivity data from near the sediment-water interface are judged to be more representative of actual conditions because the data provide a smooth chloride-depth profile that is consistent with the analytical model at this sampling location. Therefore, the "best-fit" solution to the data near the sediment-water interface provides a better estimate of actual upwelling velocity than the "best-fit" solution to the entire data set from the upper 9 ft. of sediment.

Table VII-1 includes notes indicating the quality of the upwelling analysis, which is a qualitative assessment of how well the measured data matched the chloride-depth profiles calculated using Equation 1. The quality of the upwelling analysis for about 65 percent of the chloride-depth profiles based on pore water data and for about 54 percent of the chloride-depth profiles based on sediment-conductivity data are judged to be "good." For these chloride-depth profiles the chloride concentrations generally increase monotonically with depth with little scatter and there is a good correspondence between the observed and calculated chloride-depth profiles. For these analyses, there is a high degree of confidence in the calculated upwelling velocities. On the other hand, the quality of the upwelling analysis for about 8 percent of the chloride-depth profiles based on pore water data and about 14 percent of the chloride-depth profiles based on sediment conductivity data are described as "poor." In general, these analyses are judged to be "poor" because the observed chloride concentrations do not increase monotonically with depth as illustrated above for location OL-GP-40182. For these analyses there is significant uncertainty associated with the calculated upwelling velocity. A few of the chloride-depth profiles were not analyzable either because of sparse or sporadic data; a total of seven of the chloride-depth profiles developed from pore-water data and 18 of the profiles developed from sediment-conductivity data were not analyzable.

At locations where the analysis of the chloride-depth profiles were judged to be poor and that are located within remediation areas that will be unaffected by operation of the hydraulic containment systems, additional borings were advanced in the Phase VI Pre-Design investigation to collect pore-water data with Vibracores to better determine the upwelling velocities. An example of such a location is OL-GP-40182, which is located at the mouth of Ninemile Creek and was discussed above. Plots of the chloride-depth profiles developed from sediment conductivity data from this location and plots of the chloride-depth profiles developed from pore-water data from a Phase VI Vibracore located near (OL-VC-40302) are shown below.

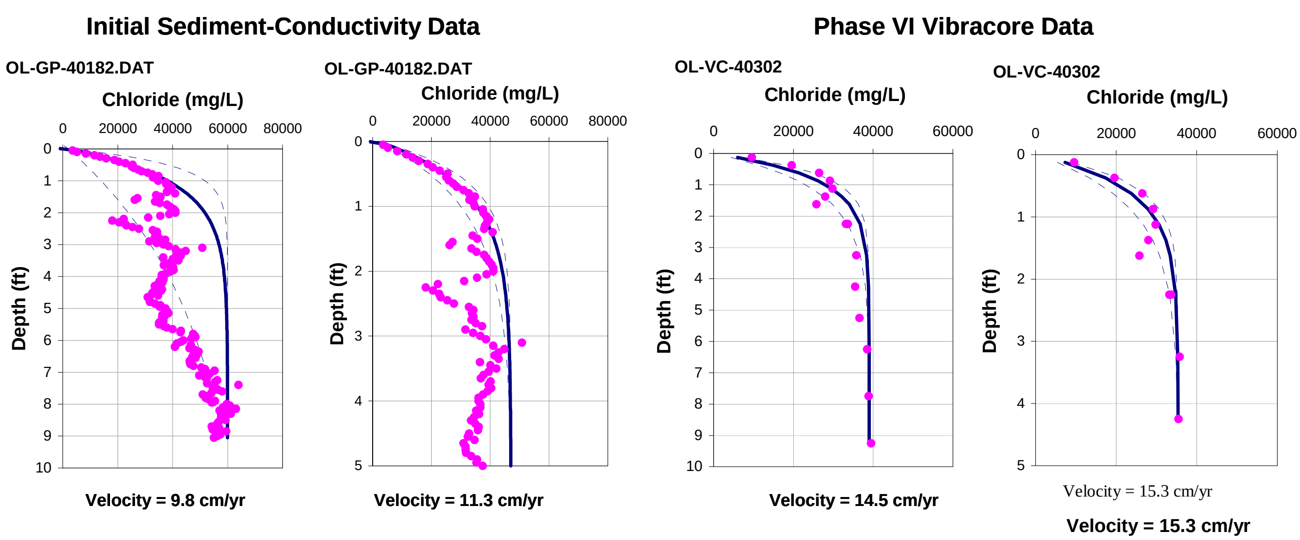

The analysis of the chloride-depth profiles developed from sediment-conductivity data from the upper 10 ft. and the upper 5 ft. from OL-GP-40182 resulted in estimated upwelling velocities of 9.8 cm/yr and 11.3 cm/yr, respectively[11]. These analyses, though, are based solely on fitting the data from the upper 1.25 ft. as the data from greater depths have significant scatter and do not correspond with the calculated chloride-depth profile. The analysis of the chloride-depth profiles developed from pore-water data from the upper 10 ft. and the upper 5 ft. from the Phase VI data collected at OL-VC-40302 resulted in estimated upwelling velocities of 14.5 cm/yr and 15.3 cm/yr, respectively. These data, with the exception of one data point from about 1.5 ft., fit the calculated chloride-depth profiles quite well. As a result, the upwelling velocity calculated from the Phase VI pore-water data is judged to be a better estimate of the actual upwelling velocity at this location.

[11] The NYSDEC has indicated that their analyses of these data produce an upwelling velocity as high as 21 cm/yr (NYSDEC, April 25, 2010).

At some locations, the calculated upwelling velocity based on the "best-fit" solution exceeded a seepage velocity (as defined in Equation 1) of 50 cm/yr, which was judged to be the upper bound velocity that could be estimated by this method. For these locations, Table VII-1 notes that the velocity is greater than the Darcy velocity that corresponds to a seepage velocity of 50 cm/yr[12]. None of the locations where the seepage velocity was estimated to be greater than 50 cm/yr are located within proposed capping areas. The hydraulic containment system proposed to the east of the mouth Ninemile Creek was designed specifically to reduce groundwater upwelling velocities in that portion of Remediation Area A where seepage velocities estimated from the chloride-depth profile method exceeded 50 cm/yr.

[12] The upwelling velocities listed on Table 1 are Darcy velocities. The Darcy velocity by definition is equal to the seepage velocity multiplied by the porosity. Since the porosity is always less than one, the Darcy velocity is always less than the seepage velocity.

Section 5
Upwelling Velocities for Cap Design in Areas without Hydraulic Containment

Groundwater upwelling velocities in Remediation Area E and in Model Areas A1, A2 and C2 are expected to be only minimally affected by operation of the hydraulic containment systems and thus upwelling velocities with the cap are expected to be similar to current upwelling velocities[13]. For each of these areas, a cumulative frequency distribution of upwelling velocities was developed based on the chloride-depth profiles within the areas for use in cap design. In calculating the frequency distributions the following data treatment criteria were used to obtain a data set in which point estimates of upwelling velocities were relatively uniformly distributed within the areas:

1. At locations with upwelling velocity estimates from both pore-water and sediment-conductivity data, the velocity calculated from the pore-water data was selected.
2. At locations with duplicate or triplicate sets of pore-water data or sediment-conductivity data, the highest calculated upwelling velocity from the replicates was selected.
3. When upwelling velocities were calculated from both chloride-depth profiles from the upper 5 ft. and chloride-depth profiles from the upper 10 ft., the higher calculated upwelling velocity was selected unless one of the analyses were judged to be poor.
4. At locations where the 90 percent upper confidence interval on the calculated upwelling velocity was greater than 50 percent of the best-fit value, the value corresponding to the 90 percent upper confidence interval was selected.
5. In Model Area A1, the upwelling velocity in the near shore area that will be affected by the hydraulic containment system was specified as 1.4 cm/yr, which corresponds to the upwelling velocity through the silt and clay unit (refer to Section 8).
6. In Remediation Area E, the upwelling velocity in the near shore area that will be affected by the Harbor Brook containment system was not considered in developing the cumulative frequency distribution of upwelling velocities in Remediation Area E because the area affected by the containment system is only a very portion of Remediation Area E.

[13] Exceptions are 1) in that portion of Model Area A1 that is located in proximity to the proposed hydraulic containment system located east of the mouth of Ninemile Creek, and 2) in that portion of Remediation Area E located in proximity to the eastern end of the Harbor Brook hydraulic containment system.

7. In Model Area C2[14] only upwelling estimates from pore-water data were selected as chloride-profiles constructed with sediment-conductivity data were "noisy" and apparently affected by presence of Solvay materials in the sediment.

8. In Remediation Area E there are two small areas with radii of about 25 ft. where many sets of chloride-depth profiles were obtained and for which an upwelling velocity was calculated for each set. A single upwelling velocity was selected to represent the upwelling velocity in each of these areas; this value was specified as the average of the estimates from pore-water data.

These data treatment criteria for developing cumulative frequency distributions of upwelling velocities are biased towards overestimating the actual upwelling velocity, as the higher of the estimates was selected at several decision points.

Results

The upwelling velocities used to calculate the cumulative frequency distributions are listed on Table 1 and the selected data are shown in map view on Figures 14 to 16[15]. On these figures, the values used to develop the cumulative frequency distribution are shown in bold typeface, the values not used are shown in light-grey typeface. Selected statistics of the cumulative frequency distribution for each of the areas, and the number of upwelling velocities used to construct the distribution, are listed below.

	Model Area A1	**Model Area A2**	**Model Area C2**	**Remediation Area E**
count	54	29	12	126
median	1.00	3.22	1.66	1.10
mean	1.33	4.08	2.71	1.49
standard deviation	1.97	2.96	2.62	1.80

The mean calculated upwelling velocity in Model Area A1 is 1.33 cm/yr with a standard deviation of 1.97 cm/yr, the mean upwelling velocity in Model Area A2 is 4.08 cm/yr with a standard deviation of 2.96 cm/yr, the mean upwelling velocity is Model Area C2 is 2.71 cm/yr with a standard deviation of 1.04 cm/yr, and the mean upwelling velocity in Remediation Area E is 1.49 cm/yr with a standard deviation of 1.80 cm/yr. The highest upwelling velocities occur in Model Area A2 and are associated with recent deposits from Ninemile Creek.

Probability plots of the upwelling distributions are shown in graphic form below with the upwelling velocity plotted on a logarithmic scale on the x-axis and the frequency percentile plotted on a probability scale on the y-axis.

---

[14] The upwelling velocity frequency distribution for Model Area C2 is based on upwelling velocity estimates from the area offshore of the Department of Transportation turnaround that will be unaffected or only partially affected by hydraulic containment systems as shown on Figure 15.

[15] The values shown on Figures 14 to 16 represent the values listed on Table 1 in the column labeled “Upwelling Velocity” and not the values adjusted for the confidence interval where appropriate.

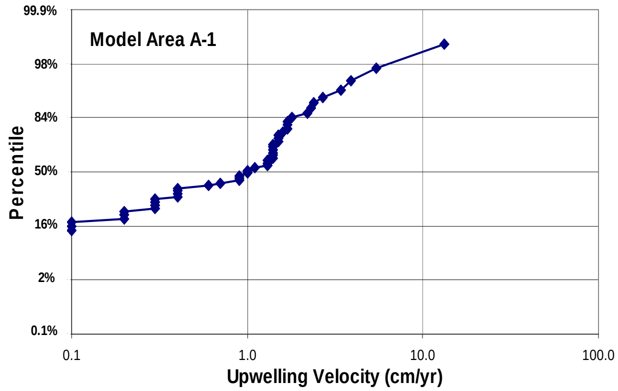
Model Area A-1
Percentile
99.9%
98%
84%
50%
16%
2%
0.1%
0.1
1.0
10.0
100.0
Upwelling Velocity (cm/yr)

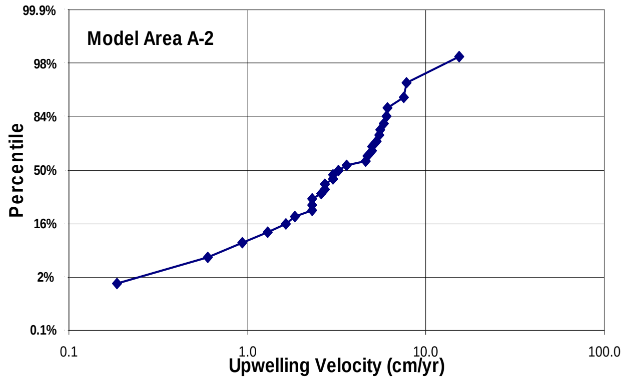
Model Area A-2
Percentile
99.9%
98%
84%
50%
16%
2%
0.1%
0.1
1.0
10.0
100.0
Upwelling Velocity (cm/yr)

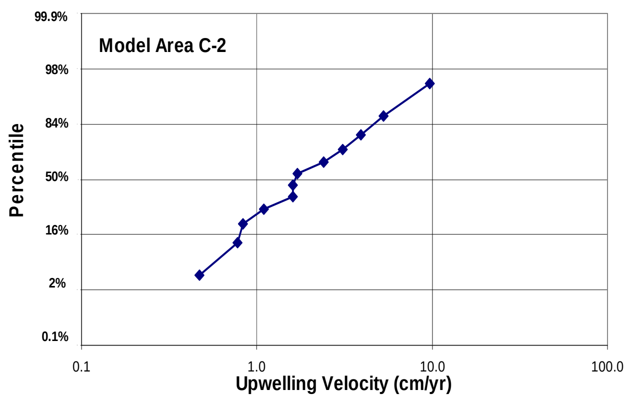
Model Area C-2
Percentile
99.9%
98%
84%
50%
16%
2%
0.1%
0.1
1.0
10.0
100.0
Upwelling Velocity (cm/yr)

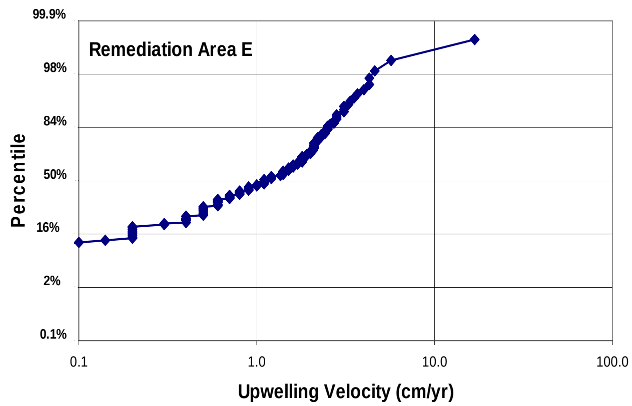
Remediation Area E
Percentile
99.9%
98%
84%
50%
16%
2%
0.1%
0.1
1.0
10.0
100.0
Upwelling Velocity (cm/yr)

Section 6
Evaluation of Uncertainty in Calculated Upwelling Velocities

This section evaluates the uncertainties associated with upwelling velocities calculated with the chloride-depth profile method. In evaluating the chloride-depth profiles, the best estimates of aquifer and chemical parameters have been utilized in the analyses. This section briefly discusses the uncertainty associated with the input parameters, the uncertainty associated with reproducibility of results from co-located borings, and the uncertainty associated with the use of a “best fit” solution to Equation 1 to estimate the upwelling velocity.

Sensitivity to Model Parameters

The sensitivity of calculated upwelling velocities to dispersion length, porosity and chloride factor was evaluated. Sensitivity analyses were conducted using the data from a subset of sample locations (specifically Geoprobe location GP-40168 and Vibracore locations VC-30179, VC-40091, VC-40092, VC-40297, VC-40302, VC-60303, and VC-70058) having estimated upwelling velocities that ranged from 3.3 to 15.3 cm/yr. The sensitivity analyses consisted of the following four evaluations:

1. Increasing the dispersion length from 0.1 ft. to 0.8 ft
2. Decreasing the porosity to the lowest porosity value measured in the vicinity of the location
3. Increasing the factor that converts conductivity to chloride from 0.8 to 1.0 (only for sediment conductivity data)
4. Decreasing the factor that converts conductivity to chloride from 0.8 to 0.64 (only for sediment conductivity data)

The results of these sensitivity evaluations indicate the calculated upwelling velocities are sensitive to porosity and dispersion length, but not very sensitive to the chloride adjustment factor. The porosity and dispersion lengths used in the analyses of upwelling velocities described in Attachment VII and shown on Figures 14 to 16 are the best-estimates of the parameter values. The results of the sensitivity evaluations for porosity and dispersion length that were conducted for the chloride-depth profiles from the selected sample locations are contained in Attachment XI.

Reproducibility of Results

The reproducibility of calculated upwelling velocities was evaluated by comparing the upwelling velocities calculated from sediment conductivity data with those calculated from the Vibracore data at each of the thirty locations with both types of data and by comparing calculated upwelling velocities from multiple sediment-conductivity borings advanced close to one another. Overall the calculated velocities from co-located Vibracore and sediment-conductivity borings compare well. The results of these evaluations are listed on Table 2 and plots of these data are contained in Attachment IX.

At 47 locations, multiple sets of sediment conductivity data were collected. The upwelling velocities at locations with multiple sets of conductivity data are listed on Table 3. At most locations, the upwelling velocities calculated from each set of data are similar.

The reproducibility of calculated upwelling velocity was also assessed by comparing sediment conductivity data taken in different seasons at the same location. Chloride profiles based on sediment conductivity were obtained during spring and fall seasons at several locations (OL-GP-40183, OL-GP-40184, OL-GP-40185, OL-GP-40186, and OL-GP-70107). The upwelling velocities determined in different seasons for these locations are comparable, except in cases where the data are difficult to analyze due to exceeding the maximum measurement capability of the probe (OL-GP-70107). Distinct seasonal trends could not be reliably identified. At four locations, profiles were obtained during the summer months in both 2007 and 2008 (OL-GP-40074, OL-GP-40010, OL-GP-70053, and OL-GP-70054). The upwelling velocity determinations were comparable, except in cases where the data were difficult to analyze due to the measured values exceeding the maximum measurement capability of the probe.

Model Fit

The uncertainty of the upwelling velocities calculated with a "best fit" solution to Equation 1 was evaluated by calculation of a confidence interval (CI) for the calculated velocity. This uncertainty is primarily related to scatter in the chloride or conductivity depth profile data. The confidence interval is calculated as:

$$b \pm f \cdot s_b \tag{4}$$

where b is the calibrated parameter value, f is the confidence interval factor (for a 90% CI, f=1.645), and s_b is the standard deviation of the estimated parameter value. The standard deviation of a parameter value is a function of the perturbation sensitivities and the observation variances (Aster et al. 2005, Doherty, 2008):

$$s_b^2 = \sigma^2 \left(\underline{X}^T \underline{X} \right)^{-1} \tag{5}$$

where $\underline{X}$ is a matrix of the sensitivities of observations to parameters (calculated using forward difference perturbations) and σ^2 is an *m*-vector containing the observation variance calculated according to (Doherty, 2008):

$$\sigma^2 = \frac{\Phi}{m-n} \tag{6}$$

where Φ is the residual sum of squares, *m* is the number of observations, and *n* is the number of parameters.

Because there is only one parameter, the sensitivity matrix $\underline{X}$ has *m* rows and only one column, making it a vector. As such, calculation of $\underline{X}^T\underline{X}$ is simply:

$$\sum_{i=1}^{m} x_i^2 \tag{7}$$

where x_i is the *i*th row in the sensitivity vector.

The calculated confidence intervals for each of the upwelling velocities are listed on Table 1. At most locations, the confidence interval is relatively small compared to the magnitude of the estimated upwelling velocity.

This formal analysis of uncertainty is based on the assumption that the boundary conditions for Equation 1 are fixed. In practice though, there is some uncertainty relative to the lower boundary condition. For the analyses that were judged to be "good" as listed on Table 1, the uncertainty related to the lower boundary condition is small, but for analyses judged as "fair" or "poor," there may be additional uncertainty related to the magnitude of the lower boundary condition.

Another measure of model fit is the correspondence between the upwelling velocities calculated based on "best-fit" solution to the upper 5 ft. of data and the upwelling velocities based on "best-fit" solution to the upper 10 ft. of data. For locations where the upwelling results from the two sets of analyses are similar, this is an indication that the uncertainty associated with the upwelling estimate is low; whereas, when the two estimates differ significantly it indicates uncertainty regarding the estimated upwelling velocity. The upwelling velocities estimated from the upper 5 ft. of data and the upper 10 ft. of data are listed in Attachment VII.

Summary

The evaluations of the uncertainties in the upwelling velocities quantified with the chloride-depth profile method have indicated a high degree of confidence in the calculated upwelling velocities, but as with all evaluations based on field data, there is some uncertainty associated with individual evaluations of upwelling velocities. The spatial consistency of results, as shown on Figures 14, 15 and 16, increased the confidence associated with estimates at individual locations.

Section 7
Analysis of Upward Groundwater Flow through Silt and Clay Unit

Groundwater discharge in remediation areas offshore from the hydraulic containment systems will be less than current rates following construction and operation of the systems. In areas offshore of the hydraulic containment systems, groundwater discharge will potentially come from two sources; recharge in the area between the lake shore and the hydraulic barrier and upward groundwater flow through the silt and clay layer. The engineered design for the restoration of wetlands outboard of the barrier wall will prevent, to the extent practicable, groundwater recharge along the transitional slope from the wall to the wetlands by placing a low permeability material in this area. The locations of proposed outboard wetlands are shown on Figure 1. As a result, the only significant potential source of groundwater discharge is upward migration of groundwater through the silt and clay layer.

Groundwater levels, and hydraulic heads, in the permeable units below the silt and clay unit in Remediation Areas A, B, C and D are higher than the average water level in Onondaga Lake. This creates the potential for upward groundwater flow from the deeper units to the lake. Some of the monitoring wells completed in the sand and gravel unit along the shoreline flow at the surface, which illustrates realization of this potential. The water levels in the sand and gravel in onshore wells in the vicinity of the remediation areas are shown on the figure below (elevations are in feet AMSL)[16]. Water levels in the wells in the vicinity of the lakeshore range from 364 to 372 ft. AMSL. The average lake level is about 362.95 ft. AMSL; therefore, the water level differences between the sand and gravel zone and the lake range from about 1 ft. to 9 ft., with the smallest differences occurring at the sample location in the southeast corner of the lake near the mouth of Harbor Brook.

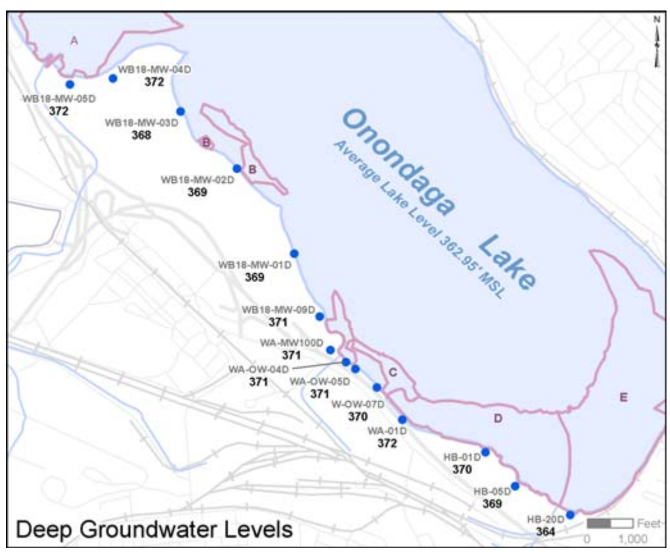

The potential for upward flow from the deep units is proportional to the water level difference. Therefore, the potential for upward flow is smaller in the southeast corner of the lake. The magnitude of the upward flow is also related to the thickness and permeability of the silt and clay unit and differences in groundwater density between the sand and gravel zone and the lake.

[16] Water level data represent best estimate of average water levels in the deep zone (O'Brien & Gere, 2009).

Several lines of evidence have been used to estimate the upward groundwater flow through the silt and clay unit, and all of these lines of evidence indicate the rate of groundwater flow is very small. From a large-scale perspective, the presence of halite brines in the unconsolidated units beneath the lake provides very strong evidence that the rate of upward groundwater flow through the sediments is very small. The existence of the brine in the sand and gravel aquifer is consistent with only the diffusive flux of chloride across the silt and clay unit as discussed in Appendix D of the Lake FS and in the USGS report by Yager and others (2007b). If upward flow of any appreciable magnitude was occurring across the silt and clay unit, the halite brine in the deep zone, which originated about 16,000 years ago during the end of the last period of glaciation, would have dissipated long ago.

Water-quality data collected from a deep boring (OL-STA-30033) advanced to bedrock in the lake in Remediation Area B also provide qualitative information on the negligible rate of upward groundwater flow through the silt and clay unit. In this boring, pore water samples were collected as the boring was advanced. A plot of water-quality data variations with depth in this deep boring is shown below along with a geologic log, location map and a schematic cross section with the well location.

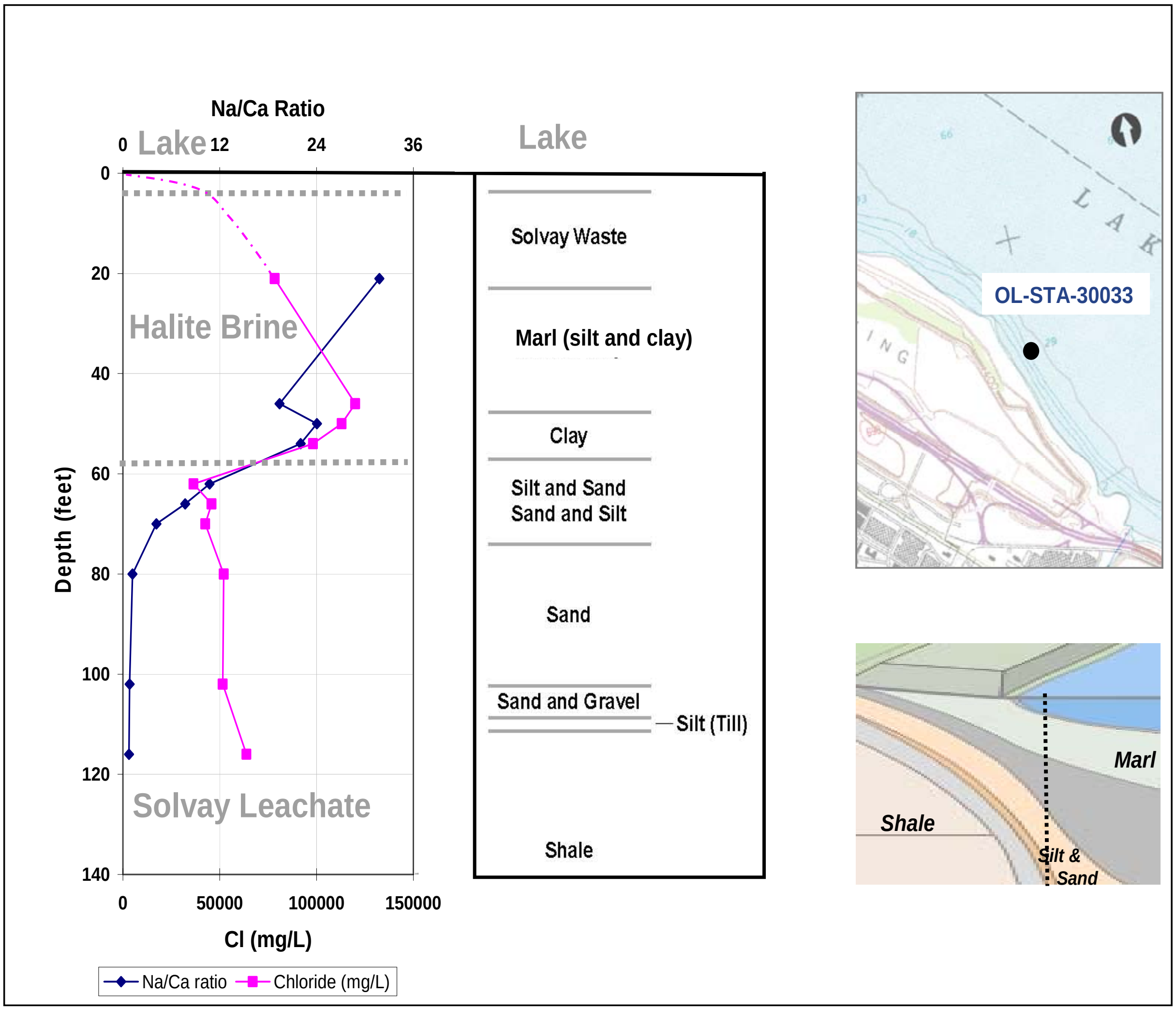

Pore water samples collected within the silt and clay unit have the characteristics of the natural halite brine and water samples in the underlying more permeable units have the characteristics of Solvay leachate. This change in water quality with depth is the result of lateral movement of Solvay leachate in the more permeable units from the nearby wastebed. Prior to operation of the wastebeds, water quality in the silt and clay unit and the underlying permeable unit most likely had the characteristics of halite brines similar to what is observed elsewhere in the lake. During or following operation of the wastebeds, Solvay leachate migrated within the more permeable units away from the wastebeds displacing the natural halite brine. This migration likely occurred prior to 1950 as dating of the groundwater in the more permeable units along the lakeshore with the tritium method indicates a groundwater age of more than 60 years. The Solvay leachate does not appear to have migrated significantly upward into the silt and clay unit as the natural halite brine in this unit has not been displaced, indicating that the rate of upward groundwater flow is very small. At an upward groundwater velocity of 2 cm/yr, over a period of 60 years, the Solvay leachate would have migrated about 10 ft. into the silt and clay unit[17]. The fact that the Solvay leachate has apparently not migrated into the silt and clay unit suggests that the upward groundwater flow rate through the silt and clay unit is significantly less than 2 cm/yr in Remediation Area B.

An estimate of groundwater flow across the silt and clay unit was also made using chloride concentration gradients in an analogous manner to that used to estimate upwelling velocities near the sediment-water interface. Pore water samples were collected in three borings in SMU 2[18] from the upper 8 ft. of the silt and clay unit and analyzed for chloride concentrations in the pore. The pore water chloride data from these borings were interpreted using Equation 1 to quantify groundwater velocity through the silt and clay unit. The calculated velocity through the silt and clay unit at all three borings was less than 0.5 cm/yr. The estimate though has significant uncertainty because the chloride concentration gradient within the silt and clay unit is small due to the fact that this unit is located tens of feet below the sediment-water interface. The results of these evaluations are contained in Attachment X.

A deep boring was advanced in Remediation Area D, approximately 2,000 ft. offshore, into bedrock which was encountered at a depth of 169 ft. below the sediment-water interface. In this boring, unlike the boring in Remediation Area B, all the pore water had the characteristics of a natural sodium-chloride brine. The chloride-depth profile from this boring could not be analyzed to determine upwelling velocities because chloride concentrations in the sand and gravel unit were lower than in the overlying fine sand and silt and the underlying bedrock, likely

[17] This distance is based on an upwelling velocity of 2 cm/yr, an effective porosity of 0.4, and a 60 year migration time frame.

[18] Borings OL-STA-20042, OL-STA-20053, OL-STA-20058 advanced in May 2006.

reflecting changes in water quality induced by historic brine production[19]. A plot of chloride concentrations with depth in this boring (OL-STA-10108), as well as sodium to calcium ratios, are shown on the figure to the right.

The USGS advanced a boring to a depth of 181 ft. near the center of the lake in the profundal zone beyond Remediation Area A. Sediment samples were collected as the boring was advanced and subsequently centrifuged in the laboratory to obtain pore water samples. These samples were analyzed for a number of analytes including calcium, sodium and chloride. The chloride-depth data have been analyzed using the techniques described above to estimate the upwelling velocity. The calculated upwelling velocity is 0.24 cm/yr as shown on the figure below.

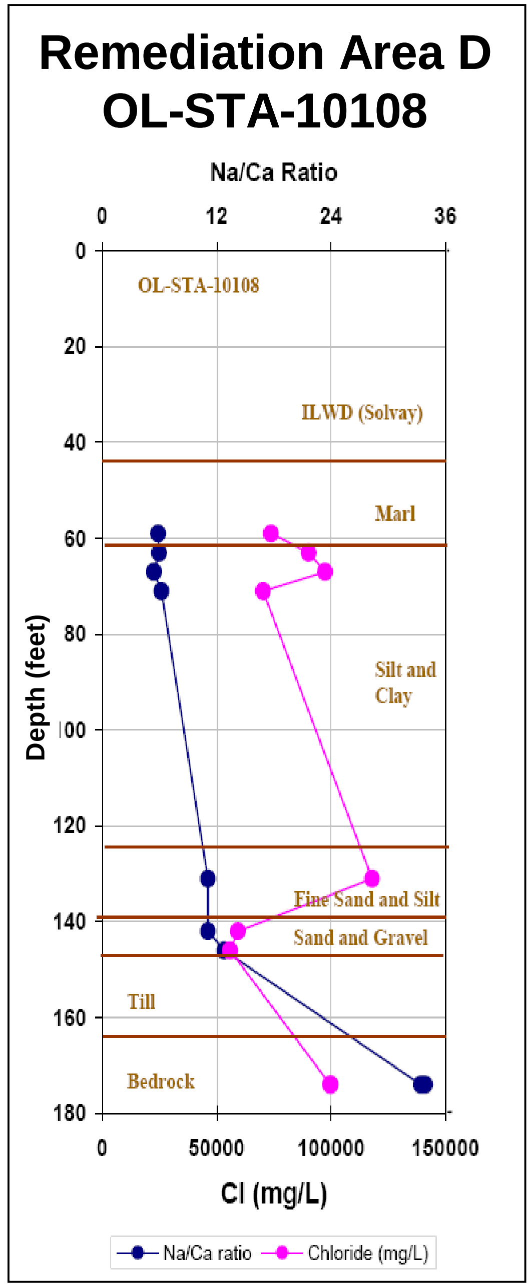

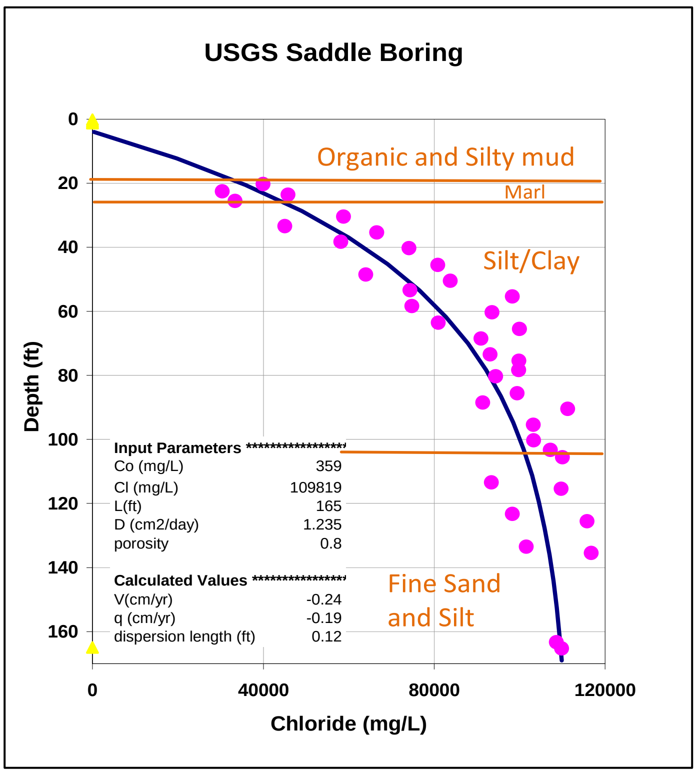

[19] The USGS (2000) reported that 11.5 million tons of salt were removed from brines produced from the groundwater system at Onondaga Lake from 1797 to 1917. This represents the salt content from the constant production of 500 gpm of brine with a chloride concentration of 60,000 mg/L over this period. Most of this production occurred from the permeable sand and gravel unit. This production lowered groundwater levels throughout the connected portion of the sand and gravel unit and induced the migration of fresher groundwater from the landward margins of the sand and gravel unit.

The silt and clay unit typically is described in the field as brown to dark gray clay with some silt with medium to high plasticity. The vertical hydraulic conductivity of the silt and clay unit averages about 1.4×10^{-7} cm/second based on testing of the silt and clay unit within the remediation areas. The vertical hydraulic conductivity of the silt and clay unit was measured[20] in multiple Shelby tube samples collected from eight borings advanced through the silt and clay unit in the Remediation Areas in the Phase VI Pre-Design Investigation. The vertical hydraulic conductivities measured in samples from the eight borings are listed on Table 4 and the locations of the borings are shown on Figure 17. At each boring location, an effective vertical hydraulic conductivity[21] was calculated from the individual measurements of hydraulic conductivity by the following equation:

$$K_{Veff} = \frac{b_T}{\sum_{i}^{n} b_i / K_{Vi}} \qquad (8)$$

where K_{Veff} is the effective vertical hydraulic conductivity for the silt and clay unit, b_T is the total thickness of the silt and clay unit, n is the number of vertical hydraulic conductivity measurements in the silt and clay unit at the boring, b_i is the thickness corresponding to measurement i, and K_{Vi} is the measured vertical hydraulic conductivity. The effective vertical hydraulic conductivities at the eight borings ranged from 5×10^{-8} cm/sec to 3×10^{-7} cm/sec, a relatively narrow range indicating that the effective vertical hydraulic conductivity of the silt and clay unit is relatively uniform.

In addition, vertical hydraulic conductivity values were calculated from consolidation test results from 11 Shelby tube samples collected from the silt and clay unit beneath Remediation Area D in the Phase I Pre-Design Investigation. The locations of the borings in which these samples were collected are also shown on Figure 17, and the calculated vertical hydraulic conductivies are listed on Table 4. The calculated vertical hydraulic conductivities ranged from 6×10^{-8} cm/sec to 3×10^{-7} cm/sec, a range that is consistent with the data collected in the Phase VI Pre-Design Investigation. The method used to analyze these data and the results of the analyses are described in detail in Attachment XIII.

The thickness of the silt and clay unit beneath the lake is variable, ranging from about 15 ft. to over 70 ft. across the Remediation Areas. A map of the thicknesses of the silt and clay unit beneath much of Onondaga Lake is shown on Figure 3. In much of the eastern part of Remediation Area D and in adjacent Remediation Area E, the silt and clay unit is over 60 ft. thick. The unit is thinnest along the shoreline in the western portion of Remediation Area D, but the unit thickens rapidly away from the shoreline.

---

[20] The vertical hydraulic conductivity was measured using a flexible wall permeameter by ASTM D 5084.

[21] The effective vertical hydraulic conductivity is defined as the value of the vertical hydraulic conductivity that will produce the correct estimate of groundwater flux through the silt and clay unit using the equation $v = K_v$ * *hydraulic gradient* where the hydraulic gradient is the water-level difference across the silt and clay unit divided by the total thickness of the silt and clay unit.

The rate of upward groundwater flow through the silt and clay unit can be estimated with Darcy's law: $v = ki$ where v is the upwelling velocity, k is the vertical hydraulic conductivity, and i is the hydraulic gradient. This equation is valid if the density of the groundwater on either side of the silt and clay unit is approximately the same, which is generally the case as brines occur both in the marl overlying the silt and clay unit and in the underlying fine sand and silt unit and the sand and gravel unit. If the density is not the same, the velocity can be estimated with the following equation:

$$v = -k\left(\frac{\partial h_f}{\partial z} + \left(\frac{\rho - \rho_f}{\rho_f}\right)\right) \quad (9)$$

where h_f is equivalent fresh-water head, ρ is average density between two locations where head is measured, and ρ_f is freshwater density (Parsons, 2004; Appendix D: Part A).

The large variations in the thickness of the silt and clay unit result in differences in the upward groundwater flow in Remediation Area D, with the larger upward groundwater flows occurring near the shoreline where the silt and clay unit is the thinnest. Evaluations of potential upwelling velocities were conducted considering the water level differences measured at the various monitoring locations along the shoreline in Remediation Area D and the density variations in groundwater[22]. These evaluations indicate that upwelling velocities will generally be less than 2 cm/yr adjacent to the shoreline where the silt and clay unit is thinnest, to less than 1 cm/yr where the silt and clay unit is greater than about 30 ft. thick[23]. The calculated upwelling velocities at selected monitoring locations, based on water levels in deep and intermediate well pairs, are listed on Table 5.

The silt and clay unit beneath the lake at Remediation Area D appears to be the thinnest adjacent to the East Flume. A boring was advanced and monitoring wells were installed on the spit of land beneath the East Flume and the lake to determine the characteristics of the silt and clay unit and groundwater conditions in this area (boring HB-SB-213 and monitoring wells HB-MW-213D, HB-MW-213I and HB-MW-213S). Monitoring wells HB-MW-213I and HB-MW-213D are screened in the marl above the silt and clay unit and in the sand and silt unit below the silt and clay unit, respectively. Based on the water level difference between these two wells, the

---

[22] Groundwater density was estimated based on the total dissolved solids concentrations in groundwater. Standard QA/QC procedures were used to validate the water quality data that were the basis for the measurements of total dissolved solids.

[23] These estimates were calculated using a water-level difference across the silt and clay unit of 7 ft. and vertical hydraulic conductivities for the silt and clay unit in the range of 1.4×10^{-7} cm/yr.

thickness of the silt and clay unit and the higher of the two estimates of the vertical hydraulic conductivity described above, the upward groundwater velocity is less than 3 cm/yr[24].

In Remediation Area A offshore of the proposed hydraulic containment system the thickness of the silt and clay unit is slightly greater than 30 ft., and the water level difference between the deep zone and the lake is greater than 9 ft. Based on these parameter values, the estimated upwelling velocity through the silt and clay unit in this area is about 1.4 cm/yr. In Remediation Area B offshore of the proposed hydraulic containment system the thickness of the silt and clay unit ranges from about 20 to 60 ft. and the water level difference between the deep zone and the lake is on the order of 6 ft. Based on these parameters, the upwelling velocity through the silt and clay unit is in the range of 0.4 to 1.3 cm/yr. In Remediation Area C offshore of the proposed hydraulic containment system the thickness of the silt and clay unit ranges from about 15 to 40 ft. and the water level difference between the deep zone and the lake is on the order of 7.5 ft.. Based on these parameters, the upwelling velocity through the silt and clay unit is in the range of about 1cm/yr to a little more than 2 cm/yr

The groundwater model, described in the Lake FS, is an analytical tool that combines in a rigorous mathematical framework all of the important factors that affect the rate of vertical groundwater movement through the sediments beneath Onondaga Lake. The groundwater model incorporates information on the variations in thickness of each of the geologic units including the silt and clay unit, variations in hydraulic properties, and variations in density of groundwater within the subsurface. In addition, the groundwater model can explicitly represent the effects of operation of the hydraulic containment system on vertical groundwater flow through the silt and clay unit. As noted above, the groundwater model was used to estimate upwelling velocities for the Lake FS, and the results of the evaluations were that upwelling velocities in Remediation Area D following installation and operation of the hydraulic containment system would be less than 2 cm/yr. The numerical methods used to calculate flow in the groundwater model have precision limitations due to the nature of the algorithms used in the model, and our evaluations indicated that the precision of the calculations of upwelling velocities generated a maximum value of 2 cm/yr. Therefore, it was determined that upwelling velocities of less than 2 cm/yr could not meaningfully be calculated with the numerical model alone. The one-dimensional analyses of groundwater flow through the silt and clay unit described above; however, does provide additional justification for the use of 2 cm/yr as a maximum upwelling velocity within Remediation Area D with the shallow hydraulic containment system in operation.

Summary

The presence of upward hydraulic gradients from the deep groundwater zones to Onondaga Lake indicates that there is the potential for upward groundwater flow from the deep

---

[24] The upward groundwater velocity is calculated based on a vertical hydraulic conductivity of 1.4×10^{-7} cm/sec, a water level difference across the silt and clay unit of 4.92 ft. based on water levels collected on November 3, 2008 (O'Brien & Gere, 2009) and a silt and clay unit thickness of 8 ft. The hydraulic gradient is calculated as the water-level difference divided by the silt and clay thickness. The densities of groundwater at HB-MW-213I and HB-MW-213D are similar as measured total dissolved solids concentrations were 48,900 mg/L and 47,000 mg/L, respectively in November 2008.

zones to Onondaga Lake. The hydraulic containment systems that will be operated along the lakeshore at Remediation Area D, portions of Remediation Area A, and portions of Remediation Area B will capture shallow groundwater flowing towards the lake but will have a negligible effect on the potential upward flowing groundwater from the deeper groundwater zones to the lake. The evaluations described above indicate that the upwelling velocities with the hydraulic containment system in operation will generally be less than 2 cm/yr. Upwelling velocities may approach 2 cm/yr along the shoreline in the western portion of Remediation Area D where the silt and clay unit is the thinnest, but upwelling velocities may be much less than 2 cm/yr in the remainder of Remediation Area D where the silt and clay unit is much thicker. Upwelling velocities will be less than 2 cm/yr in areas offshore of the hydraulic containment systems in Remediation Areas A and B.

Section 8
Upwelling Velocities for Cap Design in Areas with Hydraulic Containment

Based on the multiple lines of evidence described in Section 7, estimates of the upwelling rates in Remediation Areas affected by operation of the hydraulic containment system have been developed. These estimates are based on the assumption that groundwater discharge in the remediation areas with operation of the hydraulic containment system will be the result only of upward groundwater flow through the silt and clay unit. The rate of groundwater flow through the silt and clay unit is a function of the hydraulic gradient across this unit, the thickness of the unit and the effective vertical hydraulic conductivity of this unit. Contour maps of equal upwelling velocities within Remediation Areas B, C and D have been developed based on best estimates[25] of vertical hydraulic conductivity for the silt and clay unit, thickness of the silt and clay unit, and groundwater level difference across the silt and clay unit. These contour maps are shown on Figures 18, 19, and 20 for Remediation Areas B, C and D, respectively.

For purposes of cap design, upwelling velocities based on best-estimates of groundwater gradient, silt and clay unit thickness and vertical hydraulic conductivity were supplemented by developing cumulative frequency distributions of upwelling velocities based on a consideration of the uncertainty/variability in the estimates of each of these three parameters. The cumulative frequency distributions were calculated using a Monte Carlo approach that is described below, following a discussion of the uncertainty/variability in each of the individual parameters.

Vertical Hydraulic Conductivity

During the Phase VI Pre-Design Investigation the vertical hydraulic conductivity of the silt and clay unit was measured in multiple Shelby tube samples collected from eight borings advanced through the silt and clay unit in the remediation areas and in addition vertical hydraulic conductivity was calculated from consolidation test results from 13 Shelby tube samples collected from the silt and clay unit in Remediation Area D in the Phase I Pre-Design Investigation. For the eight borings in which multiple measurements of vertical hydraulic conductivity were obtained, an effective vertical hydraulic conductivity for the silt and clay unit at that location was calculated. A cumulative frequency distribution of these eight effective vertical hydraulic conductivities is shown on the left-most graph below, in which vertical hydraulic conductivity is plotted along on a logarithmic scale on the x-axis and the percentile frequency is plotted on a probability scale on the y-axis. The data points on the graph plot approximately along a straight line indicating that vertical hydraulic conductivity is log-normally distributed. For purposes of the Monte Carlo simulations used to calculate the uncertainty/variability in estimated upwelling velocities, the uncertainty/variability in the vertical hydraulic conductivity was described by a log normal distribution with a mean of -6.906 log

[25] In developing these maps, a vertical hydraulic conductivity of $1.4\text{x}10^{-7}$ was used, the thicknesses shown on Figure 3 were used, and water-level differences based on average levels in sand and gravel unit monitoring wells along the shoreline as shown on page 33 subtracted from average lake levels were used.

cm/sec (1.24×10^{-7} cm/sec) and a standard deviation of 0.275.

For comparison purposes, a probability plot for all 40 individual measurements of vertical hydraulic conductivity was also prepared (the right-most graph above). These data also plot approximately along a straight line, with the exception of one extreme value at each end of the distribution, indicating that these data are also log-normally distributed. The calculated mean and standard deviation of this distribution is -6.80 log cm/sec (1.6×10^{-7} cm/sec) and 0.32, respectively. This distribution is similar to that calculated based on effective vertical hydraulic conductivities.

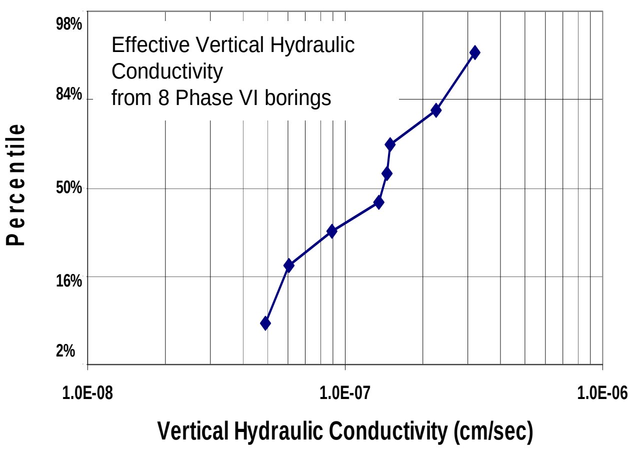

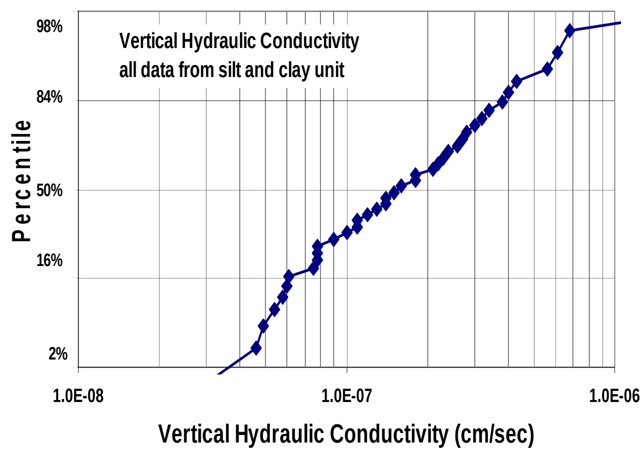

Thickness of Silt and Clay Unit

The uncertainty in the thickness of the silt and clay unit is related to the accuracy with which the contacts with the overlying marl and underlying silt and fine sand unit were picked and is related to the density of borings that penetrated the silt and clay unit. The uncertainty in picking the contacts with overlying and underlying units, for purposes of the Monte Carlo simulations, was specified as a normal distribution with ±5 ft. corresponding to a 95 percent degree of confidence. The uncertainty related to density of borings was not explicitly represented in the Monte Carlo simulations as in most areas there is a relatively good density of borings. In addition to the uncertainty described above, the silt and clay thickness varies spatially, according to the contours shown on Figure 3.

Water Level Differences

The groundwater-level difference across the silt and clay unit has not been measured at any location within the remediation areas primarily because of logistical difficulties in obtaining representative water-level measurements beneath the lake. As a conservative assumption, the water-level difference for purposes of the Monte Carlo simulations was specified based on water-levels in monitoring wells completed in the sand and gravel unit along the shoreline and lake water levels. This overestimates the actual water-level difference across the silt and clay unit, as the silt and clay unit is only a portion of the total sediment thickness between the sand and gravel unit and the bottom of the lake. If groundwater-level measurements were available for monitoring wells completed at the base of the marl and at the top of the silt and fine sand unit, the difference in water-levels across the silt and clay unit could be accurately computed and they would undoubtedly be smaller than those computed from monitoring wells in the sand and gravel unit and lake level.

For the sand and gravel monitoring wells along the lakeshore, the difference between the groundwater level in the well and lake level[26] was calculated for each date with available groundwater level data. The average and standard deviation of the water-level difference was then calculated for each monitoring location along the shoreline, and these statistics were used in the Monte Carlo simulations (assuming a normal distribution) to represent the uncertainty in water-level difference across the silt and clay unit. The average water-level differences and the standard deviations of the differences are listed in the table below.

	HB HB-01D	HB HB-05D	HB-20D	WA WA-01D	WA MW100D	WA OW-04D	WA OW-05D	WA OW-07D	WB18 MW-02D	MW18 MW-03D	WB18 MW-05D
Remediation Area	D	D	D	D	C	C	C	C	B	B	A
Average (feet)	7.07	5.55	0.71	7.45	8.49	7.74	8.18	7.46	6.26	5.16	9.45
Standard Deviation (feet)	1.16	0.70	0.32	0.45	0.40	0.51	0.56	0.60	0.63	1.05	0.49

Monte Carlo Simulation

The basic model used in the Monte Carlo simulation was the following (i.e., Darcy's Law):

$$V = K_V * \frac{\Delta H}{b} \qquad (10)$$

where V is the upwelling velocity, ΔH is the water-level difference across the silt and clay unit, and b is the thickness of the silt and clay unit. This equation assumes that the density of groundwater does not change significantly across the silt and clay unit. The steps in the Monte Carlo analysis were the following:

1. One hundred sets of stochastic random fields were generated for each of the three parameters in the basic model: vertical hydraulic conductivity, water-level difference and silt and clay thickness. For Remediation Area D parameter values were defined on a 50-ft. by 50-ft. grid, and in Remediation Areas B and C parameter values were defined a 25-ft. by 25-ft. grid. The stochastic random vertical hydraulic conductivity fields were generated using the FIELDGEN utility in the computer program PEST (Doherty, 2008). The random fields for thickness of the silt and clay unit were generated by randomly selecting a value from the normal distribution describing the

[26] The lake level was specified based on daily data from the U.S. Geological Survey gage 04240495 Onondaga Lake at Liverpool, New York.

uncertainty in estimated thickness, adding this value to the best-estimate of thickness, and then kriging these values within the domain of interest. The random water-level difference fields were generated by randomly selecting a value from the normal distribution described above at each monitoring well location along the shoreline shown on the figure on page 30 and then kriging the selected values assuming that the water-level difference is constant perpendicular to the shoreline within the domain of interest.

2. One hundred sets of parameter combinations were generated by randomly selecting values from 100 sets of random fields generated in the previous step for each parameter.
3. The upwelling velocity was calculated using Equation 10 at each grid cell in Remediation Area D and in Remediation Areas B and C for each 100 sets of parameter combinations.
4. The statistics of the calculated upwelling velocities within each subarea in Remediation Area D and in Model Areas B1/C1, B2, and C3 were computed.

Results

Selected statistics on the upwelling frequency distributions generated for each model area are listed on the table below. These statistics are based on the upwelling velocities calculated at each of the grid cells within the model area in the Monte Carlo simulations. The number of calculated upwelling velocities used to construct the frequency distribution for each model area is listed in the column labeled “count” in the table below. The mean and standard deviation of the log-transformed distributions were used to generate upwelling distributions for the Monte Carlo simulations conducted with the cap model.

Remediation Area	Area	Count	Mean (cm/year)	Log-Transformed Values	
				Mean log(cm/yr)	Std Dev log(cm/yr)
B and C	B1/C1	104700	1.02	-0.09	0.30
	B2	48400	0.51	-0.39	0.29
	C3	76300	1.50	0.07	0.30
D	East	85000	0.37	-0.56	0.34
	Center	51700	0.68	-0.28	0.31
	Western	20000	1.11	-0.06	0.31
	SMU2-ILWD	11900	1.53	0.08	0.31

Probability plots of the distributions generated from the Monte Carlo simulations are shown in graphic form below; the x-axis of each plot is the upwelling velocity plotted on a logarithmic scale and the y-axis is the frequency percentile plotted on a probability scale. Each of the distributions plots approximately as a straight line indicating that the distributions are normally distributed.

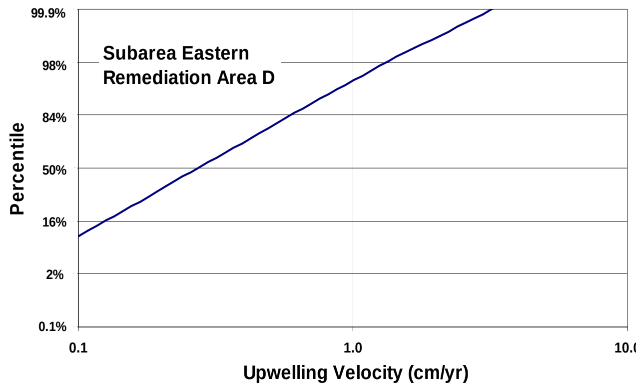
Subarea Eastern
Remediation Area D
Percentile
99.9%
98%
84%
50%
16%
2%
0.1%
0.1
1.0
10.0
Upwelling Velocity (cm/yr)

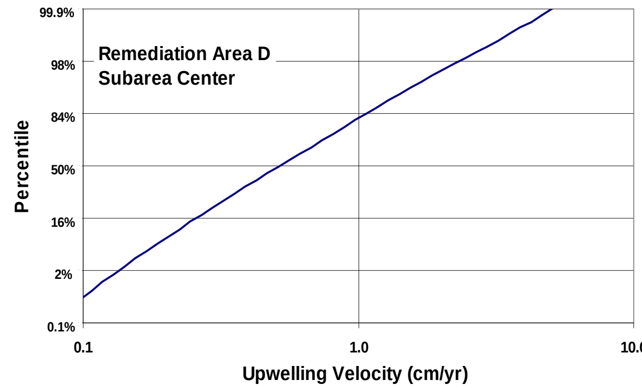
Remediation Area D
Subarea Center
Percentile
99.9%
98%
84%
50%
16%
2%
0.1%
0.1
1.0
10.0
Upwelling Velocity (cm/yr)

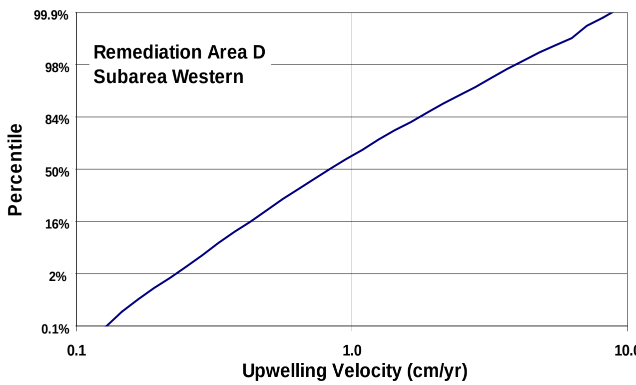
Remediation Area D
Subarea Western
Percentile
99.9%
98%
84%
50%
16%
2%
0.1%
0.1
1.0
10.0
Upwelling Velocity (cm/yr)

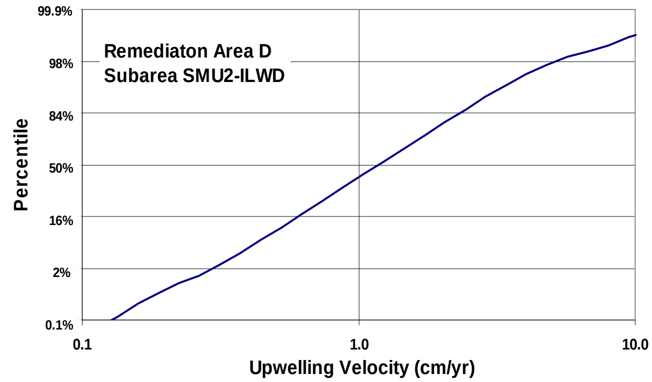
Remediaton Area D
Subarea SMU2-ILWD
Percentile
99.9%
98%
84%
50%
16%
2%
0.1%
0.1
1.0
10.0
Upwelling Velocity (cm/yr)

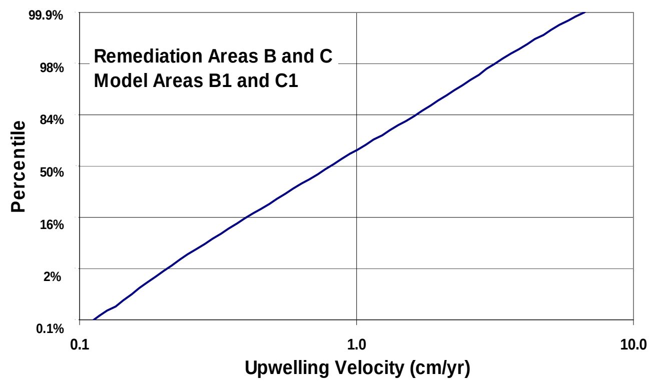
Remediation Areas B and C
Model Areas B1 and C1
Percentile
99.9%
98%
84%
50%
16%
2%
0.1%
0.1
1.0
10.0
Upwelling Velocity (cm/yr)

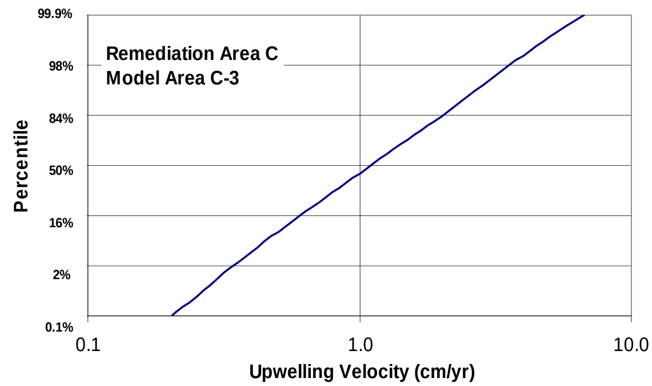
Remediation Area C
Model Area C-3
Percentile
99.9%
98%
84%
50%
16%
2%
0.1%
0.1
1.0
10.0
Upwelling Velocity (cm/yr)

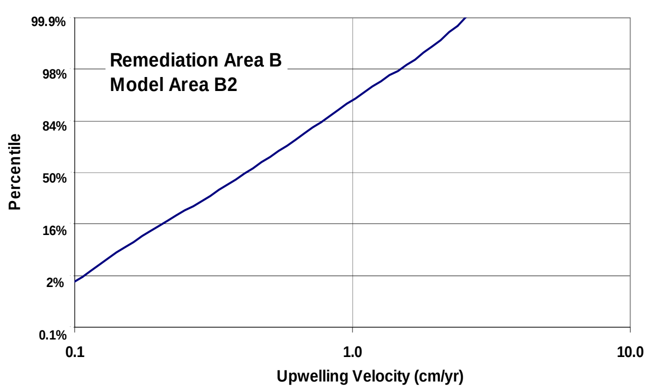
Remediation Area B
Model Area B2
Percentile
99.9%
98%
84%
50%
16%
2%
0.1%
0.1
1.0
10.0
Upwelling Velocity (cm/yr)

Remediation Area A – Model Area A1

A hydraulic containment system is also proposed along the shoreline of Remediation Area A just east of the mouth of Ninemile Creek because of the high upwelling velocities determined in the area from analysis of chloride-depth profiles constructed from both sediment-conductivity and pore-water data in this area. Conservatively it was calculated that the effect of the containment system on upwelling velocity would extend 500 ft. outward from the shoreline[27]. In the region near the shoreline the average upwelling velocity was calculated to be 1.4 cm/yr with the containment system in operation based on the thickness of silt and clay unit in this area, the average silt and clay vertical hydraulic conductivity, and the water-level difference between the sand and gravel unit and the lake in this area. This value was used in the calculation of the upwelling frequency distribution in Model Area A1 by specifying an upwelling velocity of 1.4 cm/yr at five sample locations present in the influenced area.

[27] The effect of hydraulic containment systems on upwelling velocities was discussed in Appendix D of the FS. A comparison of the tabulated upwelling velocities with distance from shore on pages DA.11-1 and DA.12-1, which show current upwelling velocities and upwelling velocities with hydraulic containment system in place, clearly shows that the effect of the hydraulic containment system extends outward at least 500 ft.

Section 9
Conclusions

This report describes the results of extensive field and analytical studies that have quantified the discharge of groundwater to the areas in Onondaga Lake where a sediment cap will be placed as part of the remedial activities undertaken to meet the requirements of the Record of Decision for the Onondaga Lake Bottom Subsite. The current rates of groundwater discharge in Remediation Areas A and E and Model Area C2, which are similar to discharge rates expected after placement of the cap, have been delineated based on the analysis of chloride depth profiles at more than 200 locations within and in the vicinity of these remediation areas. In Remediation Area D and Model Areas B1/C1, B2 and C3 the rates of groundwater discharge after placement of the cap will be significantly lower than current rates as the result of the construction and operation of a hydraulic containment system along the shoreline. Groundwater discharge rates in Remediation Area D and Model Areas B1/C1, B2 and C3 after placement of the cap were calculated based on groundwater flow rates upward through the underlying regional confining unit (the silt and clay unit).

This report describes a number of methods that were implemented in the field to estimate groundwater discharge rates, which are commonly referred to as upwelling velocities. The evaluation of upward groundwater velocity through the sediment based on the change in chloride concentrations with depth in sediment pore water was determined to be the best method for estimating current upwelling velocities in the remediation areas. This report describes the theoretical bases for the use of this method to estimate upwelling velocities and describes the extensive data collected on chloride concentrations in sediments to accurately delineate the current distribution of upwelling velocities within the remediation areas.

The upwelling velocities within the remediation areas are low. The mean measured upwelling velocity in Remediation Area E is 1.49 cm/yr, and the mean upwelling velocities in Model Areas A1, A2, and C2 are 1.33 cm/yr, 4.08 cm/yr, and 2.71 cm/yr, respectively. In Remediation Area D and Model Areas B1/C1, B2 and C2, calculated upwelling velocities with the hydraulic containment system in place are less than 2 cm/yr.

The data and evaluations described in this report provide an excellent foundation for the design of the remedy for Onondaga Lake. The upwelling velocities that are described in this report will be used in the cap model for purposes of cap design.

Section 10
References

Al-Niami, A., and K. Rushton. 1977. Analysis of Flow Against Dispersion in a Porous Media: Journal of Hydrology 33: 87-97.

Anati, D., 1994. Advection and Diffusion in Marine Sediments: DSDP Site 374 in the Eastern Mediterranean as an Example. Earth and Planetary Science Letters 128:575-589.

Andrews, C. and G. Swenson, 2004. Groundwater Flow to Onondaga Lake. Appendix D: Part A to the Onondaga Lake Feasibility Study. Prepared for Honeywell, Morristown, NJ. By Parsons. November 2004.

Aster, R.C. B. Borchers, and C.H. Thurber (2005), Parameter Estimation and Inverse Problems, International Geophysics Series, vol. 90, Elsevier Academic Press, Amsterdam.

Berg, P. and N. Risgaard-Petersen, 1998. Interpretation of Measured Concentration Profiles in Sediment Pore Water. Chemical Oceanography 43(7): 1500-1510.

Bredehoeft, J.D. and Papadopulos, I.S., 1965. Rates of Vertical Groundwater Movement Estimated from Earth's Thermal Profile. Water Resources Research, 1:325-328.

Boudreau, B. 1996. The Diffusive Tortuosity of Fine-Grained Unlithified Sediments: Geochimica et Cosmochimica Acta 60, no. 16: 3139-3142.

Cable, J., J. Martin, P. Swarzenski, M. Lindenberg and J. Steward, 2004. Advection within Shallow Pore Waters of a Coastal Lagoon, Florida. Ground Water, V42: 1011-102.

Cornett, R. J., B.A. Risto, and D. R. Lee, 1989. Measuring Groundwater Transport Through Lake Sediments by Advection and Dispersion. Water Resources Research, V.25, no. 8.

Day-Lewis, F.D., H. Karam, C. Harvey, J.Lane, 2006. Monitoring Submarine Groundwater Discharge Using a Distributed Temperature Sensor, Waquoit Bay, Massachusetts. EOS Transactions, American Geophysical Union, V.87. no. 52.

Doherty, J. (2008), PEST, Model Independent Parameter Estimation. User's Manual: 5th Edition.

Effler, S. W. editor, 1996. Limnological and Engineering Analysis of a Polluted Urban Lake. Springer-Verlag, New York.

Effler, S., S. Doerr, and C. Brooks, 1990. Chloride in the Pore Water and Water Column of Onondaga Lake, N.Y., U.S.A. Water, Air, and Soil Pollution 51:315-326.

Felmy, A. and J. Weare, 1991. Calculation of Multicomponent Ionic Diffusion from Zero to High Concentration: I. The Sys tem Na-K-Ca-Mg-Cl-SO_4-H_2O at 25º C. Geochimica et Cosmochimica Acta 55:113-131.

Kappel, W.M. 2000, Salt Production in Syracuse, New York ("The Salt City") and the Hydrogeology of the Onondaga Creek Valley. U.S. Geological Survey Fact Sheet 139-00.

Keery, J., A. Binley, N. Crook, and J. Smith, 2006. Temporal and Spatial Variability of Groundwater-Surface Water Fluxes: Development and Application of an Analytical Method Using Temperature Time Series. Journal of Hydrology, 336:1-16.

Jackson. W. and T. Anderson, 2007. Diffusion Sampler Equilibration Study Using Teflon (PTFE) and Tuffryn Membranes in Onondaga Lake Sediments. Prepared for Parsons, Liverpool, New York, February 24, 2007.

Kappel, W.M, and R. Yager, 2008, Ground-water-flow modeling of a freshwater and brine-filled aquifer in the Onondaga Trough, Onondaga County, New York—A summary of findings, U. S. Geological Survey Open-File Report 2007-1409, 12p.

Lee, D.R. 1977. A Device for Measuring Seepage Flux in Lakes and Estuaries. Limnology and Oceanography, 22: 140-147.

Maris, C. and M. Bender, 1982. Upwelling of Hydrothermal Solutions Through Ridge Flank Sediments Shown by Pore Water Profiles. Science, 216: 623-626.

Maris, C., M. Bender, P. Froelich, R. Barnes, and N. Luedtke, 1984. Chemical Evidence for Advection of Hydrothermal Solutions in the Sediments of the Galapagos Mounds Hydrothermal Field. Geochemica et Cosmochimica Acta: 48:2331-2346.

Neuman, S.P. 1990. Universal Scaling of Hydraulic Conductivites and Dispersivities in Geologic Media: Water Resources Research 26, no. 8: 1749-1758.

Neuman, S.P. 2006. Comment on Longitudinal Dispersivity Data and Implications for Scaling Behavior: Ground Water 44, no. 2: 139-141.

Neuzil, C.E., 1986. Groundwater Flow in Low Permeability Environments, Water Resources Research, 22, no. 8: 1163-1195.

New York State Department of Environmental Conservation (NYSDEC) and U.S. Environmental Protection Agency (USEPA), 2005. Record of Decision Onondaga Lake Bottom Subsite of the Onondaga Lake Superfund Site. Town of Geddes and Salina, Villages of Solvay and Liverpool and City of Syracuse, Onondaga County, New York.

Onondaga County, 2003. 2002 Annual Report: Onondaga Lake Ambient Monitoring Program.

Onondaga County, 2004. 2003 Annual Report: Onondaga Lake Ambient Monitoring Program.

O'Brien & Gere, 2008. Wastebeds 1-8 Remedial Investigation Report, Geddes, New York. Prepared for Honeywell, Morristown, New Jersey and Syracuse, New York. April

O'Brien & Gere, 2009. Remedial Investigation Revised Report Wastebed B/Harbor Brook Site.

Parsons, 2003. Groundwater Upwelling Investigation for Onondaga Lake, Syracuse, New York. Prepared for Honeywell, Morristown, New York.

Parsons, 2004. Draft Feasibility Study Report for Onondaga Lake. Prepared for Honeywell, Morristown, New York. November.

Parsons, 2005a. Onondaga Lake Phase I Pre-Design Investigation: Sampling and Analysis Plan. Prepared for Honeywell, Morristown, New Jersey and Syracuse, New York.

Parsons, 2005b. Onondaga Lake Pre-Design Investigation: Quality Assurance Project Plan. Prepared for Honeywell, Morristown, New Jersey. Syracuse, New York.

Parsons, 2006. Onondaga Lake Pre-Design Investigation: Phase II Work Plan. Prepared for Honeywell, Morristown, New Jersey and Syracuse, New York.

Parsons, 2007a. Onondaga Lake Pre-Design Investigation: Phase I Data Summary Report. Prepared for Honeywell, Morristown, New Jersey and Syracuse, New York

Parsons, 2007b, Onondaga Lake Pre-Design Investigation: Phase III Work Plan. Prepared for Honeywell, Morristown, New Jersey and Syracuse, New York.

Parsons 2007c, Onondaga Lake Pre-Design Investigation: Phase III Addendum 1. Prepared for Honeywell, Morristown, New Jersey and Syracuse, New York.

Parsons 2007d, Onondaga Lake Pre-Design Investigation: Phase III Addendum 2 Prepared for Honeywell, Morristown, New Jersey and Syracuse, New York

Parsons 2007e, Onondaga Lake Pre-Design Investigation: Phase III Addendum 3 Prepared for Honeywell, Morristown, New Jersey and Syracuse, New York

Parsons 2007f, Onondaga Lake Pre-Design Investigation: Phase III Addendum 4 Prepared for Honeywell, Morristown, New Jersey and Syracuse, New York

Parsons 2007g, Onondaga Lake Pre-Design Investigation: Phase III Addendum 5. Prepared for Honeywell, Morristown, New Jersey and Syracuse, New York.

Parsons 2007h, Onondaga Lake Pre-Design Investigation: Phase III Addendum 6 Prepared for Honeywell, Morristown, New Jersey and Syracuse, New York

Parsons 2007i, Onondaga Lake Pre-Design Investigation: Phase III Addendum 7 Prepared for Honeywell, Morristown, New Jersey and Syracuse, New York

Parsons 2008a, Onondaga Lake Pre-Design Investigation: Phase IV Work Plan. Prepared for Honeywell, Morristown, New Jersey and Syracuse, New York.

Parsons 2008b, Onondaga Lake Pre-Design Investigation: Phase IV Addendum 1. Prepared for Honeywell, Morristown, New Jersey and Syracuse, New York.

Parsons 2008c, Onondaga Lake Pre-Design Investigation: Phase IV Addendum 2. Prepared for Honeywell, Morristown, New Jersey and Syracuse, New York.

Parsons 2008d, Onondaga Lake Pre-Design Investigation: Phase IV Addendum 3. Prepared for Honeywell, Morristown, New Jersey and Syracuse, New York.

Parsons 2008e, Onondaga Lake Pre-Design Investigation: Phase IV Addendum 4. Prepared for Honeywell, Morristown, New Jersey and Syracuse, New York.

Parsons 2008f, Onondaga Lake Pre-Design Investigation: Phase IV Addendum 7. Prepared for Honeywell, Morristown, New Jersey and Syracuse, New York.

Parsons 2008g, Onondaga Lake Pre-Design Investigation: Phase IV Addendum 8. Prepared for Honeywell, Morristown, New Jersey and Syracuse, New York.

Parsons, 2009a. Onondaga Lake Pre-Design Investigation: DRAFT Phase II Data Summary Report. Prepared for Honeywell, Morristown, New Jersey and Syracuse, New York.

Parsons, 2009b, Onondaga Lake Pre-Design Investigation: DRAFT Phase III Data Summary Report. Prepared for Honeywell, Morristown, New Jersey and Syracuse, New York

Parsons, 2009c, Onondaga Lake Pre-Design Investigation: DRAFT Phase IV Data Summary Report. Prepared for Honeywell, Morristown, New Jersey and Syracuse, New York

Parsons 2009d, Onondaga Lake Pre-Design Investigation: Phase IV Addendum 6. Prepared for Honeywell, Morristown, New Jersey and Syracuse, New York.

Parsons 2009e, Microbead Marker 2008 Pre-Mobilization Field Test Data Summary Report. Prepared for Honeywell, Morristown, New Jersey and Syracuse, New York.

Parsons 2009f, Onondaga Lake Pre-Design Investigation: DRAFT Phase V Work Plan. Prepared for Honeywell, Morristown, New Jersey and Syracuse, New York.

Rosenberry, D. 2005. Integrating Seepage Meter Heterogeneity with the Use of Ganged Seepage Meters. Limnology and Oceanography: Methods, 3: 131-142.

Rosenberry, D. and J. LaBaugh, 2008. Field Techniques for Estimating Water Fluxes Between Surface Water and Ground Water. U.S. Geological Survey, Techniques and Methods 4-D2.

Sayles, F. and W. Jenkins, 1982. Advection of Pore Fluids through Sediments in the Equatorial East Pacific. Science, 217: 245-248.

Schneider, R. T. Negley, and C. Wafer, 2004. Factors Influencing Groundwater Seepage in a Large Mesotrophic Lake in New York. Journal of Hydrology, v310: 1-16.

Sebestyen, S. and R. Schneider, 2001. Dynamic Temporal Patterns of Nearshore Seepage Flux in a Headwater Adirondack Lake. Journal of Hydrology, 247:137-150.

S. S. Papadopulos & Associates, Inc. and O'Brien and Gere, 2009. Honeywell Groundwater Flow Model, Version 3. November 2009.

Swenson, G. and C. Andrews, 2004. Groundwater Model Documentation. Appendix D: Part B to the Onondaga Lake Feasibility Study. Prepared for Honeywell, Morristown, NJ. By Parsons. November 2004.

TAMS Consultants, Inc. 2002. Onondaga Lake Remedial Investigation Report, Syracuse, New York. Prepared for New York Department of Environmental Conservation, Division of Environmental Remediation.

van der Kamp, G., 2001. Methods for Determining the In-situ Hydraulic Conductivity of Shallow Aquitards - An Overview. Hydrogeology Journal, 9: 5-16.

Yager, R.M., W. Kappel, and L. Plummer, 2007a, Origin of halite brine in the Onondaga Trough near Syracuse, New York State, USA: modeling geochemistry and variable-density flow, Hydrogeology Journal, v. 15, no. 7, p. 1321-1339.

Yager, R., W. Kappel, and L. Plummer, 2007b. Halite Brine in the Onondaga Trough Near Syracuse, New York: Characterization and Simulation of Variable-Density Flow. U.S. Geological Survey, Scientific Investigation Report 2007-5058.

FIGURES

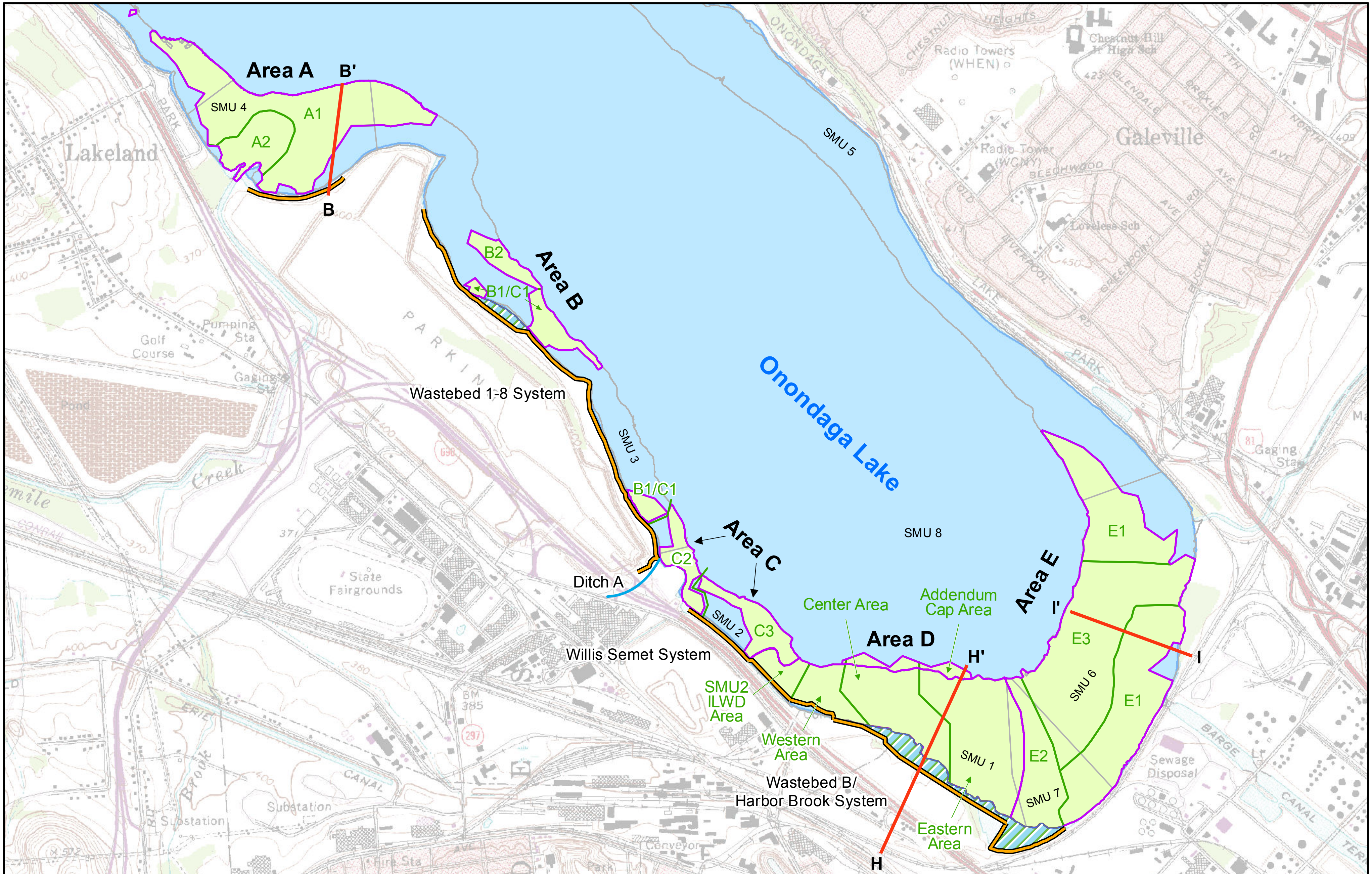

Cross Section Location
Hydraulic Containment System
Onondaga Wetlands
Remediation Area
Model Area Boundaries
Proposed Outboard Wetlands
SMU Boundary
Isolation Cap Area

0 1,000 2,000 4,000
Feet

FIGURE 1

Honeywell Onondaga Lake Syracuse, New York

Remediation Areas and Cross Section Location Map

S. S. Papadopulos & Assoc.

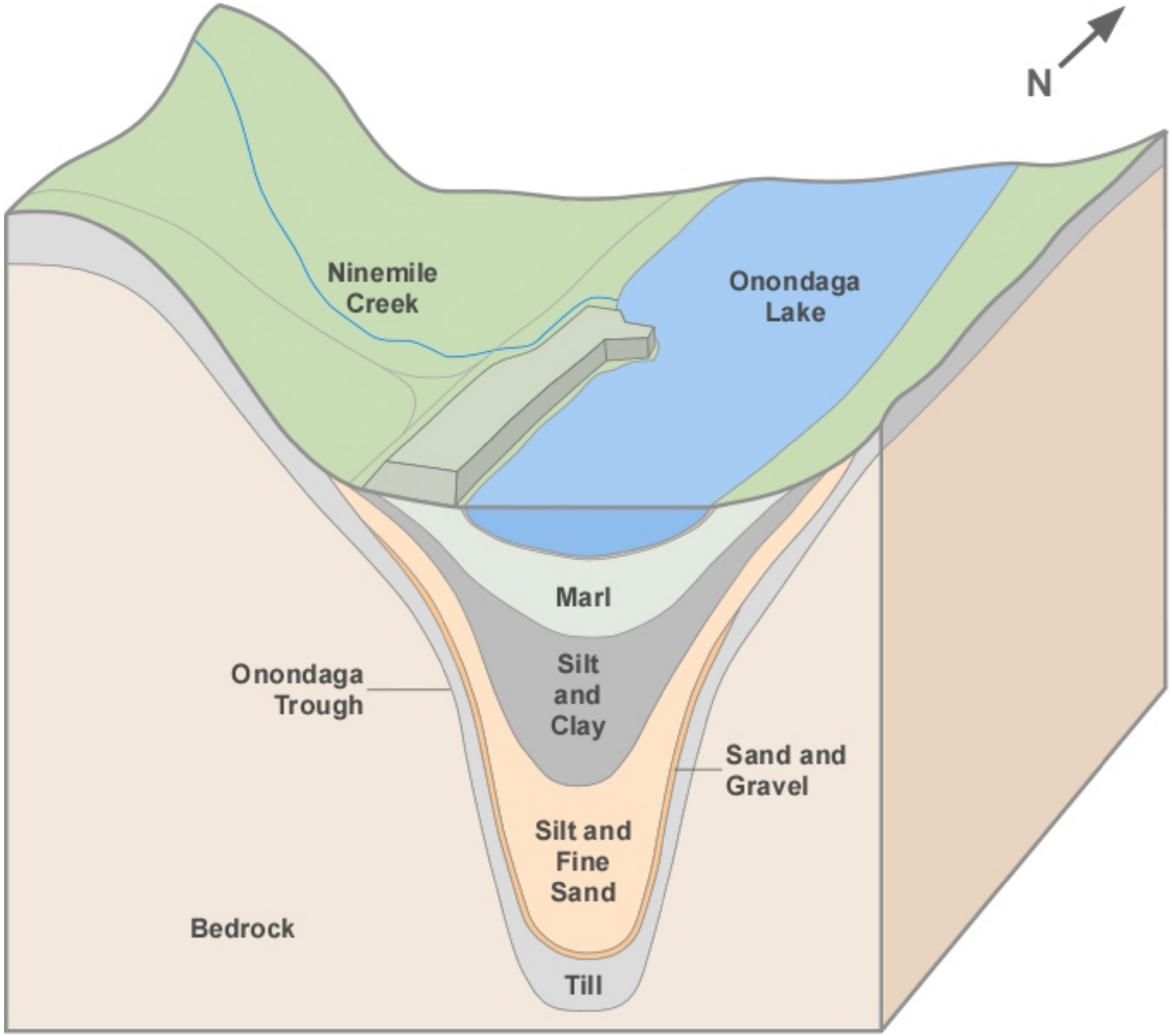

Figure 2 Hydrogeologic Setting of Onondaga Lake

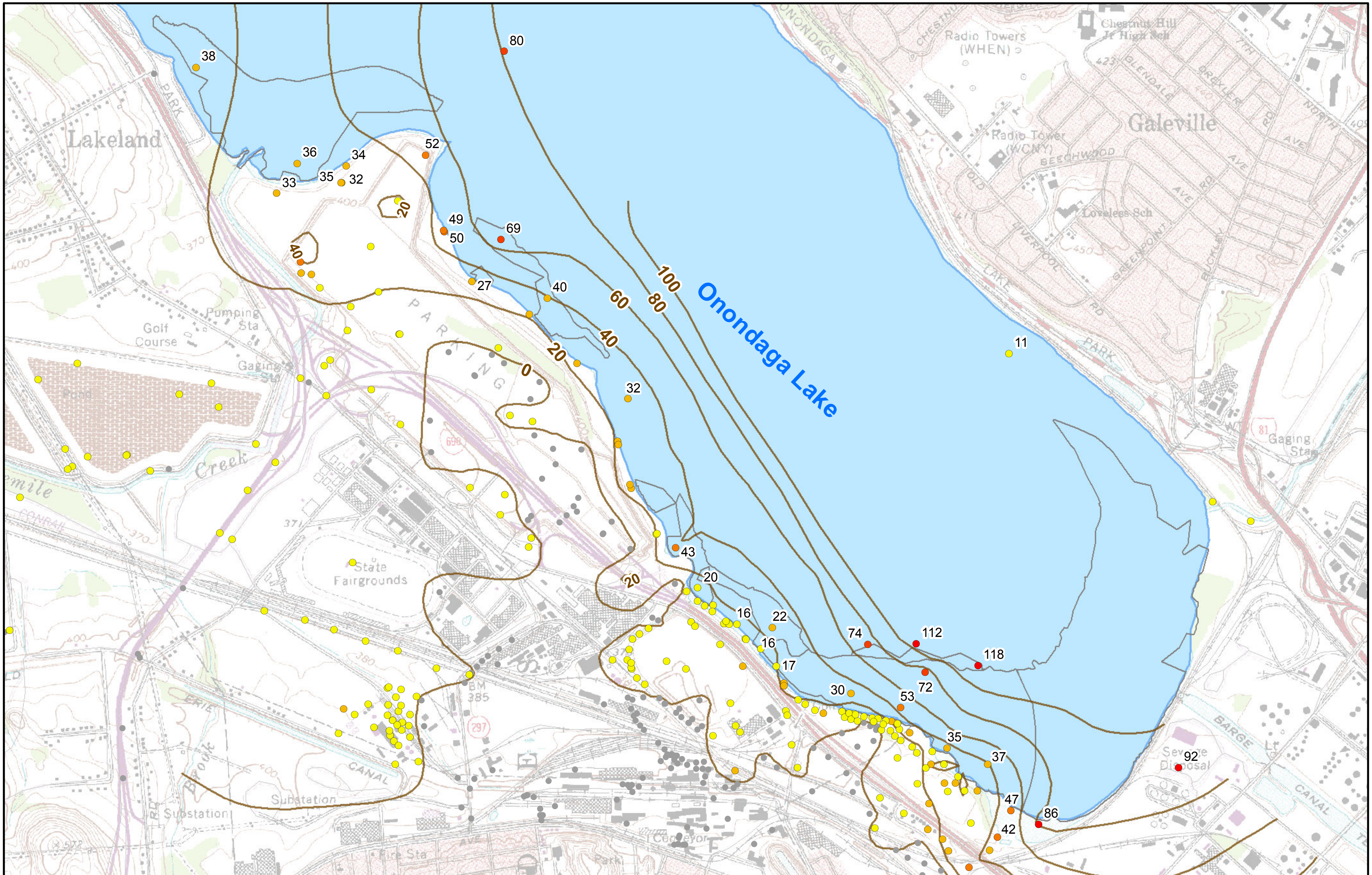

Thickness of Silt/Clay (feet)

- < 20
- 20 - 40
- 40 - 60
- 60 - 80
- > 80
- Unit Absent

Thickness Contours (feet)

Remediation Area

0 1,000 2,000 4,000
Feet

FIGURE 3

Honeywell Onondaga Lake
Syracuse, New York

Thickness of Silt and Clay Unit

$\Sigma^2\Pi$ S. S. Papadopulos & Assoc.

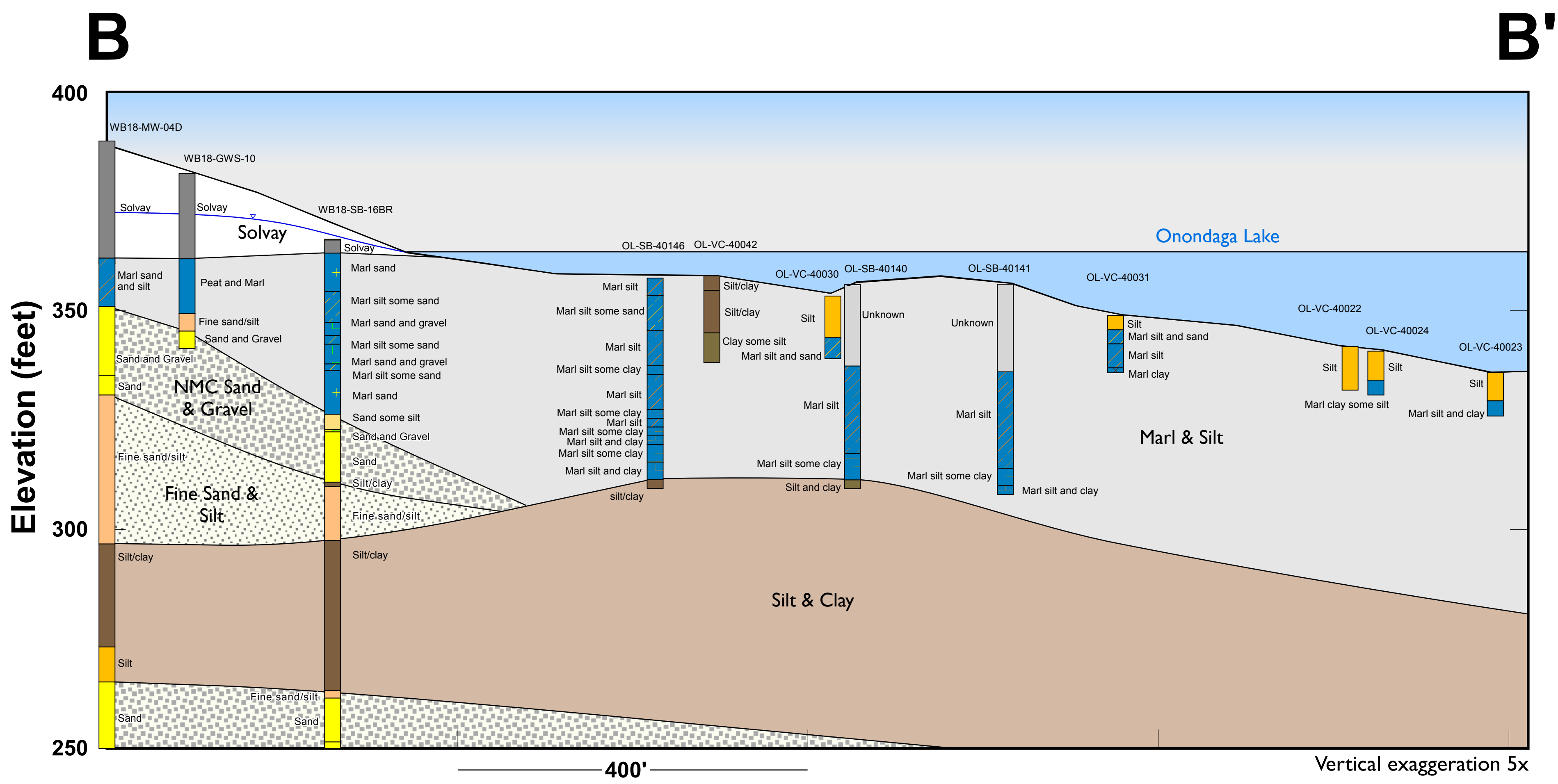

Figure 4 Remediation Area A - Hydrogeologic Cross Section B-B’

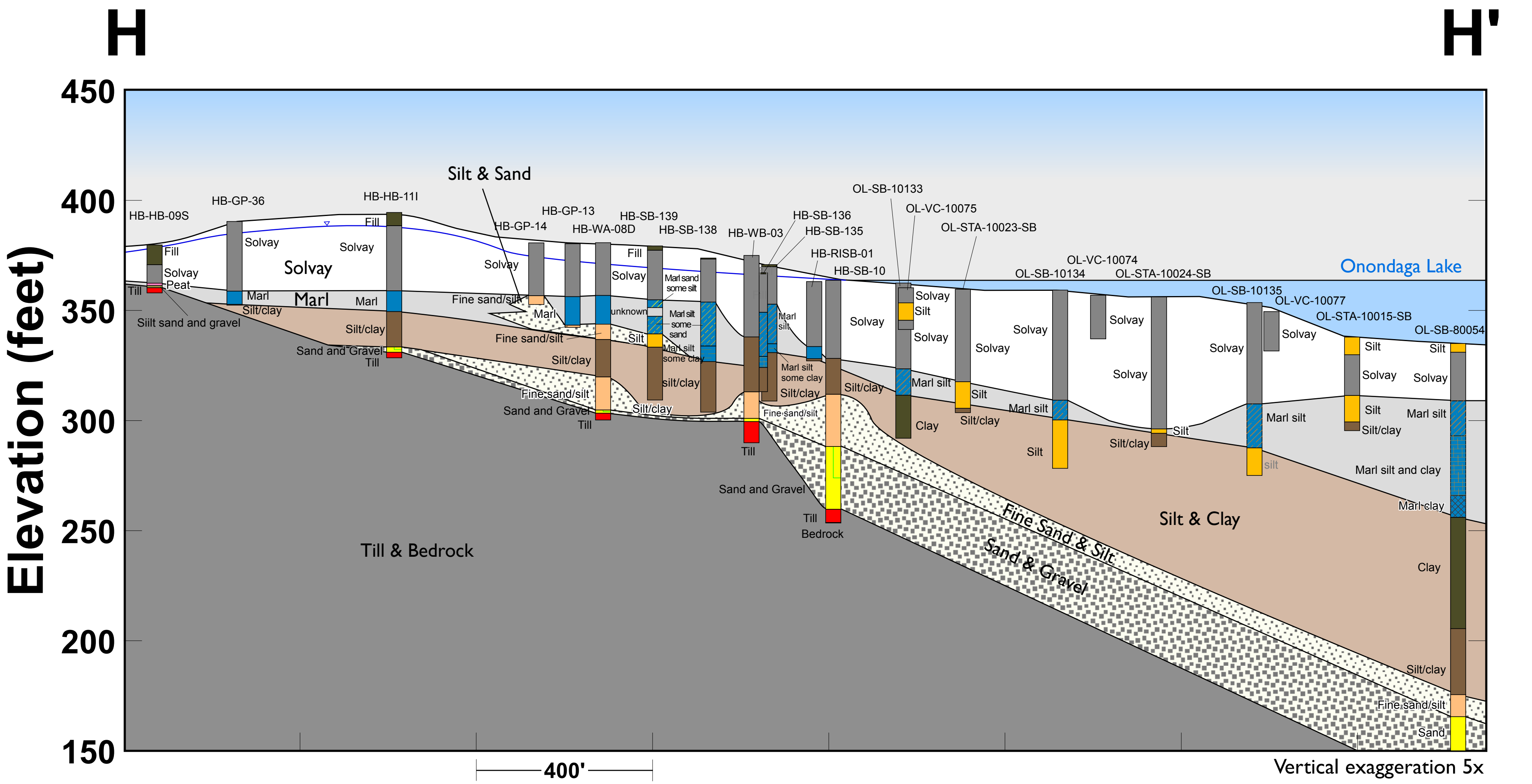

Figure 5 Remediation Area D - Hydrogeologic Cross Section H-H’

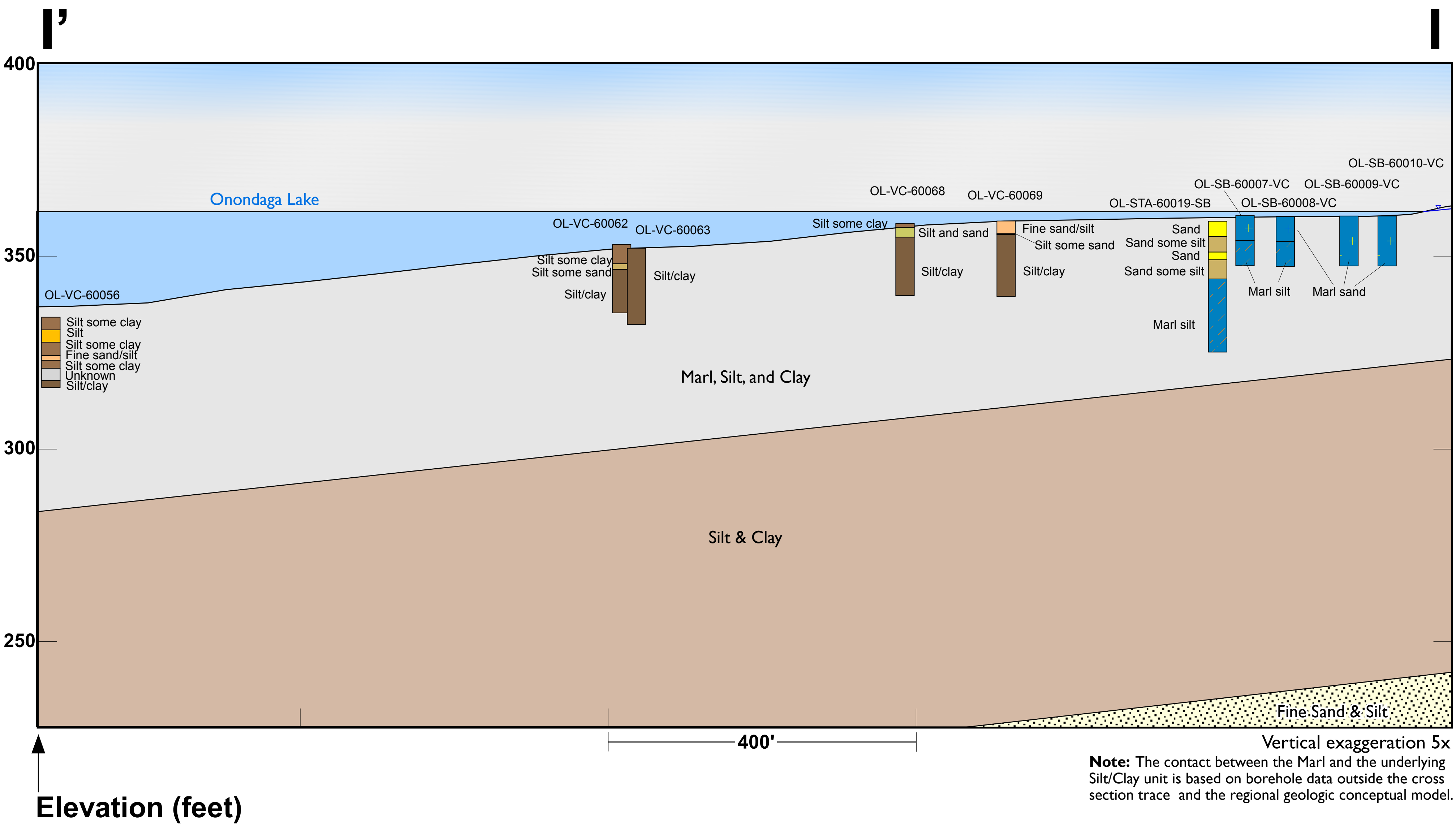

Note: The contact between the Marl and the underlying Silt/Clay unit is based on borehole data outside the cross section trace and the regional geologic conceptual model.

Figure 6 Remediation Area E - Hydrogeologic Cross Section I-I'

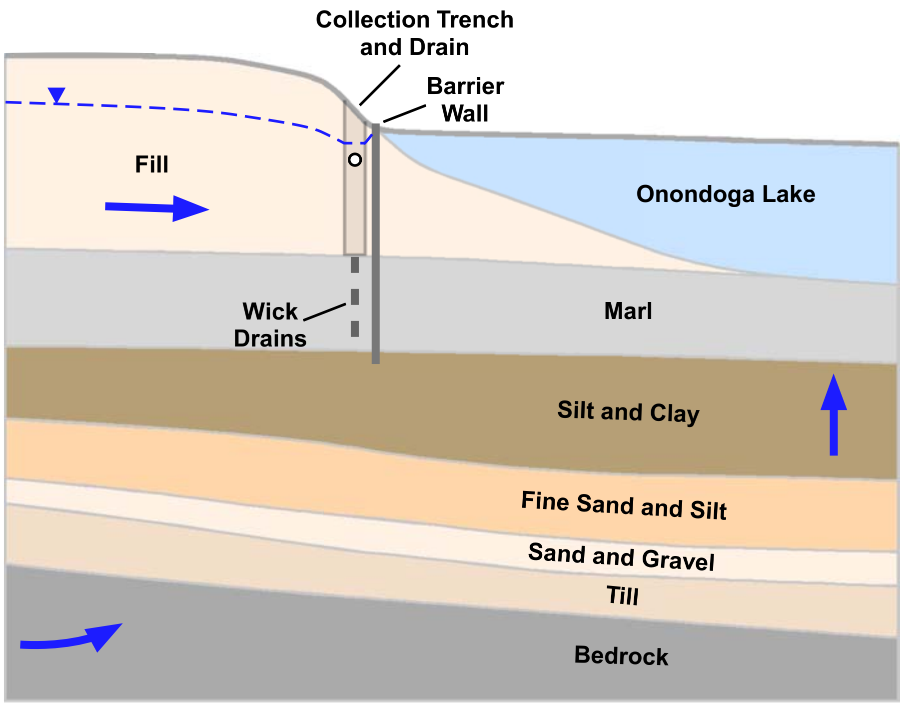

Hydraulic Containment System with Barrier Wall

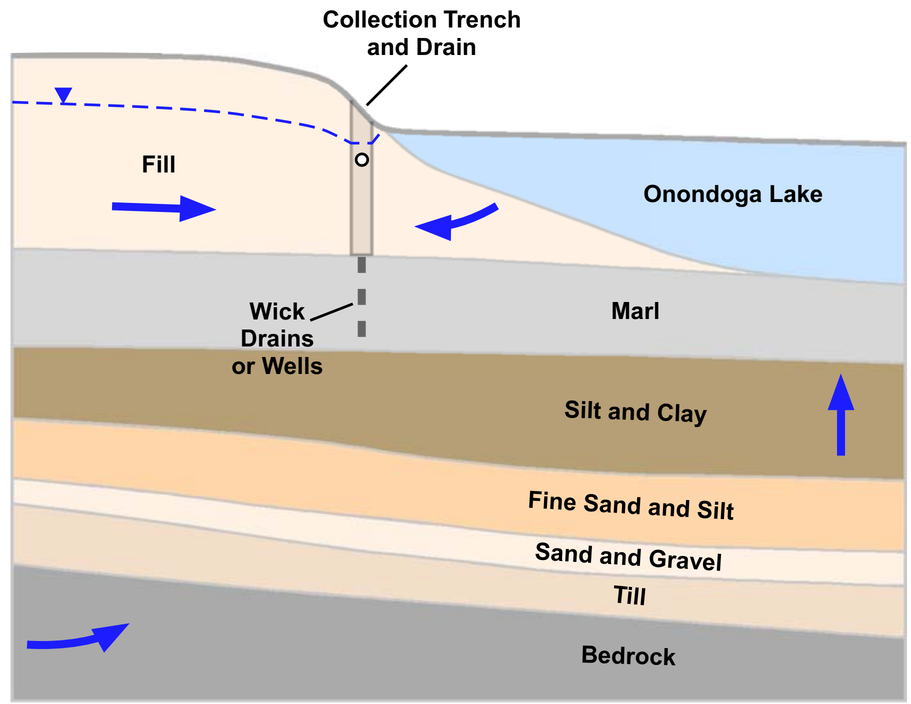

P:\815\Graphics\2009_2010 Upwelling Figure Cross Sections\Cross Section with Wick Fig 7 Nov 2010.cnv

Hydraulic Containment System without Barrier Wall

Figure 7 Schematic of Hydraulic Containment System and Groundwater Flow Through Silt and Clay Unit

S.S. Papadopoulos & Associates, Inc.

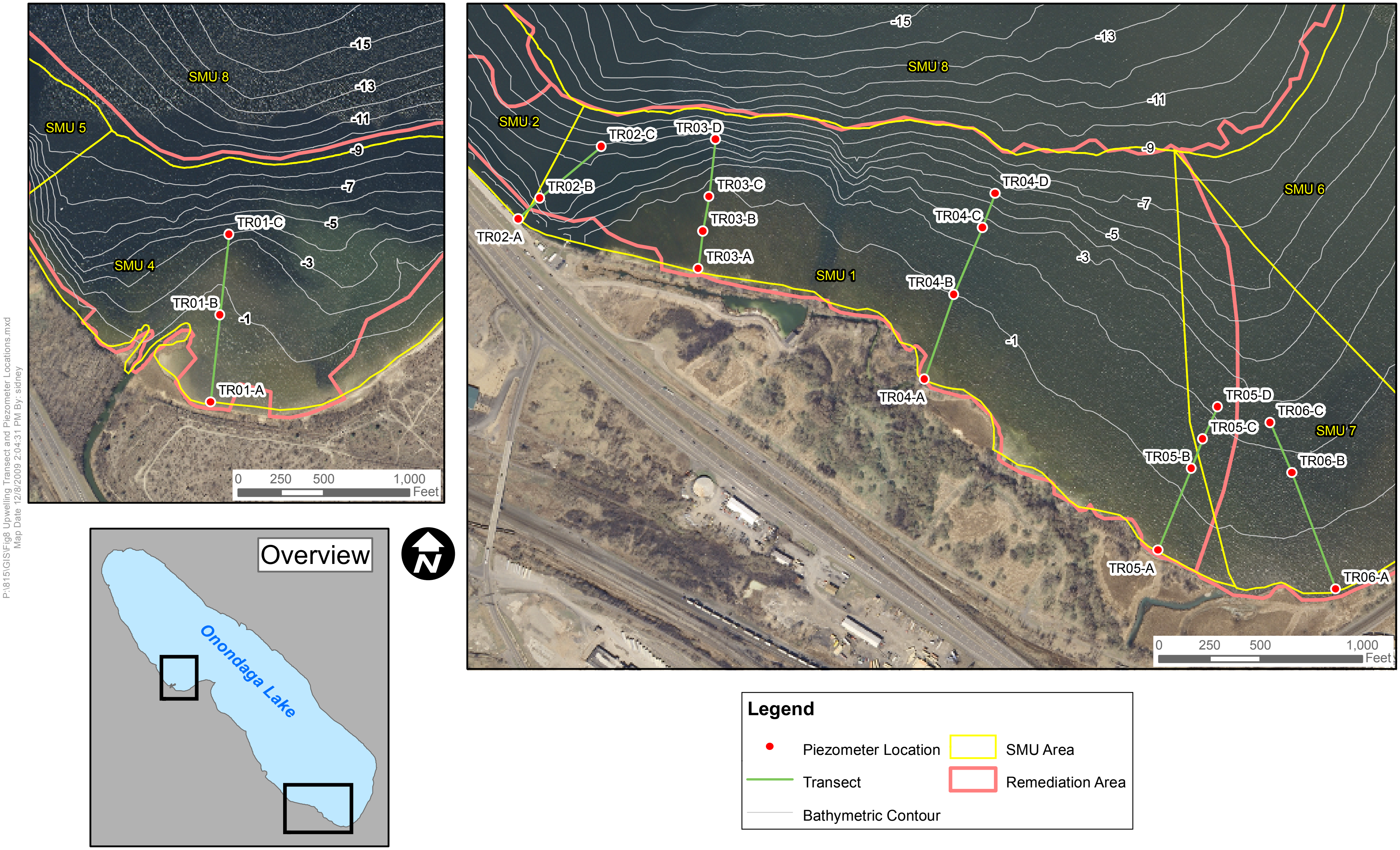

Figure 8 Upwelling Transect and Piezometer Locations

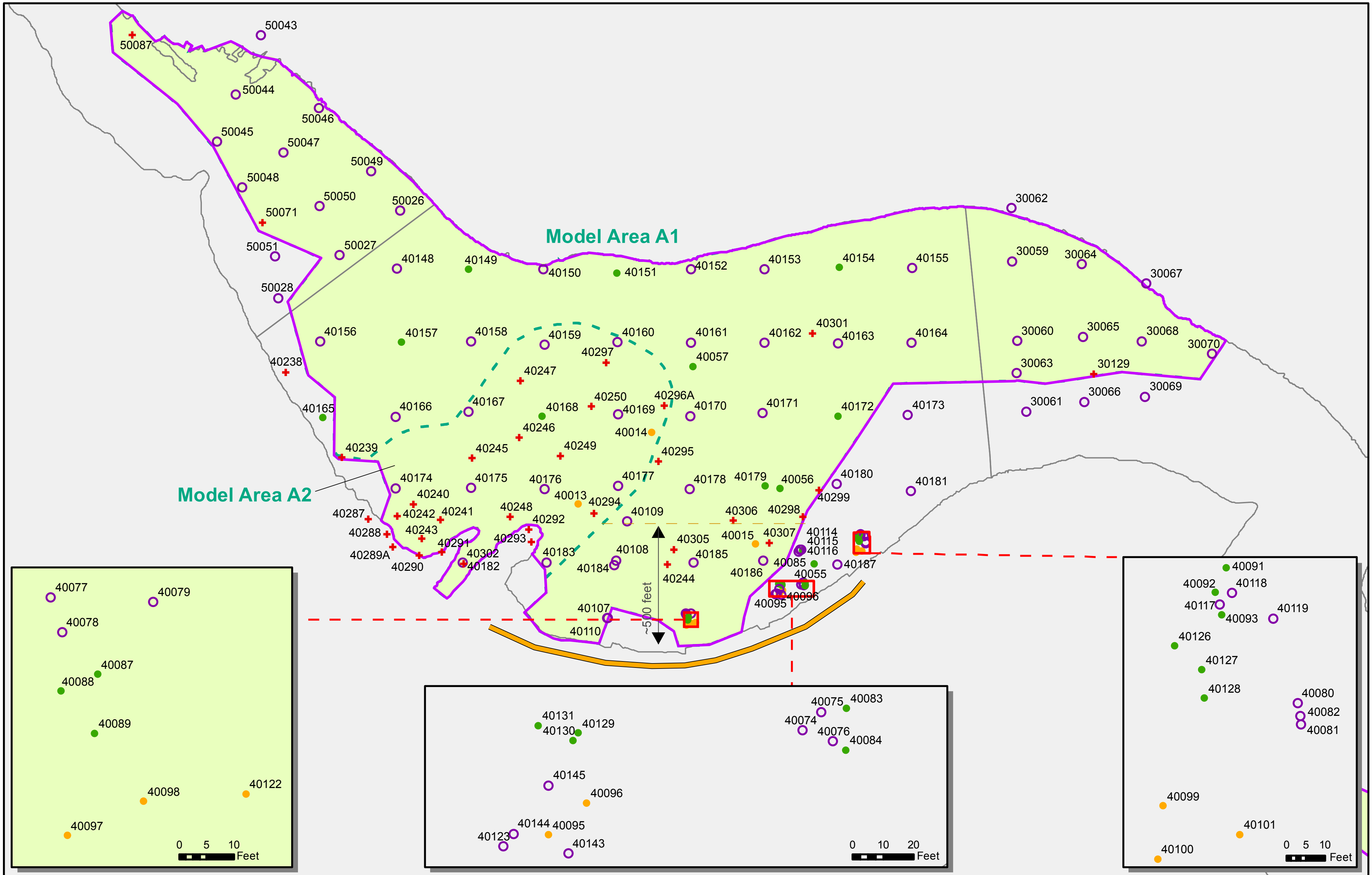

40013 Seepage Meter Location

40301 Phase V & VI Upwelling Velocity Pore Water Data Location

40162 Upwelling Velocity Sediment Conductivity Data Location

40057 Upwelling Velocity Pore Water Data Location

Hydraulic Containment System

Remediation Area

Model Area Boundary

SMU Boundary

Isolation Cap Area

N

0 250 500 1,000

Feet

FIGURE 9

Honeywell

Onondaga Lake
Syracuse, New York

Upwelling Measurement and Seepage Meter Locations - Remediation Area A

$\Sigma^2\Pi$ S. S. Papadopulos & Assoc.

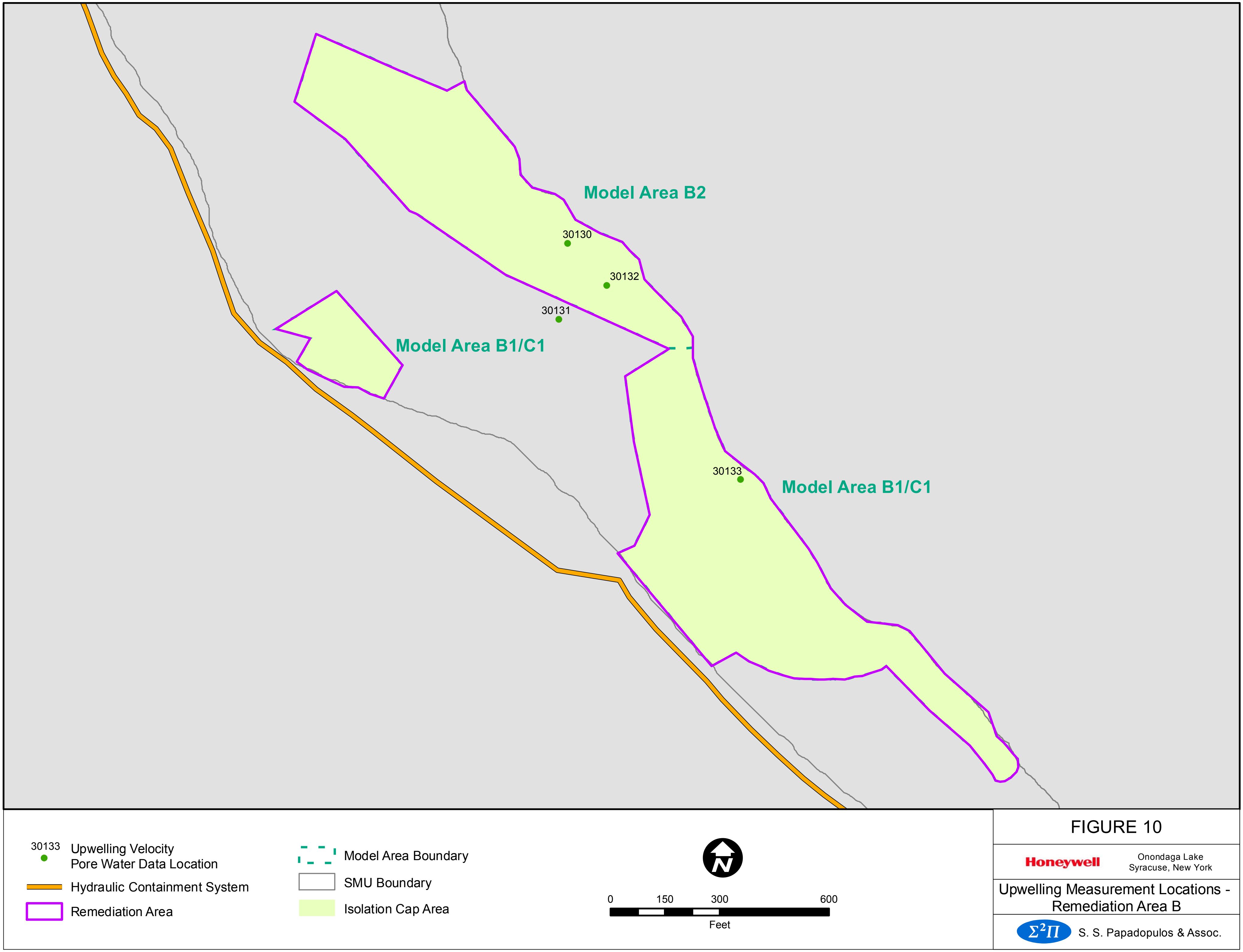

FIGURE 10

Honeywell

Onondaga Lake
Syracuse, New York

Upwelling Measurement Locations - Remediation Area B

S. S. Papadopulos & Assoc.

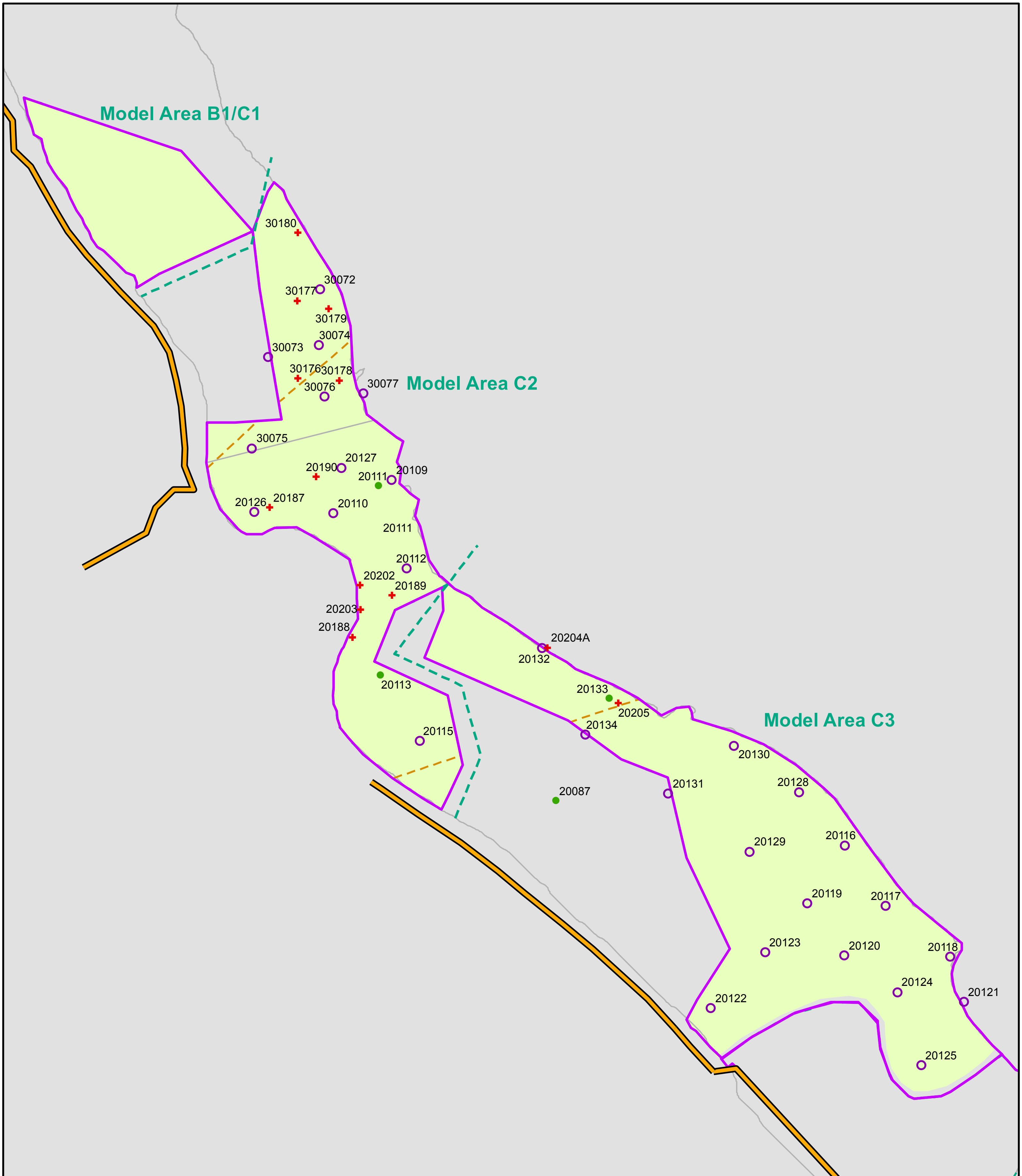

20202 Phase V & VI Upwelling Velocity Pore Water Data Location

20115 Upwelling Velocity Sediment Conductivity Data Location

20133 Upwelling Velocity Pore Water Data Location

Hydraulic Containment System

Extent of the Effect of the Hydraulic Containment System

Remediation Area

Model Area Boundary

SMU Boundary

Isolation Cap Area

0 125 250 500
Feet

FIGURE 11

Honeywell

Onondaga Lake
Syracuse, New York

Upwelling Measurement Locations - Remediation Area C

S. S. Papadopulos & Assoc.

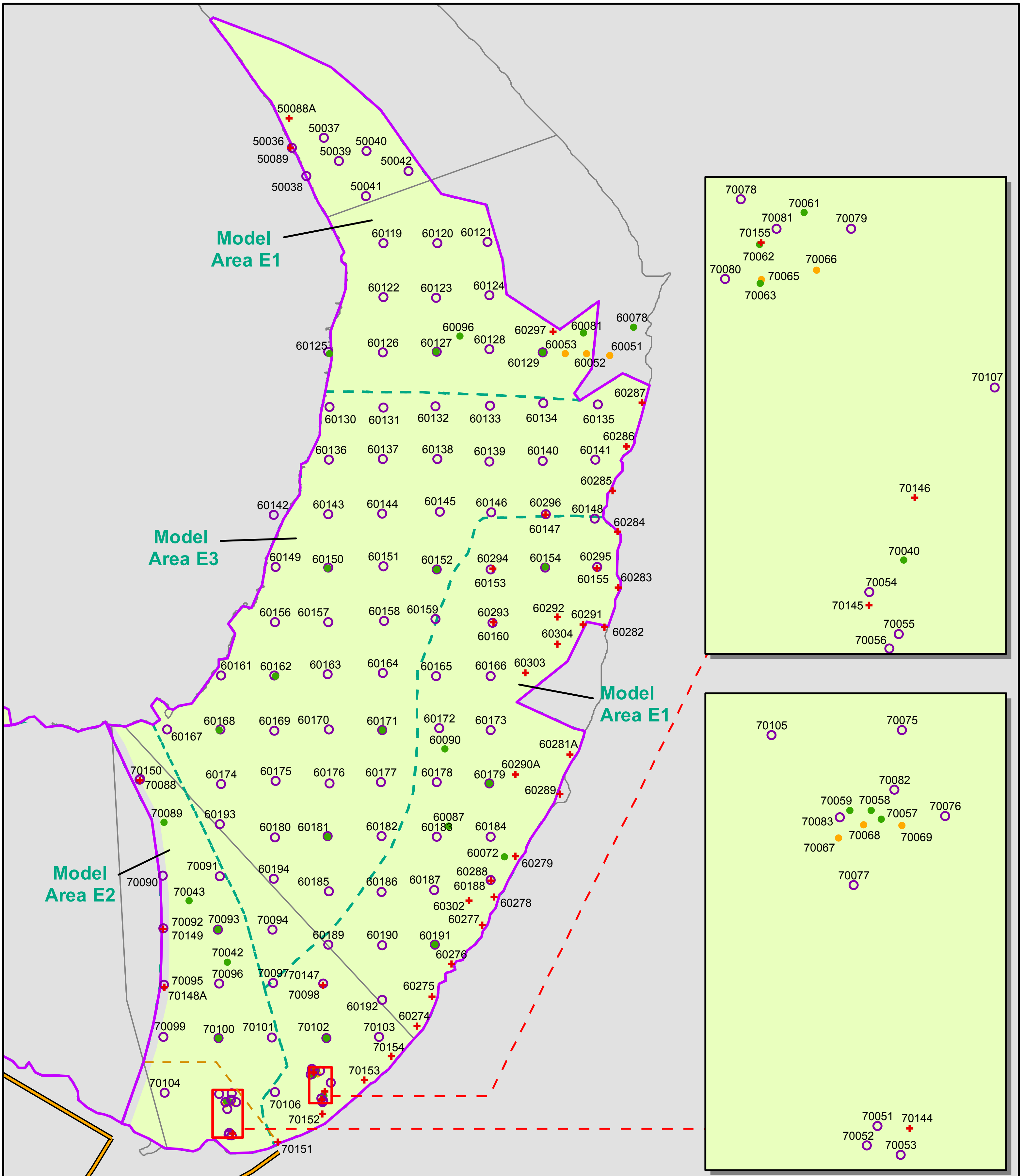

70067 Seepage Meter

70154 Phase V & VI Upwelling Velocity Sediment Conductivity Location

50041 Upwelling Velocity Sediment Conductivity Data Location

60154 Upwelling Velocity Pore Water Data Location

Hydraulic Containment System

Remediation Area

Model Area Boundaries

SMU Boundary

Isolation Cap Area

0 250 500 1,000

Feet

FIGURE 12

Honeywell

Onondaga Lake
Syracuse, New York

Upwelling Measurement and Seepage Meter Locations - Remediation Area E

S. S. Papadopulos & Assoc.

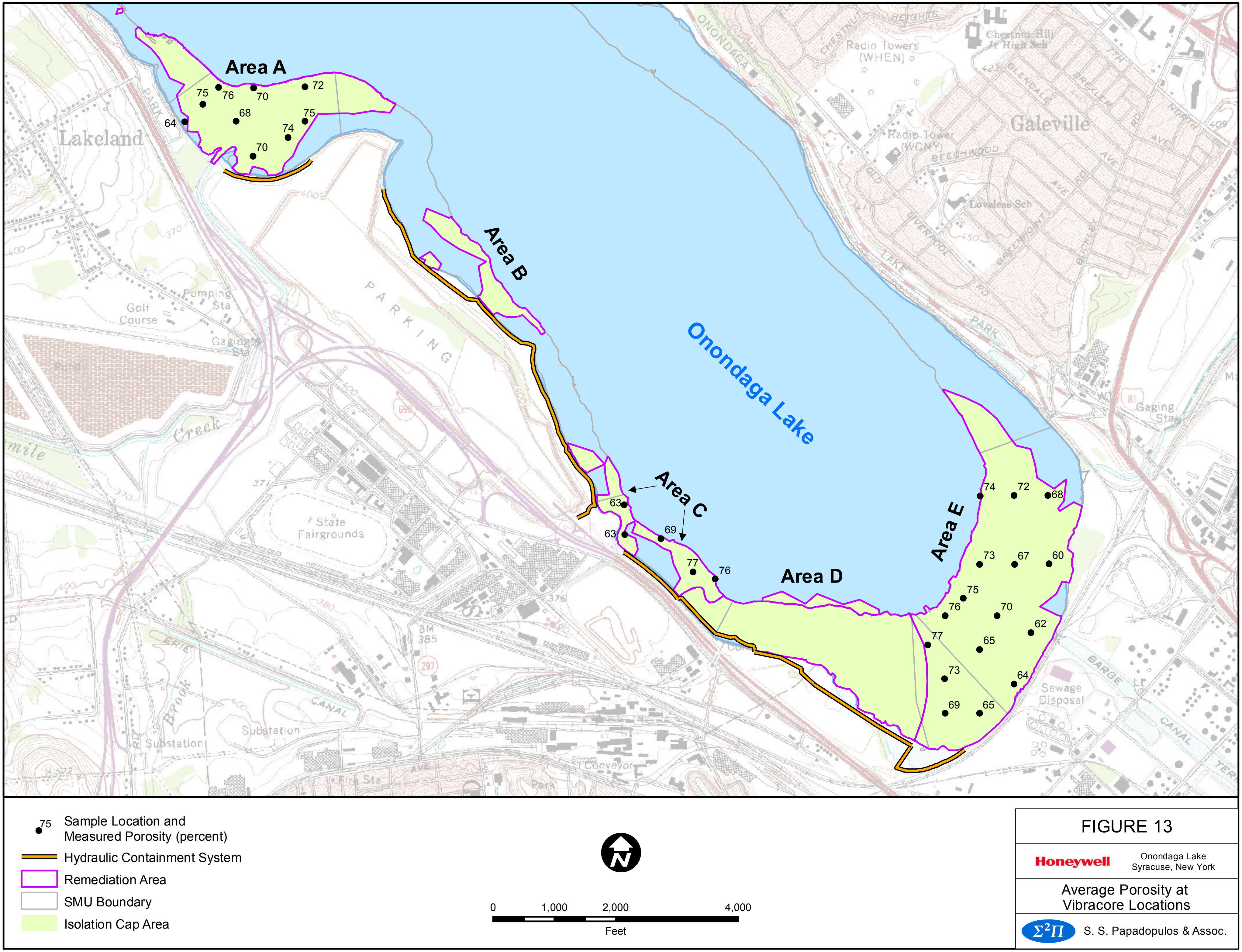

FIGURE 13

Honeywell Onondaga Lake Syracuse, New York

Average Porosity at Vibracore Locations

S. S. Papadopulos & Assoc.

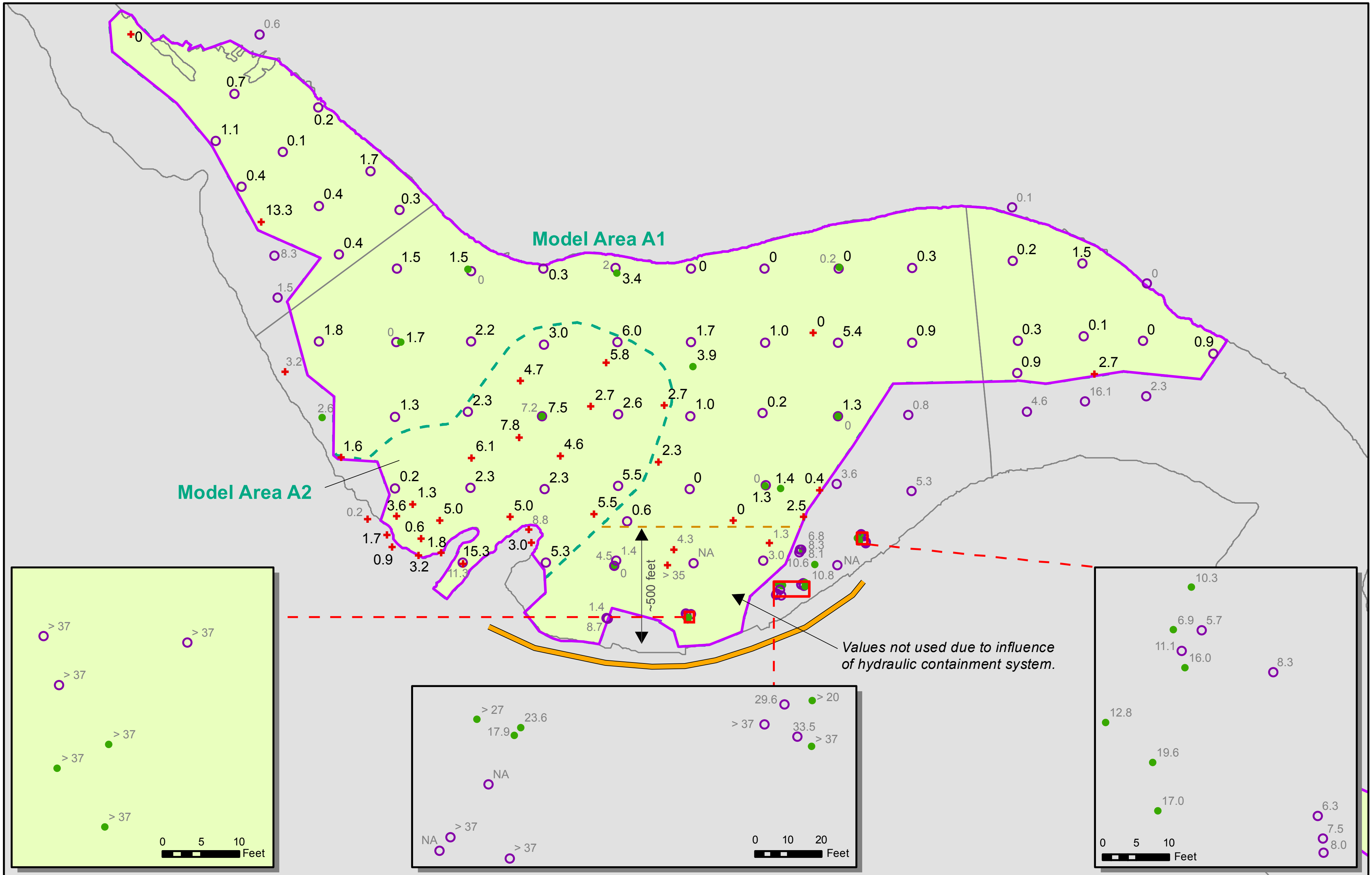

6.1 Phase V & VI Upwelling Velocity Pore Water Data (cm/yr)

5.4 Upwelling Velocity Sediment Conductivity Data (cm/yr)

1.2 Upwelling Velocity Pore Water Data (cm/yr)

Hydraulic Containment System

Remediation Area

Model Area Boundary

SMU Boundary

Isolation Cap Area

Note: Upwelling velocity values that are in light grey type are not used in the cap design analysis.

0 250 500 1,000
Feet

FIGURE 14

Honeywell

Onondaga Lake
Syracuse, New York

Upwelling Velocities in Model Areas A1 and A2

S. S. Papadopulos & Assoc.

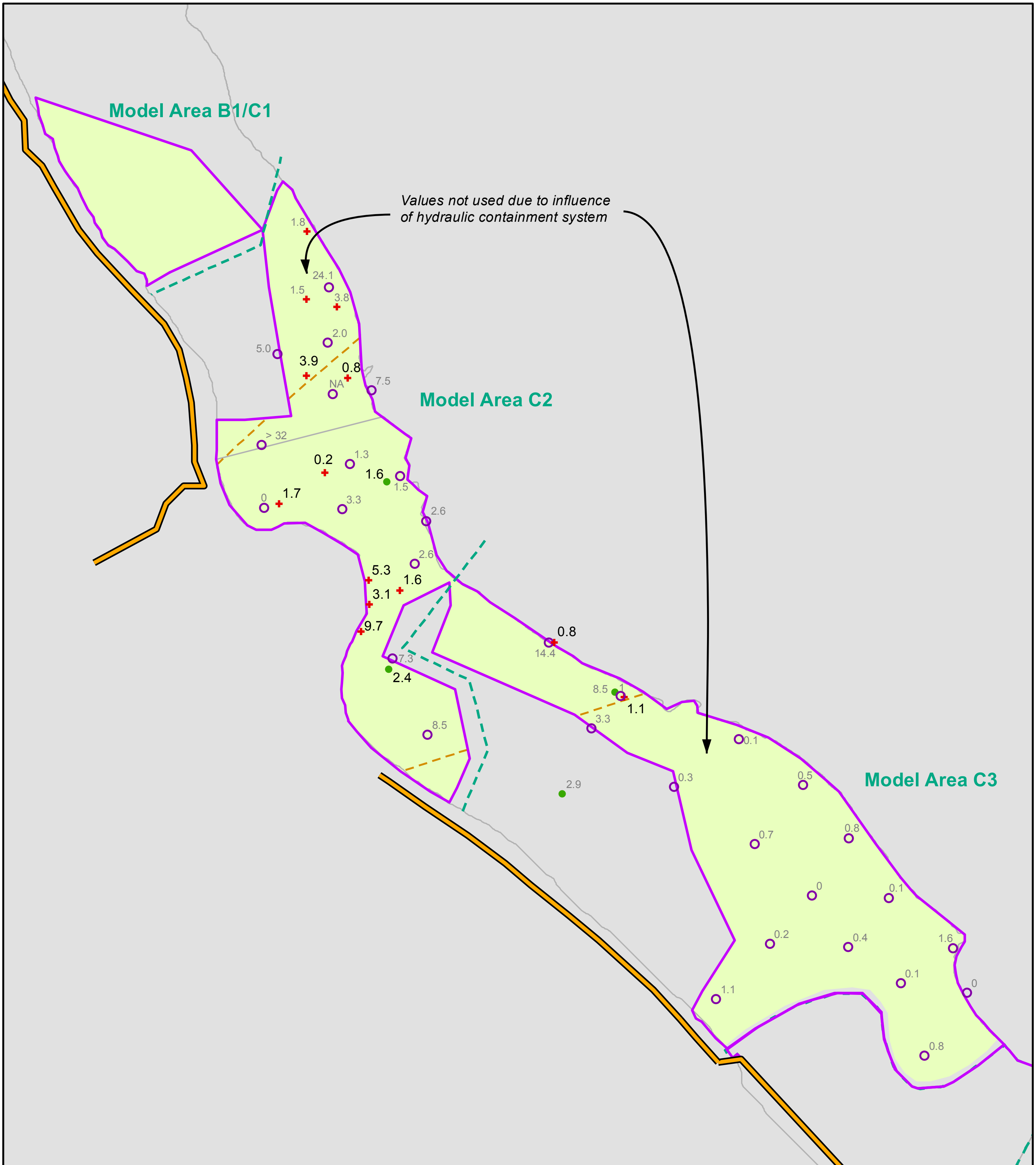

Note: Upwelling velocity values that are in light grey type are not used in the cap design analysis.

2.1 Phase V & VI Upwelling Velocity Pore Water Data (cm/yr)	Extent of the Effect of the Hydraulic Containment System
1.7 Upwelling Velocity Sediment Conductivity Data (cm/yr)	Remediation Area
0.7 Upwelling Velocity Pore Water Data (cm/yr)	Model Area Boundary
Hydraulic Containment System	SMU Boundary
	Isolation Cap Area

0 125 250 500
Feet

FIGURE 15

Honeywell
Onondaga Lake
Syracuse, New York

Upwelling Velocities
in Model Area C2

S. S. Papadopulos & Assoc.

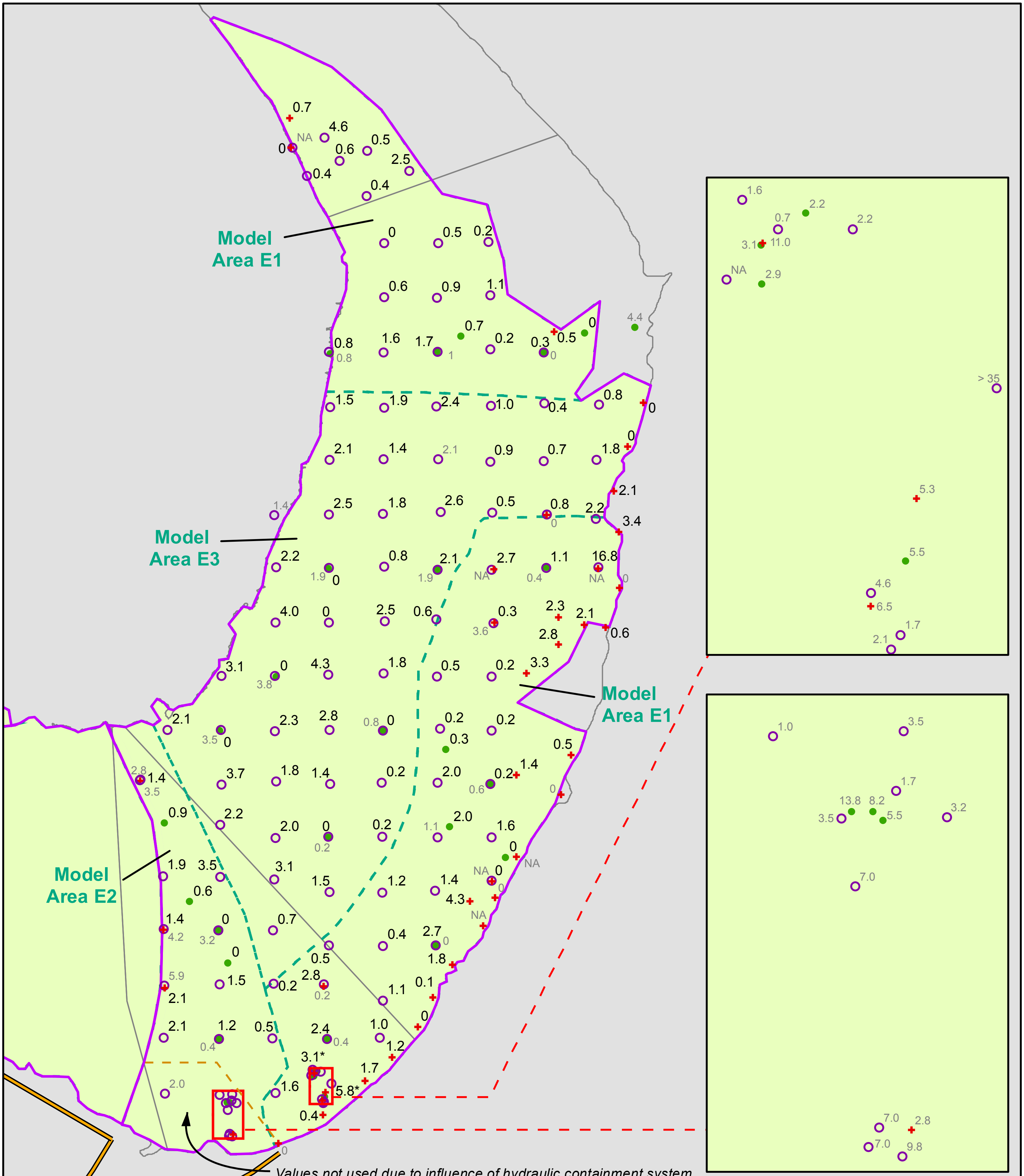

1.8 Phase V & VI Upwelling Velocity Sediment Conductivity Data (cm/yr)

3.6 Upwelling Velocity Sediment Conductivity Data (cm/yr)

4.2 Upwelling Velocity Pore Water Data (cm/yr)

Note: Upwelling velocity values that are in light grey type are not used in the cap design analysis.

Remediation Area

Model Area Boundary

SMU Boundary

Isolation Cap Area

Hydraulic Containment System

** Represents an average value.*

0 250 500 1,000

Feet

FIGURE 16

Honeywell

Onondaga Lake
Syracuse, New York

Upwelling Velocities in Model Areas E1, E2, and E3

S. S. Papadopulos & Assoc.

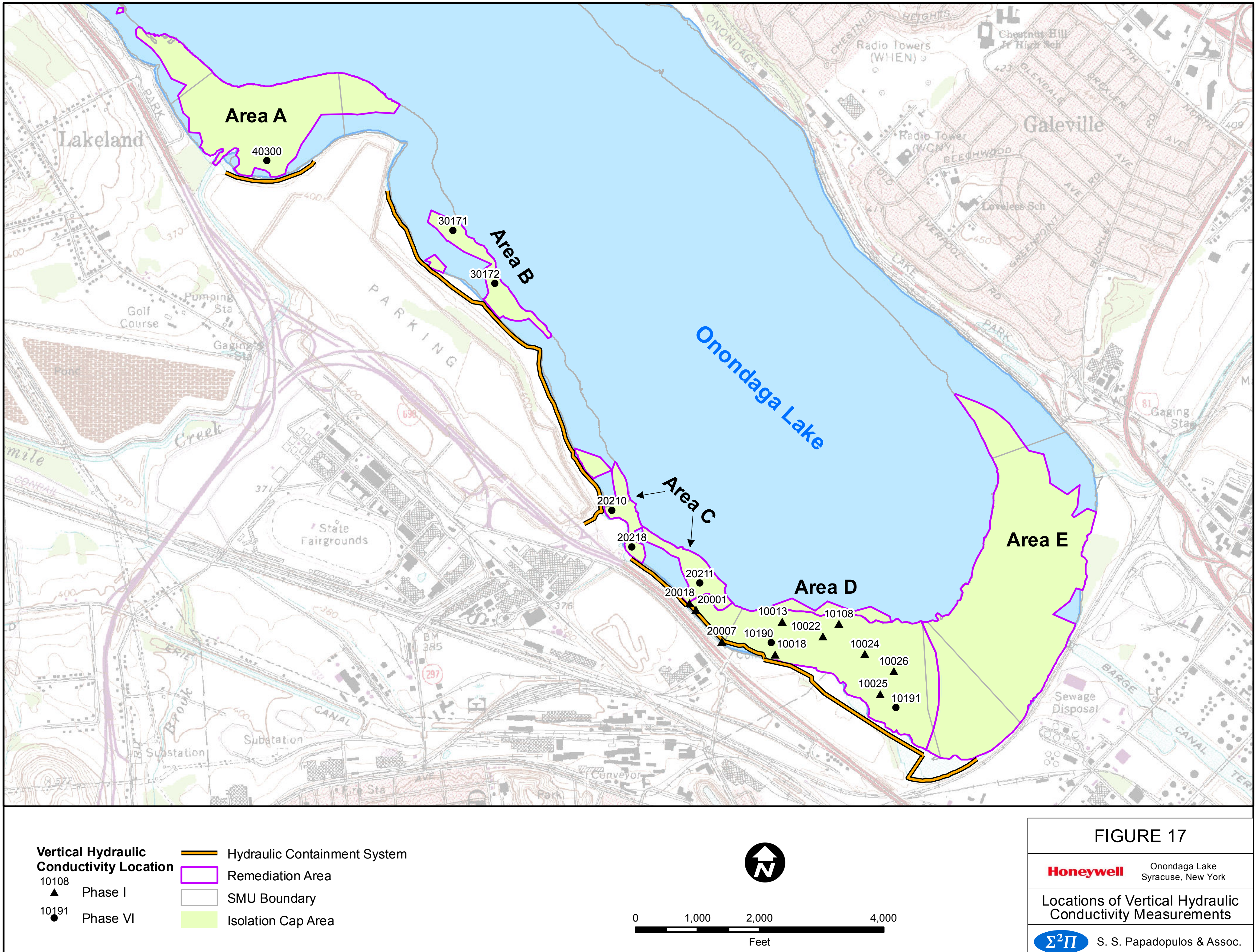

FIGURE 17

Honeywell — Onondaga Lake, Syracuse, New York

Locations of Vertical Hydraulic Conductivity Measurements

$\Sigma^2\Pi$ S. S. Papadopulos & Assoc.

4.7 Phase I to V Upwelling Velocity Pore Water Data (cm/yr)

Upwelling Velocity Contours

Hydraulic Containment System

Remediation Area

Model Area Boundary

SMU Boundary

Isolation Cap Area

0 150 300 600

Feet

FIGURE 18

Honeywell

Onondaga Lake
Syracuse, New York

Average Upwelling Velocity in Remediation Area B

S. S. Papadopulos & Assoc.

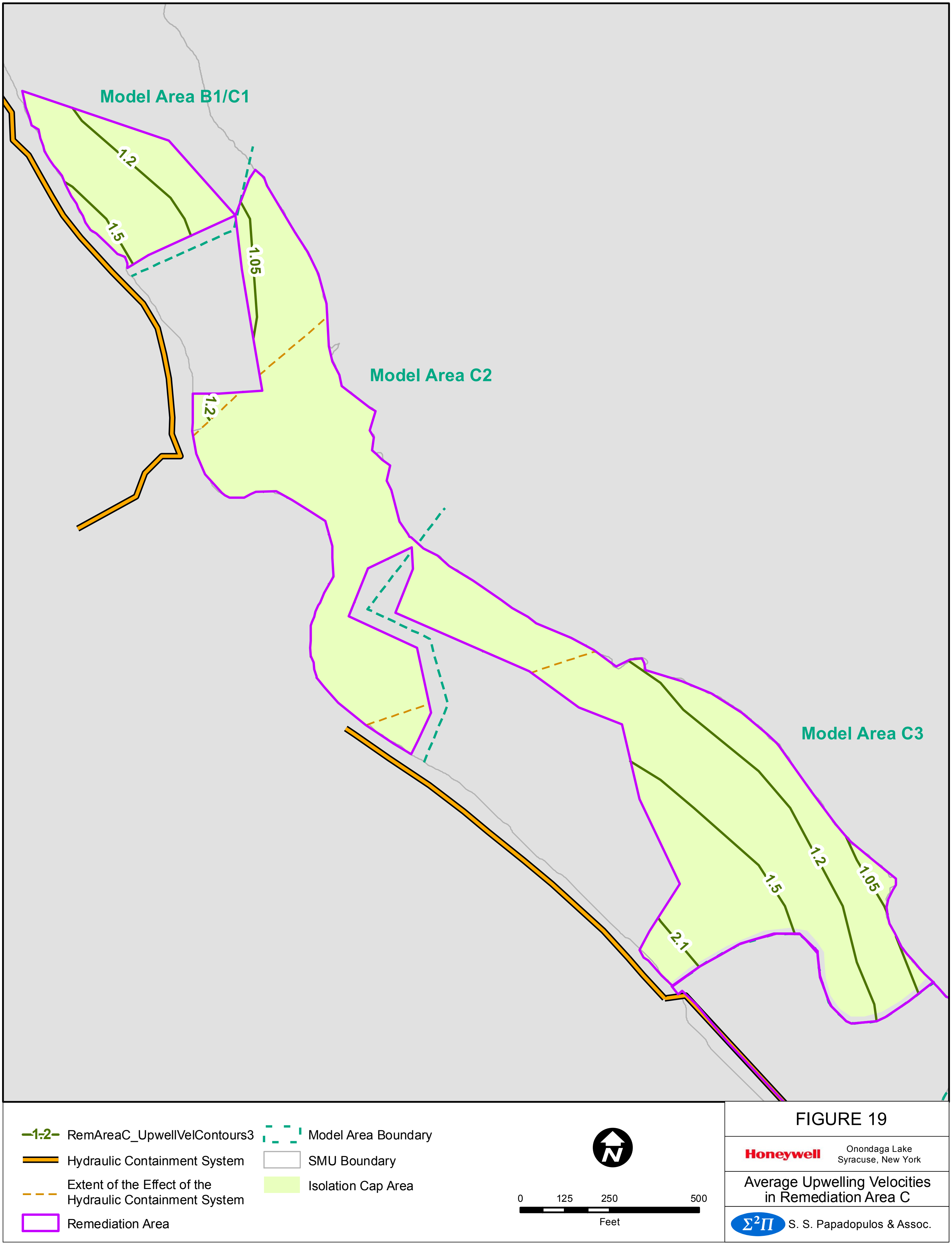

FIGURE 19

Honeywell

Onondaga Lake
Syracuse, New York

Average Upwelling Velocities in Remediation Area C

S. S. Papadopulos & Assoc.

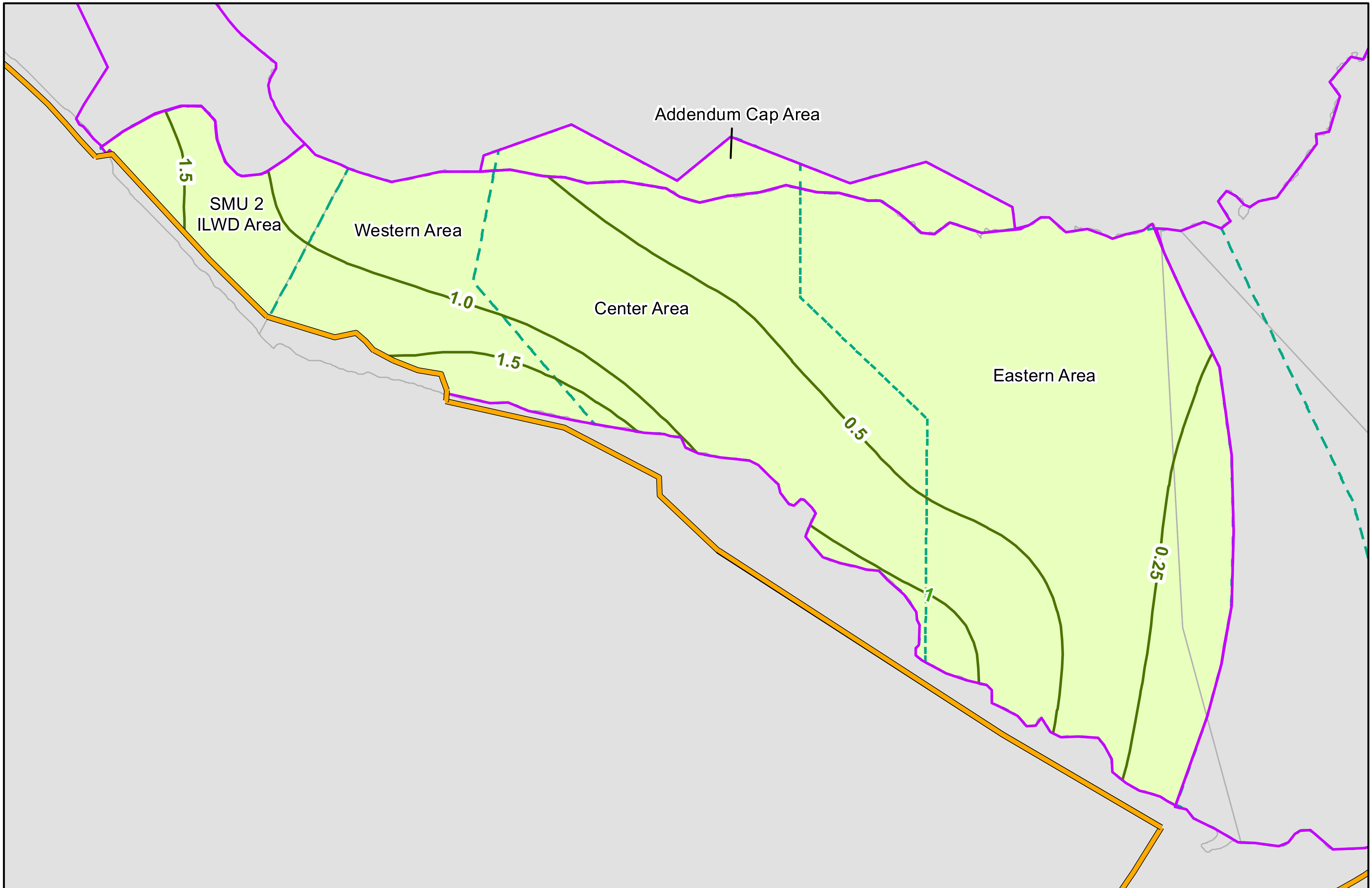

Hydraulic Containment System

Upwelling Velocity (cm/yr)

Remediation Area

Model Area Boundary

SMU Boundary

Isolation Cap Area

0 500 1,000

Feet

FIGURE 20

Honeywell

Onondaga Lake
Syracuse, New York

Average Upwelling Velocities
in Remadiation Area D

S. S. Papadopulos & Assoc.

TABLES

Table 1

Summary of Upwelling Velocities used to Develop Cumulative Frequency Distributions for Model Areas A1, A2, and C2 and Remediation Area E

Location ID	Remediation Area	Type[1]	Upwelling Velocity (cm/year)	90% Confidence Interval (+/-) (cm/year)	Depth Interval Used (feet)	Comments
30059	A1	GP	0.2	0.03	5	good
30060	A1	GP	0.3	0.05	10	good
30063	A1	GP	0.9	0.05	5	fair
30064	A1	GP	1.5	0.11	5	fair
30065	A1	GP	0.1	0.02	5	fair
30068	A1	GP	~0.0	0.04	5	fair
30070	A1	GP	0.9	0.04	5	good
30129	A1	VC	2.7	0.64	5	good
40056	A1	VC	1.4	0.18	5	good
40057	A1	VC	3.9	1.80	10	10-foot anlysis fair, 5-foot analysis poor, used 10' analysis
40109	A1	GP	0.6	0.01	5	fair
40148	A1	GP	1.5	0.15	5	fair
40149	A1	VC	1.5	0.66	5	fair
40150	A1	GP	0.3	0.03	5	good
40151	A1	VC	3.4	0.70	5	fair
40152	A1	GP	~0.0	0.02	5	good
40153	A1	GP	~0.0	0.02	5	good
40154	A1	VC	~0.0	0.16	5	good
40155	A1	GP	0.3	0.01	5	good
40156	A1	GP	1.8	0.10	10	good
40157	A1	VC	1.7	0.34	5	good
40158	A1	GP	2.2	0.12	5	good
40161	A1	GP	1.7	0.07	10	good
40162	A1	GP	1.0	0.06	5	good
40163	A1	GP	5.4	0.23	5	fair
40164	A1	GP	0.9	0.03	5	good
40166	A1	GP	1.3	0.04	5	good
40170	A1	GP	1.0	0.02	10	fair
40171	A1	GP	0.2	0.02	5	good
40172	A1	VC	1.3	0.45	5	good
40178	A1	GP	~0.0	0.11	5	good
40179	A1	VC	1.3	0.37	10	good
40239	A1	VC	1.6	0.11	10	good
40295	A1	VC	2.3	0.25	5	good
40298	A1	VC	2.4	0.27	5	good

Table 1

Summary of Upwelling Velocities used to Develop Cumulative Frequency Distributions for Model Areas A1, A2, and C2 and Remediation Area E

Location ID	Remediation Area	Type[1]	Upwelling Velocity (cm/year)	90% Confidence Interval (+/-) (cm/year)	Depth Interval Used (feet)	Comments
40299	A1	VC	0.4	0.01	10	good
40301	A1	VC	~0.0	0.11	5	good
40306	A1	VC	~0.0	0.1	5	good
50026	A1	GP	0.3	0.02	5	good
50027	A1	GP	0.4	0.04	5	good
50044	A1	GP	0.7	0.02	10	good
50045	A1	GP	1.1	0.05	5	good
50046	A1	GP	0.2	0.03	5	good
50047	A1	GP	0.1	0.02	10	good
50048	A1	GP	0.4	0.07	5	fair to poor
50049	A1	GP	1.7	0.12	5	good
50050	A1	GP	0.4	0.02	5	good
50071	A1	VC	13.3	3.42	5	good
50087	A1	VC	~0.0	0.17	5	good
40159	A2	GP	3.0	0.23	5	fair
40160	A2	GP	6.0	0.57	10	good
40167	A2	GP	2.3	0.06	10	fair
40168	A2	VC	7.5	1.38	5	good
40169	A2	GP	2.6	0.08	10	good
40174	A2	GP	0.2	0.02	5	good
40175	A2	GP	2.3	0.11	10	good
40176	A2	GP	2.3	0.57	5	fair based on upper two feet
40177	A2	GP	5.5	0.29	5	good
40183	A2	GP	5.3	0.75	10	poor
40240	A2	VC	1.3	0.39	5	good
40241	A2	VC	5.0	0.42	5	good
40242	A2	VC	3.6	0.70	5	good
40243	A2	VC	0.6	0.18	10	good
40245	A2	VC	6.1	0.38	5	good
40246	A2	VC	7.8	1.31	5	good
40247	A2	VC	4.7	0.49	10	good
40248	A2	VC	5.0	0.99	10	good
40249	A2	VC	4.6	1.38	10	good
40250	A2	VC	2.7	0.90	10	good
40288	A2	VC	1.7	0.28	5	good

Table 1

Summary of Upwelling Velocities used to Develop Cumulative Frequency Distributions for Model Areas A1, A2, and C2 and Remediation Area E

Location ID	Remediation Area	Type[1]	Upwelling Velocity (cm/year)	90% Confidence Interval (+/-) (cm/year)	Depth Interval Used (feet)	Comments
40289	A2	VC	0.9	0.31	5	good
40290	A2	VC	3.2	1.13	5	fair
40291	A2	VC	1.8	0.44	5	good
40293	A2	VC	3.0	1.15	5	fair
40294	A2	VC	5.5	0.51	5	fair
40296	A2	VC	2.7	0.68	5	good
40297	A2	VC	5.8	0.78	10	good
40302	A2	VC	15.3	4.22	5	fair
20111	C2	VC	1.6	0.54	5	fair
20113	C2	VC	2.4	0.56	5	good
20187	C2	VC	1.7	0.58	10	good
20188	C2	VC	9.7	2.81	5	good
20189	C2	VC	1.6	0.54	5	good
20190	C2	VC	0.2	0.39	10	good, adjusted based on confidence interval
20202	C2	VC	5.3	1.65	5	fair at 5 foot, poor at 10 foot analysis
20203	C2	VC	3.1	1.36	5	fair
30176	C2	VC	3.9	1.86	5	fair
30178	C2	VC	0.8	0.39	5	good
20204	C3	VC	0.8	0.07	5	good
20205	C3	VC	1.1	0.06	5	good
50037	E1	GP	4.6	0.88	5	fair
50038	E1	GP	0.4	0.02	5	good
50039	E1	GP	0.6	0.02	5	good
50040	E1	GP	0.5	0.02	10	good
50041	E1	GP	0.4	0.01	5	good
50042	E1	GP	2.5	0.09	5	fair
50088	E1	VC	0.7	0.13	5	good
50089	E1	VC	~0.0	0.21	5	good
60072	E1	VC	~0.0	0.24	5	fair
60081	E1	VC	~0.0	0.25	5	fair
60087	E1	VC	2.0	0.15	5	good
60090	E1	VC	0.3	0.08	5	good
60096	E1	VC	0.7	0.13	5	good
60119	E1	GP	~0.0	0.03	5	good
60120	E1	GP	0.5	0.02	5	good

Table 1

Summary of Upwelling Velocities used to Develop Cumulative Frequency Distributions for Model Areas A1, A2, and C2 and Remediation Area E

Location ID	Remediation Area	Type[1]	Upwelling Velocity (cm/year)	90% Confidence Interval (+/-) (cm/year)	Depth Interval Used (feet)	Comments
60121	E1	GP	0.2	0.02	10	good
60122	E1	GP	0.6	0.02	5	good
60123	E1	GP	0.9	0.03	5	good
60124	E1	GP	1.1	0.05	5	good
60125	E1	VC	0.8	0.34	5	good
60126	E1	GP	1.6	0.05	10	good
60127	E1	VC	1.7	0.47	5	fair, first data points offset
60128	E1	GP	0.2	0.02	10	good
60129	E1	VC	0.3	0.30	10	fair, adjusted based on confidence interval
60148	E1	GP	2.2	0.22	5	fair
60154	E1	VC	1.1	0.10	10	good
60155	E1	GP	16.8	3.55	5	fair to poor
60165	E1	GP	0.5	0.02	10	good
60166	E1	GP	0.2	0.04	10	good
60172	E1	GP	0.2	0.02	5	good
60173	E1	GP	0.2	0.04	5	good to five feet
60178	E1	GP	2.0	0.06	5	good
60179	E1	VC	0.2	0.60	10	fair, adjusted based on confidence interval
60184	E1	GP	1.6	0.07	5	good to five feet
60186	E1	GP	1.2	0.11	5	fair
60187	E1	GP	1.4	0.07	5	fair
60189	E1	GP	0.5	0.04	10	fair
60190	E1	GP	0.4	0.05	10	fair to 5 feet
60191	E1	VC	2.7	0.84	10	fair
60192	E1	GP	1.1	0.04	5	good
60274	E1	VC	~0.0	0.29	5	good
60275	E1	VC	0.1	0.2	5	fair to poor, adjusted based on confidence interval
60276	E1	VC	1.8	0.9	5	fair
60281	E1	VC	0.5	0.24	10	fair
60282	E1	VC	0.6	0.29	5	fair to poor
60284	E1	VC	3.4	0.49	5	good
60288	E1	VC	~0.0	0.08	5	good
60290	E1	VC	1.3	0.62	5	good
60291	E1	VC	2.1	0.19	5	fair
60292	E1	VC	2.3	0.35	5	fair

Table 1

Summary of Upwelling Velocities used to Develop Cumulative Frequency Distributions for Model Areas A1, A2, and C2 and Remediation Area E

Location ID	Remediation Area	Type[1]	Upwelling Velocity (cm/year)	90% Confidence Interval (+/-) (cm/year)	Depth Interval Used (feet)	Comments
60293	E1	VC	0.3	0.15	10	good
60294	E1	VC	2.7	0.25	5	good
60297	E1	VC	0.5	0.07	5	good
60302	E1	VC	4.3	0.53	5	good
60303	E1	VC	3.3	0.58	5	good
60304	E1	VC	2.8	0.1	5	good
70097	E1	GP	0.2	0.04	10	good
70102	E1	VC	2.4	0.63	10	good
70103	E1	GP	1.0	0.10	5	fair to 6 feet
70106	E1	GP	1.6	0.02	10	fair to 4.5 feet
70147	E1	VC	2.8	0.19	5	fair to poor
70152	E1	VC	0.4	0.2	10	fair
70153	E1	VC	1.7	0.66	10	good
70154	E1	VC	1.2	0.58	10	fair at 10 foot analysis, poor at 5 foot analysis
70042	E2	VC	~0.0	0.14	5	good
70043	E2	VC	0.6	0.49	5	good, adjusted based on confidence interval
70089	E2	VC	0.9	0.17	10	good
70090	E2	GP	1.9	0.08	5	good
70091	E2	GP	3.5	0.29	5	fair to 6.5 feet
70093	E2	VC	~0.0	0.27	5	good
70096	E2	GP	1.5	0.06	5	good
70099	E2	GP	2.1	0.14	5	good to fair
70100	E2	VC	1.2	0.45	5	good
70101	E2	GP	0.5	0.02	10	good
70148	E2	VC	2.1	0.21	5	good
70149	E2	VC	1.4	0.38	5	good
70150	E2	VC	1.4	0.29	5	good
60130	E3	GP	1.5	0.10	5	good
60131	E3	GP	1.9	0.08	5	fair to poor
60132	E3	GP	2.4	0.15	5	good
60133	E3	GP	1.0	0.06	5	good
60134	E3	GP	0.4	0.04	10	good
60135	E3	GP	0.8	0.02	10	fair
60136	E3	GP	2.0	0.07	5	good
60137	E3	GP	1.4	0.08	5	good

Table 1

Summary of Upwelling Velocities used to Develop Cumulative Frequency Distributions for Model Areas A1, A2, and C2 and Remediation Area E

Location ID	Remediation Area	Type[1]	Upwelling Velocity (cm/year)	90% Confidence Interval (+/-) (cm/year)	Depth Interval Used (feet)	Comments
60139	E3	GP	0.9	0.10	5	fair
60140	E3	GP	0.7	0.04	10	fair
60141	E3	GP	1.8	0.27	5	fair to poor
60143	E3	GP	2.5	0.12	5	good
60144	E3	GP	1.8	0.09	5	good
60145	E3	GP	2.6	0.18	5	good
60146	E3	GP	0.5	0.02	10	good
60149	E3	GP	2.2	0.12	5	good
60150	E3	VC	~0.0	0.10	5	good
60151	E3	GP	0.8	0.08	5	fair to good
60152	E3	VC	2.1	0.47	5	good
60156	E3	GP	4.0	0.20	5	good
60157	E3	GP	~0.0	0.11	10	fair at 10' analysis
60158	E3	GP	2.5	0.15	5	good
60159	E3	GP	0.6	0.05	5	good to fair
60161	E3	GP	3.1	0.13	5	good
60162	E3	VC	~0.0	0.23	5	fair
60163	E3	GP	4.3	0.22	5	good
60164	E3	GP	1.8	0.21	5	fair
60167	E3	GP	2.1	0.06	5	good
60168	E3	VC	~0.0	0.23	5	good
60169	E3	GP	2.3	0.13	5	fair
60170	E3	GP	2.8	0.09	5	good
60171	E3	VC	~0.0	0.18	5	good
60174	E3	GP	3.7	0.15	5	good
60175	E3	GP	1.8	0.11	5	good
60176	E3	GP	1.4	0.06	5	good
60177	E3	GP	0.2	0.04	5	good
60180	E3	GP	2.0	0.06	5	good
60181	E3	VC	~0.0	0.04	5	good
60182	E3	GP	0.2	0.05	5	good
60185	E3	GP	1.5	0.21	5	fair
60193	E3	GP	2.2	0.08	5	good
60194	E3	GP	3.1	0.30	10	5-foot analysis good, 10-foot analysis poor
60285	E3	VC	2.1	0.63	5	good

Table 1

Summary of Upwelling Velocities used to Develop Cumulative Frequency Distributions for Model Areas A1, A2, and C2 and Remediation Area E

Location ID	Remediation Area	Type[1]	Upwelling Velocity (cm/year)	90% Confidence Interval (+/-) (cm/year)	Depth Interval Used (feet)	Comments
60286	E3	VC	~0.0	0.35	5	fair
60287	E3	VC	~0.0	0.77	5	good
60296	E3	VC	0.8	0.24	5	fair
70094	E3	GP	0.7	0.02	5	good

Notes:

1 The upwelling estimates are based on evaluations of chloride-depth profiles developed from pore water analyses obtained from Vibracore (VC) borings and from sediment conductivity data collected with a Geoprobe (GP) direct push conductivity probe.

"NA" - indicates the chloride depth profile does not have a form suitable for analysis.

Table 2

Comparison of Upwelling Velocities at Locations with Pore Water and Sediment Conductivity Data

Location ID	Upwelling Velocity (cm/year)	
	Pore Water	Sediment Conductivity
20111	1.6	~ 0, 2.6
20113	2.4	1.0, 7.3
20118	0.7	0.5, 1.6
20119	~ 0	~ 0
20133	8.5	1.0
40149	1.5	~ 0
40151	3.4	2.0
40154	~ 0	0.2
40157	1.7	~ 0
40165	2.6	0.5
40168	7.5	7.1
40172	1.3	~ 0
40179	1.3	~ 0
40184	NA	4.5, 0.4
60125	0.8	0.6, 0.8, 0.9
60127	1.7	1.0
60129	0.3	~ 0
60150	~ 0	2.4, 1.9, 2.1
60152	2.1	1.9
60154	1.1	0.4
60162	~ 0	2.1, 3.8, 2.6
60168	~ 0	3.2, 3.5, 3.5
60171	~ 0	0.8
60179	0.2	0.6
60181	~ 0	0.2
60191	2.7	2.1
70089	0.9	2.5
70093	~ 0	3.2
70100	1.2	0.4
70102	2.4	0.4

Note: "NA" indicates the chloride-depth profile does not have a form suitable for analysis.

Table 3

Comparison of Upwelling Velocities at Locations with Multiple Sets of Sediment Conductivity Data

Location	Upwelling Velocity (cm/yr)	
	Largest	Other
20111	2.6	~ 0
20113	7.3	1.0
20115	8.5	1.0
20116	0.8	~ 0
20117	0.1	~ 0
20118	1.6	0.5
20121	~ 0	~ 0
20122	1.1	0.9
20123	0.2	~ 0
20128	0.5	0.1
20129	0.7	0.3
20130	0.1	~ 0
20132	14.4	1.1
30061	4.6	4.2
30071	>32	0.9
30072	24.1	1.2
30073	5.0	4.8
30075	>32	18.9, 7.7, 13.0, NA, NA, NA
30076	>32	1.3, 0.5, NA
40074	>37	>37
40076	33.5	NA
40079	>37	>37
40110	8.7	NA
40163	5.4	5.4
40183	5.3	2.3
40184	4.5	0.4
40185	NA	NA
40186	3.0	NA
60125	0.9	0.8, 0.6
60130	1.5	0.3, 0.5

Table 3

Comparison of Upwelling Velocities at Locations with Multiple Sets of Sediment Conductivity Data

Location	Upwelling Velocity (cm/yr)	
	Largest	Other
60136	2.1	2.0, 1.8, 1.1
60142	1.4	1.3, 0.7
60143	2.5	2.5, 0.4
60149	2.2	2.2, 2.1
60150	2.4	2.1, 1.9
60156	4.0	3.4
60161	3.1	2.5, 1.9
60162	3.8	2.6, 2.1
60163	4.3	3.3
60167	2.1	1.9, 1.9
60168	3.5	3.5, 3.2
60170	2.8	2.2, 1.8
70051	7.0	4.9
70053	9.8	6.3, NA
70054	4.6	0.8
70088	3.5	2.8, 1.9
70107	>35	~ 0 , NA

Note: "NA" indicates the chloride-depth profile does not have a form suitable for analysis.

Table 4

Measured Values of Vertical Hydraulic Conductivity of Silt and Clay Unit

Location	Sample Interval (feet, BGS)	Representative Thickness (feet)	Vertical Hydraulic Conductivity (cm/sec)	Silt and Clay Thickness (feet)	Effective Vertical Hydraulic Conductivity (cm/sec)
Phase VI Data					
OL-SB-10190	42-44	6	4.30E-07	30	8.89E-08
	52-54	10	5.40E-08		
	62-64	10	7.80E-08		
	72-74	4	4.00E-07		
OL-SB-10191	60-62		1.00E-06	37	3.19E-07
	70-72	13	6.80E-07		
	80-82	10	1.80E-07		
	90-92	14	3.40E-07		
OL-SB-20210	28-30	6	2.80E-08	43	1.36E-07
	38-40	10	3.00E-07		
	48-50	10	4.60E-08		
	58-60	10	2.20E-07		
	68-70	6.5	3.80E-07		
OL-SB-20211	37-39	8	6.00E-08	22	6-07e-8
	47-49	14	6.10E-08		
	59-61	0	4.70E-05		
OL-SB-20218	18-20	11	4.90E-08	11	4.90E-08
	27-29	0	6.60E-06		
	37-39		2.10E-04		
OL-SB-30171	25-27	14	1.10E-07	69	1.50E-07
	47-49	16	2.60E-07		
	57-59	15	6.10E-07		
	77-79	16.5	1.10E-07		
	90-92	7.5	7.80E-08		
OL-SB-30172	20-22	8	1.80E-07	40	1.45E-07
	28-30	9	5.60E-07		
	38-40	10	7.50E-08		
	48-50	12.5	1.60E-07		
OL-SB-40300	53-54	10	1.50E-07	36	2.26E-07
	62--64	9.5	2.70E-07		
	71-73	10	2.40E-07		
	82-84	6.5	3.20E-07		
Phase I Data					
OL-STA-10013	41-43		1.40E-07		
OL-STA-10018	48-50		7.80E-08		
OL-STA-10022	64-66		2.30E-07		
OL-STA-10024	64-66		1.20E-07		
OL-STA-10025	52-54		9.00E-08		
OL-STA-10026	50-52		5.80E-08		
OL-STA-20001	45-47		1.30E-07		
OL-STA-20007	39-41		1.00E-07		
OL-STA-20018	47-49		1.40E-07		
OL-STA-10108	64-66		2.80E-07		
OL-STA-10108	68-70		2.10E-07		

Table 5

Calculated Vertical Groundwater Velocities across the Silt and Clay Unit at Selected Monitoring Well Locations

Well ID	Water Level Elevation (feet, NAVD 88)	Density (g/cm3)	Midscreen Elevation (feet, NAVD 88)	Freshwater Head (feet, NAVD 88)	Silt and Clay Thickness (feet)	Vertical Velocity (cm/year)
HB-HB-20D	363.7	1.11	233.5	378.0	86	0.31
HB-HB-20I	363.5	1.02	330.5	364.2		
HB-HB-05D	368.7	1.07	275	375.3	30	0.82
HB-HB-05I	365.1	1.07	328.9	367.6		
WA-WA-1D	370.3	1.04	268.5	374.4	24	1.43
WA-WA-1I	364.5	1.04	335.4	365.7		
WA-WA-3D	373.2	1.02	311.9	374.4	23	1.15
WA-WA-3I	367.2	1.03	345.5	367.9		
WB18-MW-03D	368.3	1.06	233.3	376.4	55	0.30
WB18-MW-03I	365.3	1.08	321.3	368.8		
WB18-MW-02D	369.1	1.06	273.3	374.8	21	1.62
WB18-MW-02I	364.0	1.07	338.3	365.8		

Notes: Water level data, density data and silt and clay thickness from (O'Brien & Gere 2008 and 2009). Water level data represent best estimate of average water levels. Upwelling velocity calculated using Equation (4).